2019

Investigating the Anti-Cancer Properties of Novel Hybrid 1,4-Dihydropyridine Derivatives in U-87MG Glioblastoma Cell

Tendai Hunyenyiwa
Andrews University, hunyenyiwa@andrews.edu

ABSTRACT

INVESTIGATING THE ANTI-CANCER PROPERTIES OF NOVEL HYBRID 1,4-DIHYDROPYRIDINE DERIVATIVES IN U-87MG GLIOBLASTOMA CELL LINE.

By

Tendai Hunyenyiwa

Co-Chairs: Denise L. Smith and Desmond H. Murray

ABSTRACT TO GRADUATE STUDENT RESEARCH

Thesis

Andrews University

College of Arts and Sciences

Title: INVESTIGATING THE ANTI-CANCER PROPERTIES OF NOVEL HYBRID 1,4-DIHYDROPYRIDINE DERIVATIVES IN U-87MG GLIOBLASTOMA CELL LINE.

Name of researcher: Tendai Hunyenyiwa

Name and degree of faculty co-chairs: Denise L. Smith, PhD. and Desmond H. Murray PhD.

Date completed: July 2019

Glioblastoma is the most devastating of brain cancers with a very high death rate and a low survival rate of less than 15 months after diagnosis. Glioblastoma is a cancer of astrocytes which are the majority of the brain glial cells that support neurons and help create the blood-brain barrier among other functions. The current approach to treating this disease is surgical removal of the main tumor, followed by radiotherapy and limited chemical intervention by the use of temozolomide (TMZ). This disease is characterized by high invasion and recurrence after surgical removal of the main tumor as a result of cancerous astrocytes migrating from the main tumor site to other parts of the brain. Novel dihydropyridines were synthesized and their effects tested on glioblastoma cell line U-87MG to screen for their anti-cancer activities. Cell viability assays were performed to

establish the (lethal concentration) LC_{50} of these compounds. The novel hybrid dihydropyridines reduced the cell viability of U-87MG cells, with the substituted aromatic compounds being more potent than substituted heteroaromatic compounds.

Andrews University

College of Arts and Sciences

INVESTIGATING THE ANTI-CANCER PROPERTIES OF NOVEL HYBRID 1,4-DIHYDROPYRIDINE DERIVATIVES IN U-87MG GLIOBLASTOMA CELL LINE.

A Thesis

Presented in Partial Fulfillment

Of the Requirements of the Degree

Master of Science

By

Tendai Hunyenyiwa

2019

INVESTIGATING THE ANTI-CANCER PROPERTIES OF NOVEL HYBRID 1,4-DIHYDROPYRIDINE DERIVATIVES IN U-87MG GLIOBLASTOMA CELL LINE.

A Thesis

Presented in Partial Fulfillment

Of the Requirements of the Degree

Master of Science

By

Tendai Hunyenyiwa

APPROVAL BY THE COMMITTEE

_____

Denise L. Smith, Ph.D., Co-chair

_____

Desmond H. Murray, Ph.D., Co-chair

_____ _____7/19/2019_____

Robert Zdor, Ph.D. Date Approved

For

Letwine and Oscar Hunyenyiwa

Tafara

TABLE OF CONTENTS

ACKNOWLEDGEMENTS

I would like to extend my sincere gratitude to Dr. Denise Smith for being such an amazing advisor and mentor throughout the program. Her undeniable enthusiasm for science and contagious excitement for discovery drew me to the project and kept me going. I am so thankful for the lengths you had to go through just to see me progress and grow as a scientist and human in society. I would also like to thank Dr. Murray, for being an awesome co-advisor. Thank you for giving me an opportunity to reignite my interest in chemistry and research. Your advice and mentorship assisted me through this project. I am grateful to Dr. Zdor, for your commitment to this project and your willingness to work through the scheduling. Your external view on this project, which brought exciting questions to the subject were always a joy to tackle. I am grateful to all of you for your genuine support in my future endeavors and all the recommendation letters you wrote.

I would like to extend my gratitude to the Department of Biology and Department of Chemistry and Biochemistry for providing me with the facilities that made this project possible. I am also thankful for the grants awarded by Andrews University Grant in Aid, Dr. Smith and Dr. Murray's research grant and the Biology Department funding for financially supporting this project. Thank you, Dr. Lyons for being a helpful and supportive graduate student advisor. I am also grateful to Angela S. for the best assistance and a great listening ear.

I am very grateful to my awesome cohort: Priscilla and Christina for all the adventures and Friday rewinding, as well as Christian, Jeremy and Austin. You carried me through the whole period; from long nights writing, making the grad-room a

breathing space and Nikki's brunch. I am super thankful for Priscilla; you have been an awesome lab-mate and inspiration for my goals, team glio forever.

I am very grateful for my friends: Nathan Hwang, Ben Hiramoto, and Nadia Bastien and, especially Candys Rambeloson, who went above and beyond in helping me with editorial and technical issues. I am thankful for my American family, people who helped take care of me to this point, my home away from home: Mrs. Clark, Mrs. Rosenwinkle, Mrs. Tsikira, Mrs. Mosheti, and the Beesons.

Finally, and most importantly I would like to thank my mother Letwine Hunyenyiwa for believing, supporting and praying for me throughout this project. You are my inspiration and the undying sacrifices you make for me urge me to move on. I am thankful to God, for granting me the opportunity and carrying me through the whole process, providing comfort and encouragement and hope for the future

CHAPTER 1

INTRODUCTION

Cancer

Cancer, a collection of diseases characterized by uncontrolled cell division results in the destruction of body tissues and patient death if untreated. The uncontrolled cell division is a result of genetic mutations that can be inherited or acquired during the person's lifetime. Exposure to various carcinogens (cancer-causing agents) can lead to these mutational events. Most cancer develops in stages characterized by cellular changes starting with hyperplasia (an increase in the cell division), followed by dysplasia, (a noticeable change in morphology of the cells), which then leads to the development of *in-situ* cancer (a stationary form of cancer), and finally malignant cancer (capable of invading and metastasizing).

Cancer diseases have created a burden on the world's population with an estimated 18.1 million new cases and 9.1 million deaths in 2018 (Bray et al., 2018). Of the 9.1 million cancer deaths, the leading causes include lung, breast, prostate, and colorectal cancer, making these four cancers the most commonly studied. However, less common cancers such as brain cancers deserve research attention.

Brain cancers with an incident rate of 1.6 % of all cancers worldwide may be counted as one of the rarer cancers (Bray et al., 2018). One of the most lethal and fastest progressing cancers in this group affects the glial cells called astrocytes. This cancer has

been of interest lately in the US as it has claimed the lives of two US Senate members within the span of 10 years. This cancer is Glioblastoma multiforme.

Glioblastoma Multiforme

Glioblastoma multiforme (GBM), with a survival rate of less than 5%, has the highest death rate in comparison to all the other brain cancers (Da Fonseca et al., 2011), and most patients die within two years of diagnosis (Gallego, 2015). GBM mostly targets the elderly and is more common in males (Morgan et al., 2017). GBM can be divided into primary and secondary depending on the genetic pathways involved. The primary GBM affects the elderly with a mean age of 64, while secondary GBM affects younger people with a mean age of 45 years old (Ohgaki et al., 2004). Genetically, primary and secondary GBM have characteristic mutations. Primary GBM (80%) is characterized by high expression of epidermal growth factor receptor, while secondary GBM (20%) is associated with overexpression of mutant TP53 gene (Kleihues and Ohgaki, 1999).

GBM is a glioma which originates from astrocytes while other gliomas can arise from different glial cell types such as oligodendrocytes (Zong et al., 2012). Verkhratsky and Butt (2013) state that astrocytes constitute the largest proportion of the brain glial cells (20-50%). These star-shaped cells have multiple brain functions including secretion of the extracellular matrix, uptake, and regulation of neurotransmitters, and regulation of the blood-brain barrier.

The World Health Organization (WHO) has divided astrocytomas into four groups or grades (increasing in severity) based on morphological, cellular, genetic and biochemical properties. Grade I, also called pilocytic astrocytoma, is characterized by

benign cystic tumors in the cerebral hemispheres, affecting mostly young people (Huang et al., 2005). Grade II is low-grade astrocytoma, associated with infiltration and targets young to middle aged people, 20-50 years old. Grade III is anaplastic astrocytoma; it is a rare but malignant type of cancer. It is characterized by invasion but can be distinguished from glioblastoma by its inability to infiltrate the blood vessels. Grade IV or GBM is characterized by high proliferation and invasion.

Invasion

GBM cells aggressively invade the normal brain tissue and surrounding blood vessels which reduces the effectiveness of tumor resection. The micro-tumors (small tumors that form around the main tumor mass) also referred to as neurospheres are usually found about 3 cm away from the primary tumor area (Lara-Velazquez et al., 2017), where they are shielded from the radiation therapy by embedding into normal tissue. The invasive cells migrate through the space surrounding the blood vessels called the perivascular space. They can also travel through the brain parenchyma and white matter neuronal tract.

There are two ways in which the glioblastoma cells can invade the surrounding tissue: as a single cell or as a sheet of cells (collective migration) from the primary tumor (Gandalovičová et al., 2017). Glioblastoma cells can invade because they are transformed to be mobile, gain the ability to degrade extracellular matrix and increase the expression of necessary enzymes for these processes. The cells first develop membrane extensions (invadopodia) as a morphological change which allows them to attach to the extracellular matrix (Demuth and Berens, 2004). Sarkar et al. (2006) documented that tenascin-C an

extracellular matrix glycoprotein is highly expressed in glioma cells and promotes the formation of membrane extensions for migration.

Invasive cells produce proteolytic degradation enzymes (matrix metalloproteinases) that allow them to degrade the extracellular matrix for invasion (Gandalovičová et al., 2017). These matrix metalloproteinases (MMPs) are produced in all cancers during progression and growth (Egeblad and Werb, 2002). High levels of two metalloproteases (MMP-2 and MMP-9) are expressed in glioblastoma cells and are believed to aid in extracellular matrix degradation during the invasion (Ramachandran et al., 2017). MMP-2 and MMP-9 are upregulated in the glioblastoma cells during the invasion phase through the Hedgehog pathway (Chang et al., 2015).

Another protein family involved in migration and invasion is ADAM (a disintegrin and metalloprotease domain); these proteins cleave and therefore inactivate CD44 a cellular adhesion molecule, among other functions, which leads to cell migration (Takamune et al., 2008). Nakamura et al. (2004) discovered a high expression of ADAM-12 and ADAM-17 enzymes in glioblastoma cells which presents as a potential target for anti-invasive drugs. These ADAM proteins are upregulated in glioblastoma and aid in the cell proliferation by increasing the amount of tumor necrosis factor through prodomain shedding (Kodama et al., 2004).

Neurospheres

Neurospheres are spherical structures that form *in vitro* from the cells or tissue of embryonic or adult central nervous system (Reynolds and Weiss, 1992). They are characterized by the ability to self-renew, proliferate and differentiate. Prior to the discovery of neurospheres, the scientific community believed that adult brains did not

undergo neuronal genesis. Kaplan and Hinds (1977), however, managed to show that new neurons could be formed in an adult brain. The discovery of neuronal stem cells and the development of neurospheres were then successfully propagated from the hippocampus of the rat (Reynolds et al., 1992).

Neurospheres are physically characterized by a few neuronal stem cells which rapidly divide and get embedded into already differentiating cells. They are formed from the culturing of neuronal stem cells which originate from the sub ventricular zone or sub granular zone of the hippocampus (Pastrana et al., 2011). When the tissue from these two regions of the brain is cultured in media that promotes cell proliferation, then cells grow into small aggregations of de-differentiated cells. Neurospheres can also form from brain cancer stem cells (Kim et al., 2015).

Neurospheres provide a good study model of tumor formation in brain cancer. Reynolds and Weiss (1992) showed that the study of neurospheres can improve the prognosis of gliomas as they can be used as biomarkers for tumor development. They are also used to study brain cell and tissue regeneration as well as neuronal stem-like characteristics. Studying neurospheres formed from tumors can lead to medicinal therapies that prevent cancer relapse by targeting cancer stem cells (Gilbert and Ross, 2009).

GBM Treatment Regimen

GBM is generally treated by surgery, radiotherapy, and chemotherapy. Surgery is helpful in removing the primary tumor mass, but it does not remove all the cancer cells as many cells will have invaded into the normal tissue. Radiotherapy following the surgery

reduces the number of remaining cancer cells around the primary tumor site; but this method is not effective as many of the invasive cells have migrated far from the initial tumor mass (Giese et al., 2003). In conjunction with surgery and radiation therapy, patients are also treated with chemotherapeutic agents, the most common one being temozolomide (TMZ). This drug targets the invasion process by altering DNA bases in GBM cells through methylation (Stupp et al., 2005). However, TMZ is highly susceptible to resistance as the cancer cells mutate (Gallego, 2015). Castro and Aghi (2014) tested another drug used to treat GBM called bevacizumab, which targets angiogenesis. This drug has helped increase the survival for some patients by a few years, however, because of the development of drug resistance and the high death rates for most patients, it is not optimal. There is a need to develop new additional drugs for the treatment of GMB.

Hybrid Compounds

For decades, scientists and medical personnel have focused on the single molecule-single target paradigm in drug discovery where a single very specific target of the disease is addressed (Kong et al., 2009). Diseases, however, are complex in nature, rarely resulting from a single abnormality but have complex networks and different factors contributing to their development (Scotti et al., 2017). Complex diseases such as malaria and cancer are also prone to drug resistance due to mutations in the target. One approach to overcome the issues of complexity and resistance is the use of combination drugs. This method involves a cocktail or mixture of single target drugs so that the drugs are administered together at once. This method was not very effective due to high

resistance, low margin of safety, and adverse side effects (Berube 2016), therefore new strategies for drug development were needed.

A new paradigm of drug discovery, the use of hybrid drugs, is now being investigated. This method of drug discovery has developed over the past two decades with studies of malaria (Cavalli and Bolognesi, 2009) and cancer. The advancement in cellular/molecular biological techniques in the areas of genomics, proteomics, and genetics has provided new targets for drugs and facilitated this approach.

For example, bleomycin; a three-component anti-cancer hybrid drug was among the first be studied in early 2000 (Meunier, 2008). The other drug on the pioneering forefront in hybrid drug studies is artemisinin which is an anti-malarial pharmacophore (a part of the molecule that has biological activity) which has been studied since the 1980s (Muregi and Ishih, 2010). The FDA has also noted an increase in multitarget drugs since the 2000s (Ramsay et al., 2018).

Hybrid drugs are medications composed of two or more pharmacophores covalently bonded together into a single molecule (Micheal, 2017). These molecules can be formed through conjugation whereby a molecular linker is used to join the pharmacophores together. They can also be fused molecules which result from the direct linkage of pharmacophores via a functional group or merged molecules in which the pharmacophores are attached together without a linker, but instead, they are formed due to overlapping motifs (Gediya and Njar, 2009).

Many hybrid drugs appear to improve the pharmacodynamics and pharmacokinetics of the drugs. They have also been found to reduce resistance to drugs as one pharmacophore may inhibit resistance of the other, which is the driving force in

developing hybrid drugs for cancer therapy. There is a potential increase in drug efficacy when using hybrids as they have more than one biological target. Some anti-cancer hybrid drugs are being developed to decrease drug turnover, increase efficacy, delivery, lower toxicity, and reduce resistance to chemotherapy drugs. The use of hybrid drugs instead of combination drugs lowers the dosage of drugs administered which is likely to increase the safety margin of the drug.

Dihydropyridines

Dihydropyridines are heterocyclic compounds. They are synthesized through a Hantzsch dihydropyridine synthesis process which is a condensation reaction of aldehydes (organic compounds with carbon double-bonded to oxygen) with two beta-ketoesters (a ketone on the beta-carbon of an ester) and a nitrogen-donating group usually an ammonium salt (Velena et al., 2016).

Most dihydropyridines are known for their role in reducing blood pressure with a number of derivatives that are FDA approved for treatment (Fig. 1). They are calcium channel blockers which block L-type calcium channels thereby relaxing the cardiac smooth muscles allowing for more blood flow. However, dihydropyridines have demonstrated anti-cancer activities in breast cancer (Naziroglu et al., 2017) and HeLa cancer cells (Firuzi et al., 2013). They also inhibit the influx of calcium and this inhibition has been implicated in reducing chemotherapy drug resistance (Zarrin et al., 2010).

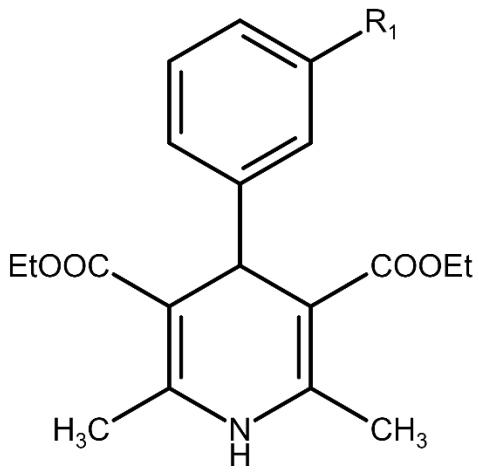

Figure 1: The generic structure of commercially available dihydropyridines, with an electron withdrawing group at position R.

Dihydropyridines act on GBM cells by inhibiting the T-voltage gated calcium channels (prominent in invasive cells) and calcium activated potassium channels which contributes to cancer cell survival (Niklasson et al., 2017). Niklasson et al. (2017) demonstrated that the dihydropyridine nifedipine increased the median survival rate in a GBM mouse model. These compounds also reduce the rate of invasion and migration of tumor cells by inhibiting the activation of ADAM10 in pancreatic cancer (Woods et al., 2015). ADAM 10 enhances cell proliferation and invasion by activating a cascade that requires calcium; therefore, blocking calcium influx inhibits this process (Woods et al., 2015).

In other cancer studies dihydropyridines showed major activity against the development of multidrug resistance. Dihydropyridines inhibit the P-glycoproteins which are involved in drug resistance (Zhou et al., 2005). Studies have shown that dihydropyridines elevate the cellular concentration of mitoxantrone (a chemotherapy drug) four-fold in comparison to initial levels. Firuzi et al., (2013) demonstrated that inhibition of the P-glycoprotein, a drug resistance protein, decreased drug resistance.

A pharmacophore of interest is boronic acid. Boronic acids are Lewis acids belonging to the organoborane group and is characterized by the presence of a carbon-boron bond. Boronic acid functional group is found in the anti-cancer drug bortezomib, used to treat prostate and bladder cancer (Lashinger et al., 2005). Scarano et al. (2013) used boronic acid as a means of drug delivery in an ovarian cancer cell line through its ability to bind cell surface carbohydrates. The boronic acid pharmacophore has also been shown to increase drug lipophilicity which promotes drug passage across cell membranes (Issa et al., 2011).

Objectives and Hypothesis

In this research, I will: (1) synthesize novel hybrid dihydropyridine compounds, (2) determine the effects of these compounds on cellular cytotoxicity and determine the lethal concentration (LC_{50}) of these compounds in U-87MG cells, (3) document the effects of the hybrid compounds on cell morphology and neurosphere formation, (4) measure the effects of the compounds on cell migration, and (5) measure the effects of the hybrid compounds on cell invasion. I hypothesize that novel dihydropyridine derivatives will reduce the growth and proliferation of U-87MG cancer cells as well as reduce the mobility and invasiveness in these cells.

CHAPTER 2

CHEMISTRY

Dihydropyridine Synthesis

Seventeen novel hybrid dihydropyridine molecules were synthesized and tested for their anti-cancer and anti-invasion activities on the U-87MG glioblastoma cell line. They were synthesized using the classical Hantzsch dihydropyridine synthesis reaction. This involves the condensation of an aldehyde, two equivalents of a beta-keto ester and a nitrogen donating ammonium salt which gives 1,4-dihydropyridine carboxylates.

The mechanism for dihydropyridine synthesis involves a few more classic mechanisms to make necessary intermediates. A Knoevenagel condensation product is formed as an intermediate through the condensation of an aldehyde and one of the beta-keto esters. Another important intermediate that is formed is the ester enamine made from the condensation of the other beta-keto ester with the ammonium salt. The further condensation of these two intermediates through Michael addition created the final product of 1,4-dihydropyridines.

Novel hybrid dihydropyridines were synthesized using substituted aromatic, heteroaromatic aldehydes and substituted cinnamaldehydes. The experimental procedure to synthesize these dihydropyridines involved the reflux of all the reagents in water and ethanol for 2.5 hours followed by collection of the solid by cooling it in saturated sodium chloride.

Hantzsch Reaction Mechanism

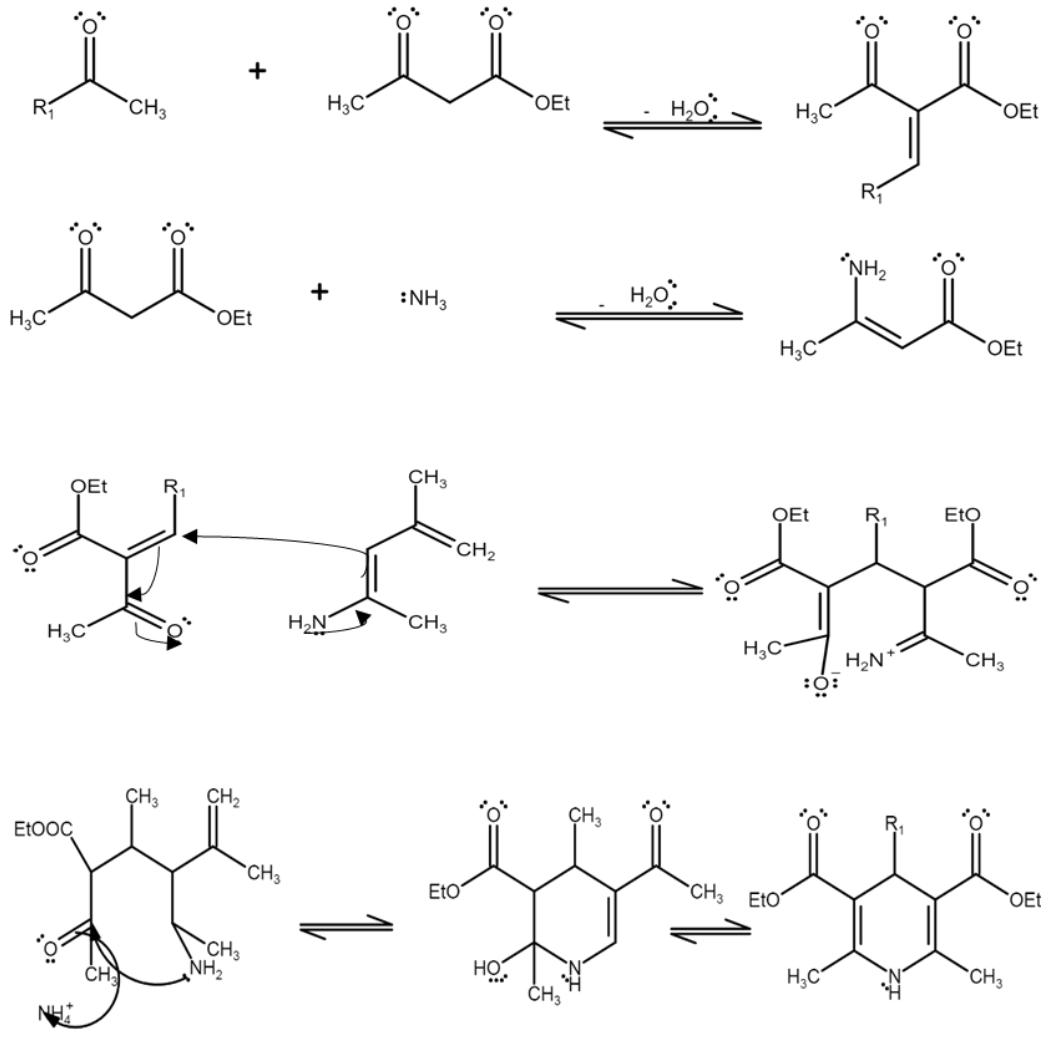

Figure 2: The general Hantzsch mechanism for the formation of dihydropyridines.

Materials

The substituted benzaldehydes, heteroaromatic aldehydes, and substituted cinnamaldehydes were purchased from Aldrich, Acros Organics and Frontier Science. The starting materials and products were analyzed and confirmed using ^{1}H NMR spectroscopy performed on a 400 MHz JEOL JNM-ECP400 FT NMR instrument and infrared spectra using Thermo Scientific Nicolet iS50 FT-IR spectrometer.

Experimental Procedure

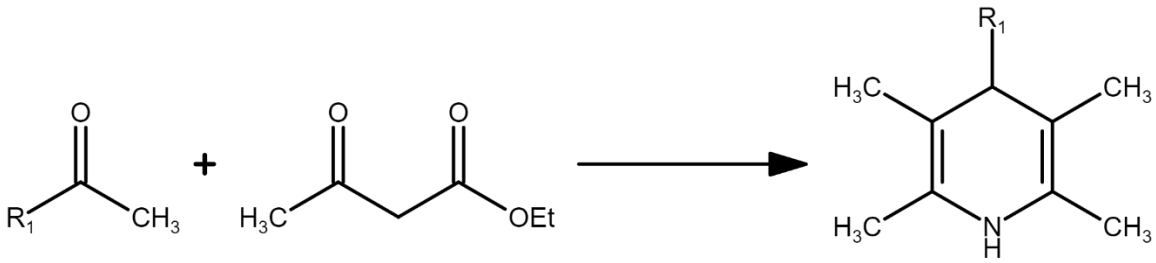

Figure 3: General equation for formation of dihydropyridines.

The solvents, 16.5 ml water and 3.5 ml ethanol, were added to a 50 ml round bottom flask containing a magnetic stir bar. The following materials were then added in order: 2.5 mmol aldehyde, 5.0 mmol ammonium carbonate, 2.5 mmol boric acid, and 5.0 mmol ethyl acetoacetate. The water-cooled condenser was attached to the round bottom flask and the reaction mixture refluxed for 6 hours. The mixture was then poured into a beaker containing 25 ml of saturated NaCl in ice and stirred for 10 minutes to terminate and neutralize the reaction. The reaction mixture was vacuum filtered and air dried to collect the solid product. The product was collected and weighed to calculate the percent yield. The products were subjected to nuclear magnetic resonance (NMR) using dimethyl

sulfoxide (DMSO) as the solvent to identify and confirm the desired products. Infrared spectroscopy (IR) was used to further elucidate the structures of the dihydropyridines made by analyzing the presence and/or absence of functional groups.

Results

Below is a list of novel hybrid compounds synthesized during this project. The list indicates the name of the compound, the acronyms that will be used from henceforth to refer to them and the NMR and IR results of the relevant peaks in identifying the dihydropyridine. Figures 4 and 5 show structures of synthesized compounds.

The starting materials showed an NMR diagnostic peak of the aldehydes between 9.7-10 ppm chemical shift representing the proton on the aldehyde and the IR diagnostic peak around the 1630-1820 region representing the carbon- oxygen double bond. These peaks, however, were not present in the products, showing that all the aldehydes had reacted forming dihydropyridines. The products had NMR diagnostic peak between position 4.5-5 ppm showing the proton at position 4 of the dihydropyridine ring. The IR spectroscopy of the products had strong peaks between region 3100-3550 for the N-H bond in the dihydropyridine ring.

Dihydropyridine NMR & IR Data

(Diethyl 2, 6-dimethyl-1, 4-dihydropyridine-3, 5-dicarboxylate-3-yl) boronic acid:(**3-FPB**) IR (ATR cm):3336 (N-H Stretch), 2980 (C-H Stretch), 1673 (C=O), 1485 (C=C); H NMR (400 MHz, DMSO-d6) δ: 1.15-1.10(6H, q, CH), 2.50 (6H, s, CH), 4.00 (4H, q,CH), 4.83 (1H, S,CH), 7.89(3H,m, Ar-H), 8.84 (1H,s,NH)

(Diethyl 2, 6-dimethyl-1, 4-dihydropyridine-3, 5-dicarboxylate-4-yl) boronic acid: (**4-FPB**) IR (ATR cm):3322 (N-H Stretch), 1654 (C=O), 1488 (C=C); H NMR (400 MHz,

DMSO-d6) δ: 1.09-1.13(6H, q, CH), 2.25 (6H, s, CH), 3.97 (4H, q,CH), 4.83 (1H, S,CH), 7.01(3H,m, Ar-H), 8.9 (1H,s,NH)

Diethyl 2, 6-dimethyl-4-(2-fluorophenyl)-1, 4-dihydropyridine-3, 5-dicarboxylate: (**2-F**) IR (ATR cm):3330 (N-H Stretch), 2981 (C-H Stretch), 1691 (C=O), 1484 (C=C); H NMR (400 MHz, DMSO-d6)

Diethyl 2, 6-dimethyl-4-(3-fluorophenyl)-1, 4-dihydropyridine-3, 5-dicarboxylate: (**3-F**) IR (ATR cm):3340 (N-H Stretch), 2981 (C-H Stretch), 1647 (C=O), 1477 (C=C); H NMR (400 MHz, DMSO-d6) δ: 1.09-1.13(6H, q, CH), 2.26 (6H, s, CH), 7.01(3H,m, Ar-H), 9.0 (1H,s,NH)

Diethyl 2,6-dimethyl-4-(4-fluorophenyl)-1,4-dihydropyridine-3,5-dicarboxylate: (**4-F**) IR (ATR cm) :3340 (N-H Stretch), 2984 (C-H Stretch), 1651 (C=O), 1505 (C=C); H NMR (400 MHz, DMSO-d6) δ: 1.09-1.14(6H, q, CH), 2.25 (6H, s, CH), 3.97 (4H, q,CH), 4.83 (1H, S,CH), 7.01(3H,m, Ar-H), 8.9 (1H,s,NH)

Diethyl 2,6-dimethyl-4-(2,3-fluorophenyl)-1,4-dihydropyridine-3,5-dicarboxylate: (**2,3-DF**) IR (ATR cm) :3342 (N-H Stretch), 2980 (C-H Stretch), 1648 (C=O), 1478 (C=C); H NMR (400 MHz, DMSO-d6) δ: 1.04-1.09 (6H, q, CH), 2.35(6H, s, CH), 3.93 (4H, q,CH), 5.14 (1H, S,CH), 7.04-1.0 (3H,m, Ar-H), 8.95 (1H,s,NH)

Diethyl 2,6-dimethyl-4-(2,4-difluorophenyl)-1,4-dihydropyridine-3,5-dicarboxylate: (**2,4-DF**) IR (ATR cm) :3373 (N-H Stretch), 2979 (C-H Stretch), 1677 (C=O), 1495 (C=C);H NMR (400 MHz, DMSO-d6) δ: 1.05-1.10 (6H, q, CH), 2.50 (6H, s, CH), 3.93 (4H, q,CH), 5.07 (1H, S,CH), 6.92-7.23 (3H,m, Ar-H), 8.86 (1H,s,NH)

Diethyl 2,6-dimethyl-4-(2,5-difluorophenyl)-1,4-dihydropyridine-3,5-dicarboxylate: (**2,5-DF**) IR (ATR cm) :3334 (N-H Stretch), 2928 (C-H Stretch), 1650 (C=O), 1488 (C=C);H NMR (400 MHz, DMSO-d6) δ:1.05 (6H, q, CH), 2.5 (6H, s, CH), 3.97 (4H, q,CH), 5.07 (1H, S,CH), 7.00 (3H,m, Ar-H), 8.97 (1H,s,NH)

Diethyl 2,6-dimethyl-4-(2-trifluoromethyl-phenyl)-1,4-dihydropyridine-3,5-dicarboxylate: (**2-TF**) IR (ATR cm) :3325 (N-H Stretch), 2981 (C-H Stretch), 1696 (C=O), 1488 (C=C);H NMR (400 MHz, DMSO-d6) δ: 1.03-1.07 (6H, q, CH), 2.43 (6H, s, CH), 3.90 (4H, q,CH), 5.40 (1H, S,CH), 7..46-7.82 (4H,m, Ar-H), 9.00 (1H,s,NH)

Diethyl 2,6-dimethyl-4-(3-trifluoromethyl-phenyl)-1,4-dihydropyridine-3,5-dicarboxylate: **(3-TF**) IR (ATR cm) :3299 (N-H Stretch), 2985 (C-H Stretch), 1670

(C=O), 1487 (C=C); H NMR (400 MHz, DMSO-d6) δ: 1.06-1.11(6H, q, CH), 2.28 (6H, s, CH), 3.97 (4H, q,CH), 4.90 (1H, S,CH), 7.45 (3H,m, Ar-H), 9.10(1H,s,NH)

Diethyl 2,6-dimethyl-4-(3-Chlorophenyl)-1,4-dihydropyridine-3,5-dicarboxylate: (**3-Cl**) IR (ATR cm) :3319 (N-H Stretch), 2979 (C-H Stretch), 1647 (C=O), 1484 (C=C);H NMR (400 MHz, DMSO-d6) δ:1.1-1.14 (6H, t,CH), 2.49(6H,s,CH), 3.99 (4H, q, CH) 4.8 (1H, s,CH), 7.1-7.2 (4H,m, Ar-H), 8.90 (1H, s, NH)

Diethyl 2,6-dimethyl-4-(4-Chlorophenyl)-1,4-dihydropyridine-3,5-dicarboxylate: (**4-Cl**) IR (ATR cm) :3355 (N-H Stretch), 2983 (C-H Stretch), 1648 (C=O), 1485 (C=C); H NMR (400 MHz, DMSO-d6) δ: 1.1-1.14 (6H, t, CH), 2.51 (6H,s, CH), 3.99 (4H,q, CH), 4.84 (1H,s,CH) 7.17-7.27 (4H, m, Ar-H), 8.89 (1H,s, NH)

Diethyl 2, 6-dimethyl-4-(2-quinoline)-1, 4-dihydropyridine-3, 5-dicarboxylate: (**2-Q**) IR (ATR cm):3404 (N-H Stretch), 2977 (C-H Stretch), 1692 (C=O), 1591 (C=C); *H* NMR (400 MHz, DMSO-d6) δ:

Diethyl 2,6-dimethyl-4-(4-quinoline)-1,4-dihydropyridine-3,5-dicarboxylate: (**4-Q**) IR (ATR cm) :3172(N-H Stretch), 2974 (C-H Stretch), 1643 (C=O), 1505 (C=C); H NMR (400 MHz, DMSO-d6) δ: 0.82-0.87(6H, q, CH), 2.50 (6H, s, CH), 3.76 (4H, q,CH), 5.68 (1H, S,CH), 7.60 (3H,m, Ar-H), 88.5 (1H,s,NH)

Diethyl 2, 6-dimethyl-4-(5-methyl-2-furfural)-1, 4-dihydropyridine-3, 5-dicarboxylate: (**5-M2-F**) IR (ATR cm):3302 (N-H Stretch), 2987 (C-H Stretch), 1650 (C=O), 1492 (C=C); *H* NMR (400 MHz, DMSO-d6) δ: 1.15-1.19 (6H, q, CH), 2.50 (6H, s, CH), 3.34 (4H, q,CH), 4.59 (1H, S,CH), 6.47(3H,m, Ar-H), 8.89 (1H,s,NH)

Diethyl 2, 6-dimethyl-4-(5-pyridine)-1, 4-dihydropyridine-3, 5-dicarboxylate: (**5-P**) IR (ATR cm):3340 (N-H Stretch), 2984 (C-H Stretch), 1651 (C=O), 1505 (C=C); *H* NMR (400 MHz, DMSO-d6) δ: 1.08-1.12 (6H, q, CH), 2.50 (6H, s, CH), 3.34 (4H, q,CH), 4.79 (1H, S,CH), 6.47(3H,m, Ar-H), 9.05 (1H,s,NH)

Diethyl 2, 6-dimethyl-4-(5-methyl-2-thiophene)-1, 4-dihydropyridine-3, 5-dicarboxylate: (**5-M2-T**) IR (ATR cm) :3342 (N-H Stretch), 2978 (C-H Stretch), 1689 (C=O), 1484 (C=C); H NMR (400 MHz, DMSO-d6) δ: 1.15-1.20 (6H, q, CH), 2.50 (6H, s, CH), 3.34 (4H, q,CH), 4.05 (1H, S,CH), 6.47(3H,m, Ar-H), 8.99 (1H,s,NH)

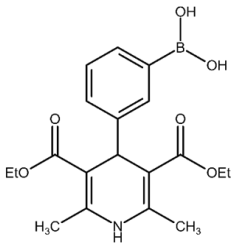

3-FPB, 53.5%
Pale yellow

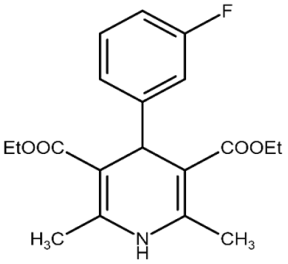

3-F, 45.8%
Light orange

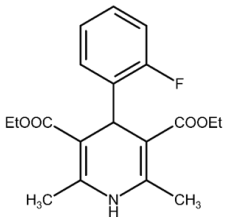

2-F, 73.4%
Dark orange

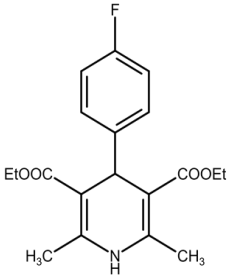

4-F, 58.4%
Sticky orange

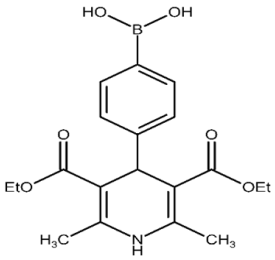

4-FPB, 57.1%
Light yellow

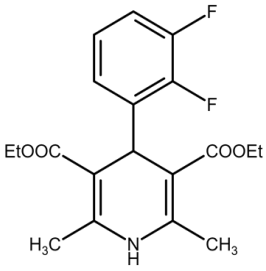

2,3-DF, 60.6%
Yellow

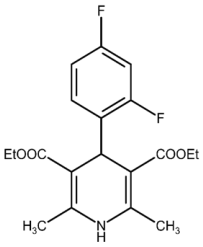

2,4-DF, 40.6%
Dark yellow

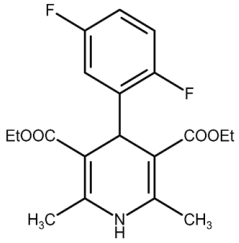

2,5-DF, 54.8%
Light yellow

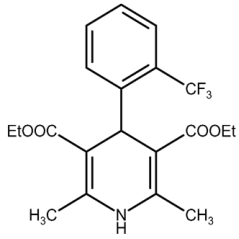

2-TF, 41.4%
Mustard yellow

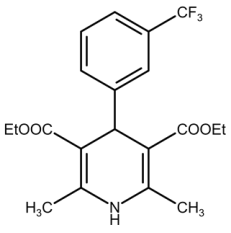

3-TF, 62.2%
Light yellow

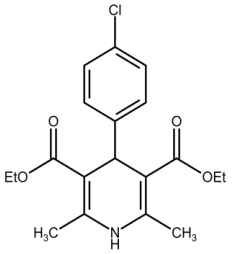

3-Cl, 53.4%
Light brown

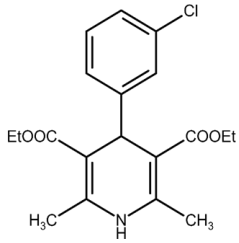

4-Cl, 47%
Sticky orange

Figure 4: The structures of the substituted aromatic novel hybrid dihydropyridines with the percentage yield and the physical characteristics of the compounds

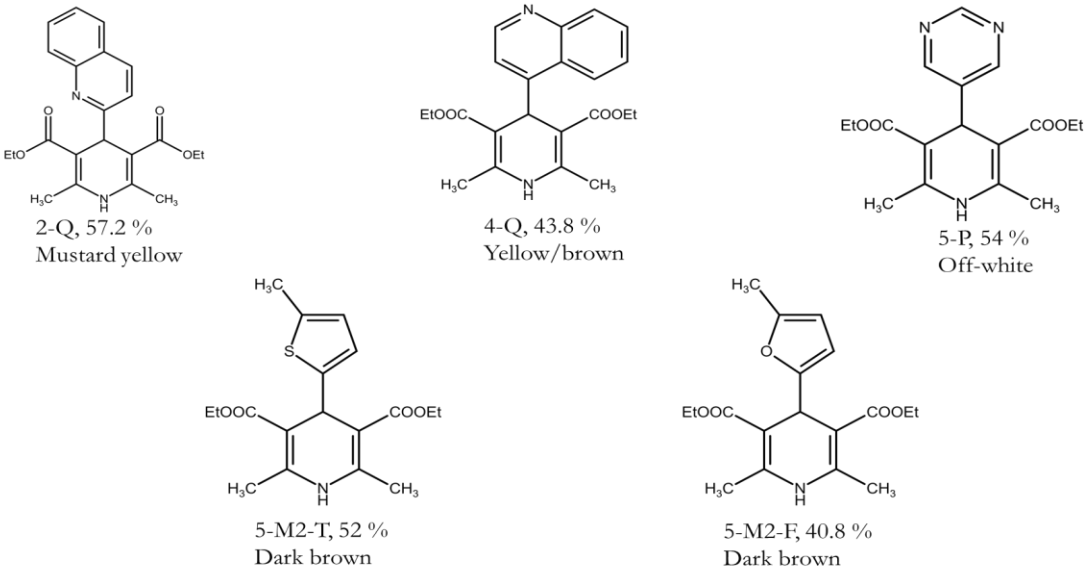

Figure 5: The structures of substituted heteroaromatic novel dihydropyridine compounds with the percentage yield and physical description.

Discussion

The synthesis of dihydropyridines following Hantzsch reaction was successful after the optimization of the method. The method was optimized for solvent by using 15% ethanol with 85% water. This eliminated the stickiness of the product and increased the yield. The method used was able to obtain yields similar to other methods such as the microwave closed system which has yields of around 50-70% (Demirayak et al. 2011). Optimization was also performed for reflux time that would give the most product, which was 6 hours. Ammonium carbonate was lost from the reaction *via* sublimation and deposition within the first few minutes of reflux, therefore, it was optimized by doubling the molarity of the salt in order to leave excess ammonium carbonate at the end of the reflux.

The novelty of the dihydropyridines synthesized is reflected in the functional groups of the aromatic rings and the use of heteroaromatic aldehydes and

cinnamaldehydes. The compounds synthesized were substituted on their aromatic rings with boronic acid, fluorine or chlorine. The lack of commercial availability of cinnamaldehydes made the substituted styrl group of dihydropyridines hard to synthesize with only two products synthesized. These products, however, could not be extracted from the flask after vacuum filtration because they were sticking to the sides of the flask and to the filter paper. They were also heavily pigmented with deep red color which could result in assay interference during biological assays.

Our novel hybrid dihydropyridines had boronic acids substituted at positions 3 and 4 (3-FPB, 4FPB), fluorine, difluoro and trifluoromethyl substituted at positions 2, 3 and 4 (2-F, 3-F, 4-F, 2, 3-DF, 2, 4-DF, 2, 5-DF, 2-TF, 3-TF) and chlorine substituted at positions 3 and 4 (3-Cl, 4-Cl). The heteroaromatic substituted dihydropyridine had substituted quinolones (2-Q, 4-Q), furfural (5-M2-F) and thiophenes (5-M2-T).

These pharmacophores are known to have medicinal effects which include anti-malarial and anti-cancer properties. The synthesized compounds were used for drug testing on U-87MG glioblastoma cells to measure their anti-invasion and anti-cancer properties. Some of our synthesized dihydropyridines have similar structures to commercially available dihydropyridines. For example, amlodipine (anti-hypertensive drug) have highly electronegative group chlorine substituted in the ortho (2) position. This may infer that in addition to anti-cancer activities, our synthesized dihydropyridines may also be potential anti-hypertensive drug candidates.

Cheminformatics

Understanding the physical properties of these compounds help predict their biological interaction with the cells and their transportation to the target sites of the disease being treated. There is a need to predict whether the drugs being synthesized have the potential to reach their target. Since the synthesized drugs are for treating brain cancer it is reasonable to make predictions towards the bioavailability of these drugs. The main pharmacological effects of interest are lipophilicity, hydrophobicity and physical properties that would help predict the drugs oral bioavailability as well as the ability to cross the blood-brain barrier.

Lipinski's rules of drug oral bioavailability state a molecule is likely to have good absorption if it has the following: (i) Molecular weight (MW) is less than 500, (ii) Calculated octanol/water partition coefficient (logP) less than 5, (iii) Presence of less than 5 hydrogen bond donors, and (iv) Presence of less than 10 hydrogen bond acceptors. This means that a small, highly lipophilic and hydrophobic molecule is likely to cross the intestinal lining and therefore have greater oral bioavailability. Violation of one of Lipinski's rules does not negate oral bioavailability, but it does reduce it.

The blood-brain barrier (BBB) protects the central nervous system from external toxins and other chemicals entering the brain tissue. This barrier is made up of capillary endothelial tight junctions and glial cells which prevent chemicals from passing through. The brain interstitial fluid also has low plasma protein concentration which reduces the permeability of plasma protein-bound lipophilic proteins. The chemicals that are able to pass through the blood-brain barrier should therefore be small, lipophilic and with low affinity to plasma proteins.

Drugs that have low molecular weight, are hydrophobic and lipophilic have a great chance of passing through the blood-brain barrier. Dihydropyridine calcium channel blockers have been used in the treatment of some brain diseases like Alzheimer's disease (Paris et al., 2011) and prevention of Parkinson's disease (Ritz et al., 2010).

Using Lipinski's rules, a prediction can be made on whether the novel dihydropyridines can cross the blood-brain barrier. A cheminformatics web software Molinspiration (https://www.molinspiration.com/) was used to predict the pharmacological and physical properties of the synthesized dihydropyridines. Table 1 shows the predicted values for the synthesized compounds.

Results

Table 1: Predicted values of biological activities of the synthesized compounds.

Drug code	Molar mass	LogP	TPSA	H-bond acceptor	H-bond donor
3-FB	373.21	3.41	105.09	4	3
4-FB	373.21	3.43	105.09	4	3
2-F	347.39	4.03	64.64	5	1
3-F	347.39	4.53	64.64	5	1
4-F	347.39	4.55	64.64	5	1
2,3-F	365.38	4.14	64.64	6	1
2,4-F	365.38	4.17	64.64	6	1
2,5-F	365.38	4.17	64.64	6	1
2-TF	397.39	4.76	64.64	7	1
3-TF	397.39	5.26	64.64	7	1
3-Cl	363.84	5.04	64.64	5	1
4-Cl	363.84	5.06	64.64	5	1
2-Q	380.44	3.99	77.53	5	1
4-Q	380.44	4.15	77.53	5	1
5-FT-2-T	379.24	2.98	105.09	5	3
5-M-2-F	364.35	3.25	123.60	5	1
5-P	331.37	1.80	90.42	7	1

Discussion

The use of software tools like molinspiration help predict the bioavailability of synthetic compounds. Although the results are just a prediction, they give information on synthesized compounds activity that helps predict the usefulness of the synthetic compound. The main elements predicted by this software were oral bioavailability, lipophilicity and the ability for the drug to pass through the blood-brain barrier. All but 3 (3-TF, 3-Cl, and 4-Cl) of the novel hybrid dihydropyridines did not violate Lipinski's rule of 5. A logP value greater than 5 was the violation for the 3 drugs. Violating only one of the rules, however, does not exclude the drug but does make it a less likely candidate.

An octanol/water partition coefficient (logP) is used to predict the lipophilicity of a compound by measuring the ability of a compound to interact with oil more than water. One of Lipinski's rules on drug availability states that a viable drug should have a logP value less than 5; values between 0 and 5 show high lipophilicity and high hydrophobicity for negative values.

The dihydropyridines synthesized are hydrophobic based on the general observation that the molecules do not dissolve in water. Hydrophobic molecules are nonpolar molecules that repel water and therefore do not dissolve in it. The dihydropyridine ring has a nitrogen that is a proton donor, two carboxylates at position 3 and 5 that are hydrogen bond acceptors; these atoms and groups increase the hydrophilicity of the compound. The overall molecule, however, is hydrophobic because of the number of hydrocarbon bonds that are nonpolar therefore increasing the hydrophobicity.

This observation was supported by the predicted total polar surface area (TPSA) of novel dihydropyridines as shown in Table 1. Polar surface area is the surface area of a molecule that arises from nitrogen or oxygen atoms plus hydrogen atoms attached to them in a molecule. The greater the TPSA the more likely the molecule is to form hydrogen bonds and therefore more hydrophobic. A TPSA of less than 140 indicates a more hydrophobic molecule and all the dihydropyridines have a low TPSA as indicated in the table.

The results predicted by the molinspiration software suggest that the synthesized dihydropyridines have oral bioavailability, high lipophilicity and hydrophobicity, and they could pass through the blood-brain barrier. Commercially available dihydropyridines have been shown to pass through the blood-brain barrier in mice with Alzheimer's (Paris et al., 2011) and humans with Parkinson's disease (Ritz et al., 2010).

CHAPTER 3

BIOLOGY

Cell Maintenance

In this project U-87MG glioblastoma cells were used to investigate the effects of novel hybrid dihydropyridines on this cancer. These cells were maintained in a humidified incubator at 5% carbon dioxide and 37 °C. The cells were cultured in minimum essential media (MEM) (Gibco) containing 10% fetal bovine serum (Gibco) and 100 U/ml penicillin/streptomycin antibiotics (Gibco). The cells were treated with trypsin/EDTA (Gibco) and routinely split with media change on a Monday, Wednesday, Friday schedule to maintain cell numbers at less than 80% confluency.

Cell Count

U-87MG cells were used to perform all the experimental screenings for the effects of novel dihydropyridines in glioblastoma cells. A cell count was obtained by detaching the cells from the dish with 2 ml of trypsin/EDTA. Using the trypan blue cell exclusion method, the total number of cells were determined using a hemocytometer and calculations for the cells needed for experimentation as follows: 12-well plate 10 000 cells/ well; 24-well plate 5000 cells/well; 60mm dish 100 000 cells/well.

Cell Viability Experimental Procedure

Cell viability experiments were set up to calculate the lethal concentration (LC_{50}), as well as the lowest effective concentration (LEC) for novel hybrid dihydropyridines in glioblastoma cells. A colorimetric MTT assay was first tried without success because of compound color interference. To eliminate this problem, a modified National Cancer Institute (NCI) assay was utilized (https://dtp.cancer.gov/discovery_development/nci-60/methodology.htm). Cells were released from the dish and counted using a hemocytometer to determine the total number of cells needed for the experiment. In a 12-well plate (Falcon), 10 000 cells per well were introduced in 1 ml of MEM media and incubated for 24 hours. The compound to be tested was diluted in DMSO at 20 mg/ml to make stock solutions. After 24 hours, the compound was diluted into 11 concentrations ranging from 0.00195mg/ml to 2mg/ml in MEM media to a final volume of 1 ml. Old media was removed from the 12-well plate and the drug introduced to the plate by putting the 11 different concentrations plus a control well with new media (Fig 6). Previous experiments in the lab showed no impact on cell viability from DMSO at concentrations used in this experiment. After 24 hours media was removed and cells were fixed using methanol for 5 minutes followed by staining with crystal violet for 5 minutes. Excess stain was removed by washing with water. Cells were then counted and quantified by picking 3 consistent spots in the wells and counting the field of view. The three field of view counts were averaged and total cell numbers per well were estimated.

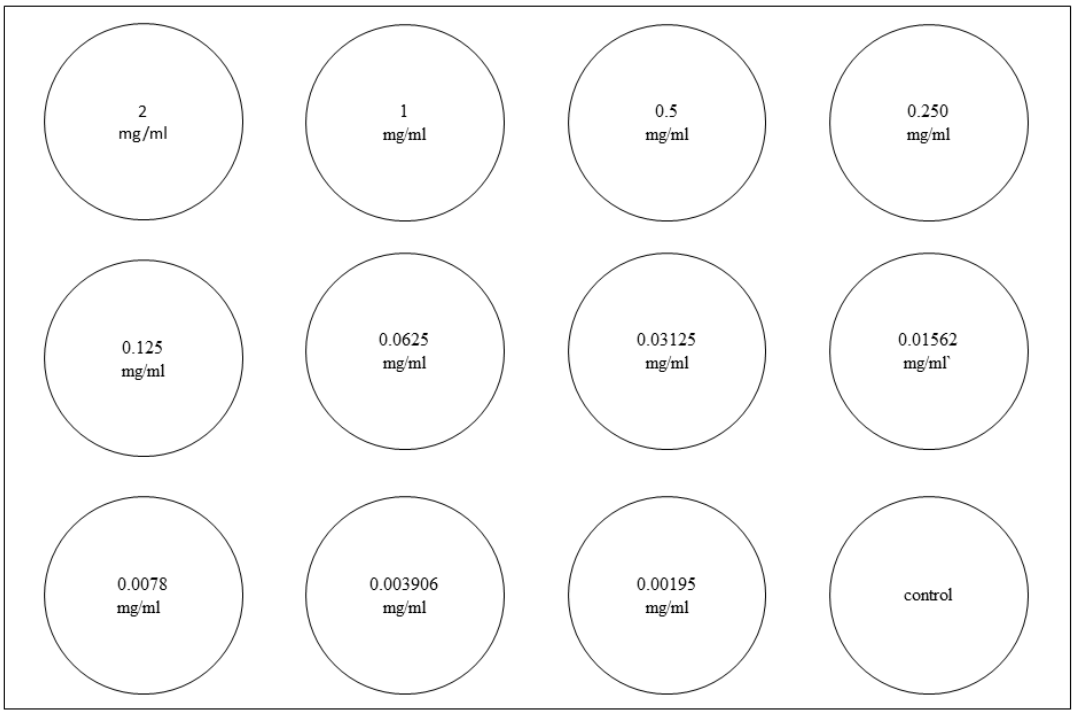

Figure 6: The representation of a 12-well plate with the 11 different concentrations in the well and a control.

Calculating LC_{50}

Three trials of the cell viability assay were run, and data were averaged. Standard deviation was calculated, and standard error bars established. Using linear regression, LC_{50} concentrations were calculated and established. To verify the calculated LC_{50}, 9 additional trial cell viability assays were performed at the linear regression-determined LC_{50} concentration. Cells were fixed and stained with crystal violet as above and 3 fields of view were counted, averaged and total cell numbers per well were calculated as above.

Results

The cytotoxicity and the LC_{50} of 14 compounds as well as the starting material ethyl acetoacetate (EAA) were measured and calculated through the cell viability assay. Figures 7-21 showing the cell viability for the 11 concentrations of the drug treated cells and untreated cells. The experiments were carried out through 3 independent trials and the results were recorded. Statistical analysis was performed using Dunnett test, to find the difference between the drug concentrations and the control. The asterisks on the graphs show the lowest concentration that was significantly different from the control, with all higher concentrations also significantly different from the control.

The dihydropyridines were cytotoxic with aromatic compounds more potent than the heteroaromatic compounds. Compounds with the same substituent on the aromatic ring but different position for example 3-FPB and 4-FPB had similar potency with the cells showing cell survival at similar concentrations.

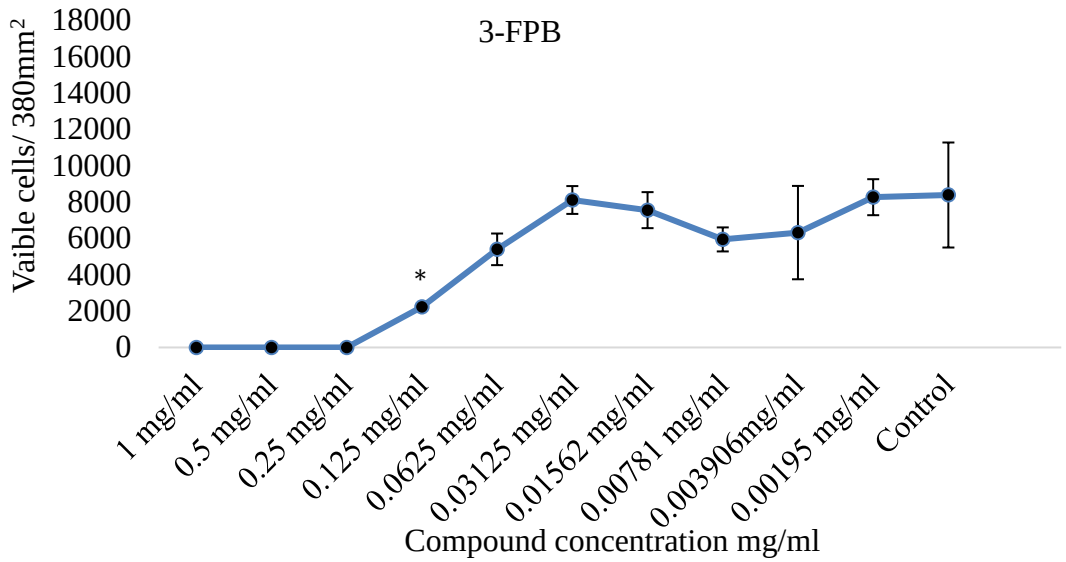

*Figure 7: Cell viability assay of 3-FPB on U-87MG glioblastoma cells. Cytotoxicity of the drug was measured by counting the number of cells per well for the 11 different concentrations and control. The error bars show the standard error, n =3 independent experiments. The lowest concentration significantly different from control is 0.125mg/ml, $p \leq 0.05$ shown by *.*

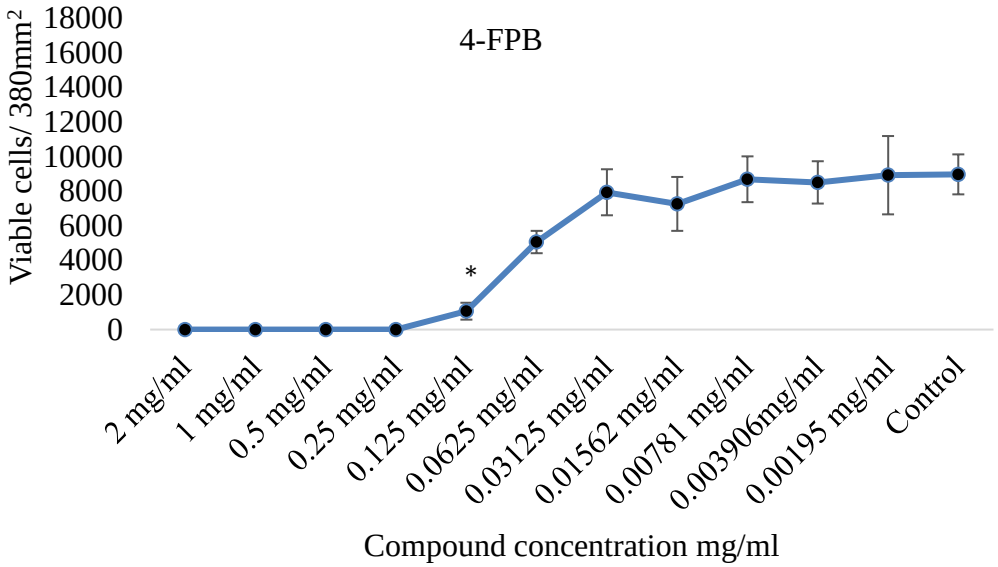

*Figure 8: Cell viability assay of 4-FPB on U-87MG glioblastoma cells. Cytotoxicity of the drug was measured by counting the number of cells per well for the 11 different concentrations and control. The error bars show the standard error, n =3 independent experiments. The lowest concentration significantly different from control is 0.125mg/ml, $p \leq 0.05$ shown by *.*

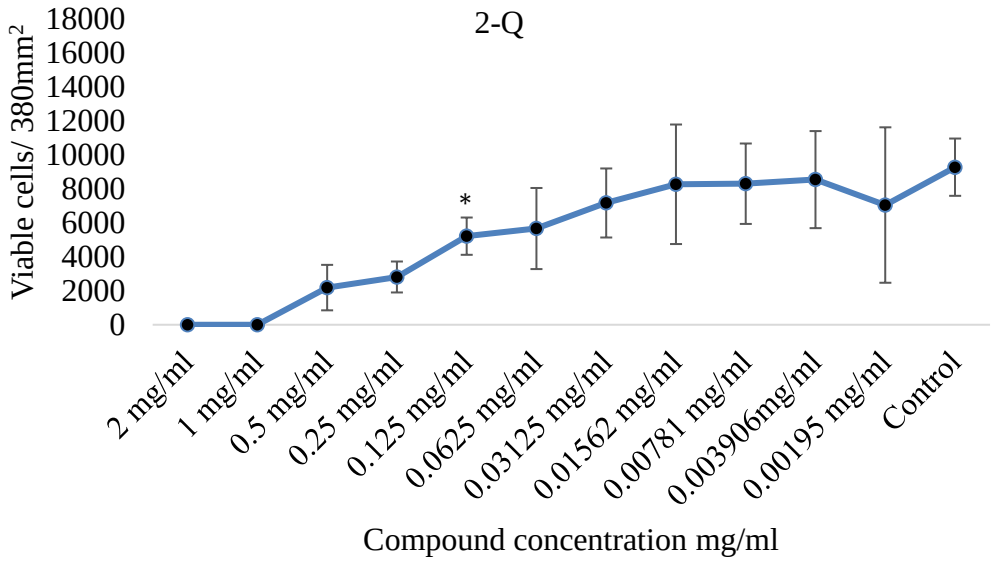

*Figure 9: Cell viability assay of 2-Q on U-87MG glioblastoma cells. Cytotoxicity of the drug was measured by counting the number of cells per well for the 11 different concentrations and control. The error bars show the standard error, n =3 independent experiments. The lowest concentration significantly different from control is 0.125mg/ml, $p \leq 0.05$ shown by *.*

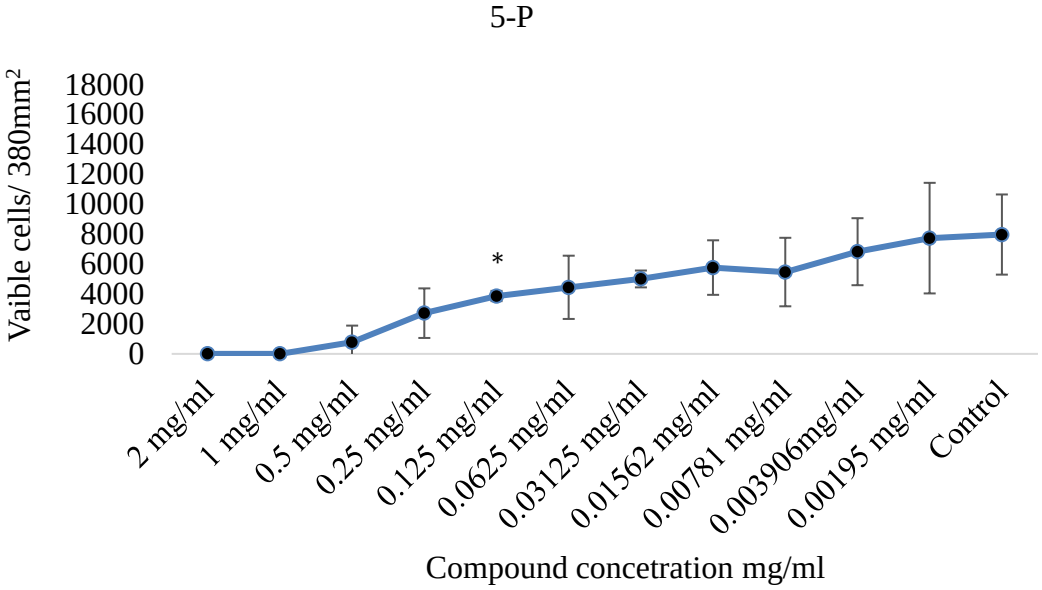

*Figure 10: Cell viability assay of 5-P on U-87MG glioblastoma cells. Cytotoxicity of the drug was measured by counting the number of cells per well for the 11 different concentrations and control. The error bars show the standard error, n =3 independent experiments. The lowest concentration significantly different from control is 0.125mg/ml, $p \leq 0.05$ shown by *.*

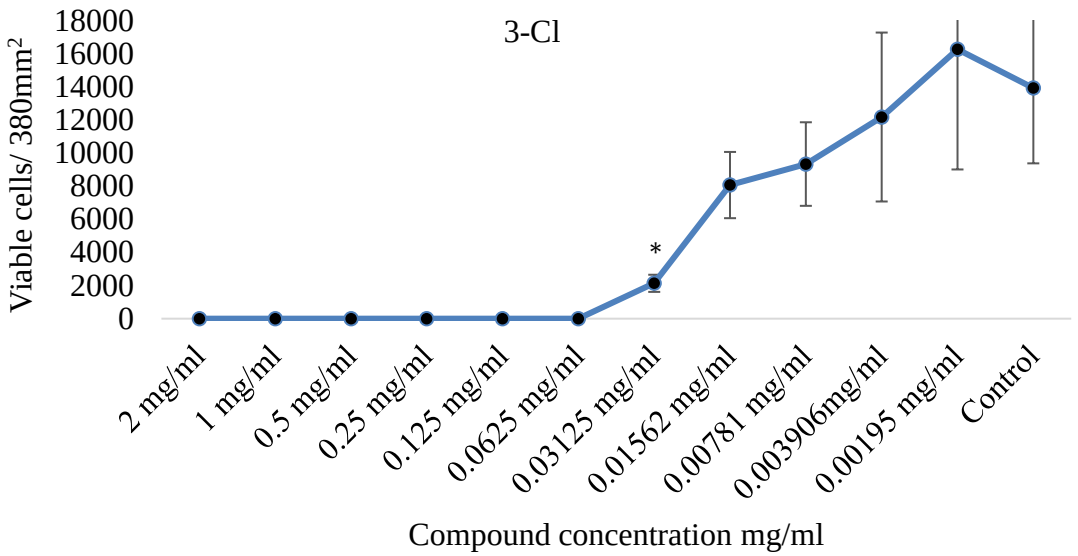

*Figure 11: Cell viability assay of 3-Cl on U-87MG glioblastoma cells. Cytotoxicity of the drug was measured by counting the number of cells per well for the 11 different concentrations and control. The error bars show the standard error, n =3 independent experiments. The lowest concentration significantly different from control is 0.03125mg/ml, $p \leq 0.05$ shown by *.*

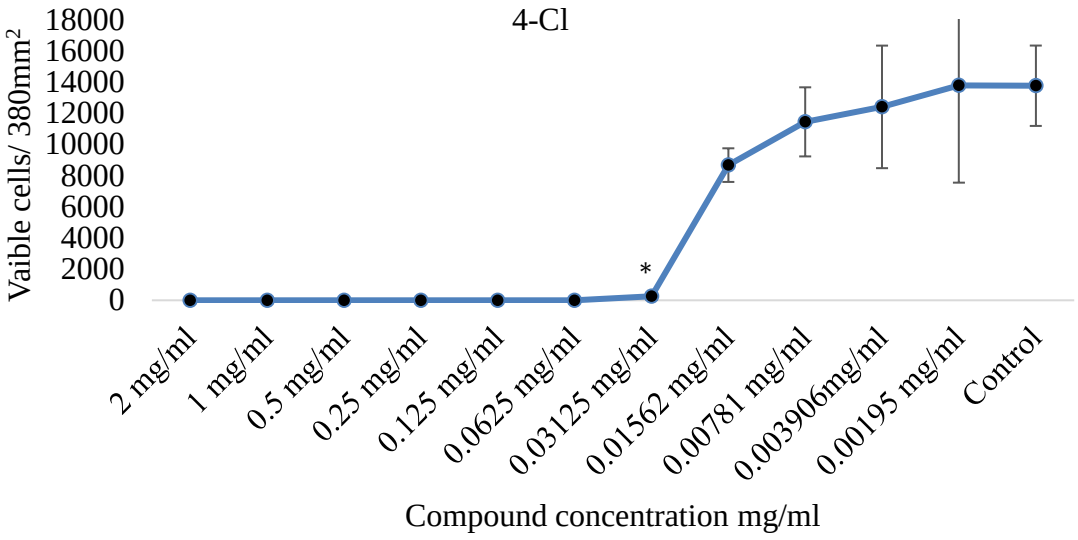

*Figure 12: Cell viability assay of 4-Cl on U-87MG glioblastoma cells. Cytotoxicity of the drug was measured by counting the number of cells per well for the 11 different concentrations and control. The error bars show the standard error, n =3 independent experiments. The lowest concentration significantly different from control is 0.03125mg/ml, $p \leq 0.05$ shown by *.*

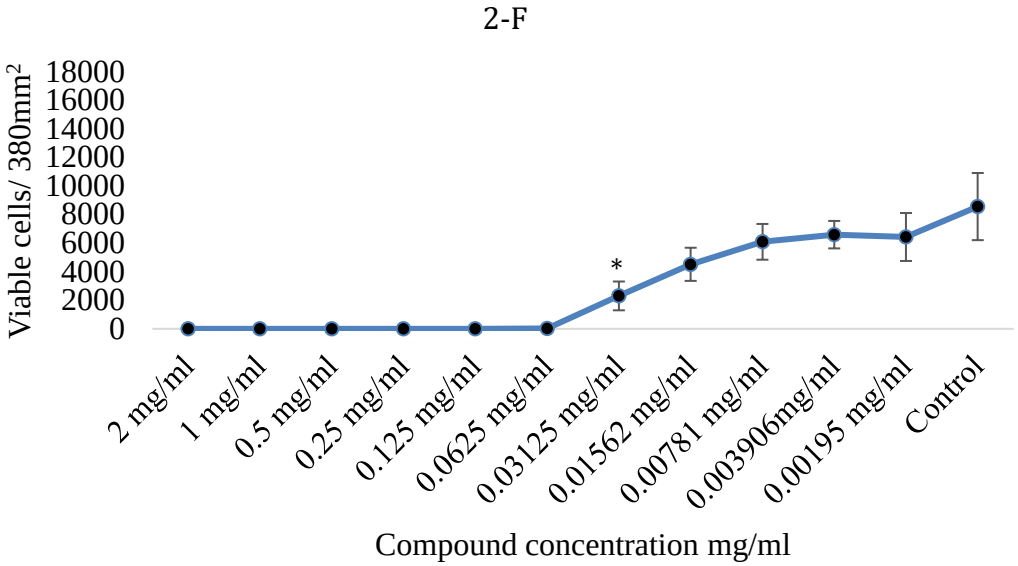

*Figure 13: Cell viability assay of 2-F on U-87MG glioblastoma cells. Cytotoxicity of the drug was measured by counting the number of cells per well for the 11 different concentrations and control. The error bars show the standard error, n =3 independent experiments. The lowest concentration significantly different from control is 0.03125mg/ml, $p \leq 0.05$ shown by *.*

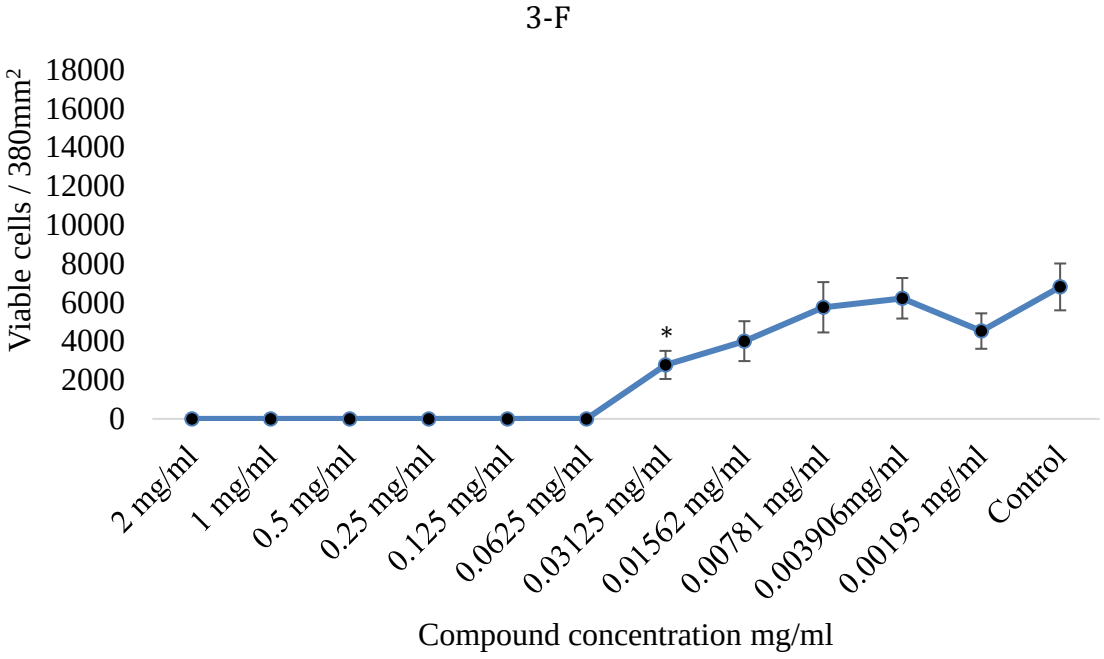

*Figure 14: Cell viability assay of 3-F on U-87MG glioblastoma cells. Cytotoxicity of the drug was measured by counting the number of cells per well for the 11 different concentrations and control. The error bars show the standard error, n =3 independent experiments. The lowest concentration significantly different from control is 0.03125mg/ml, $p \leq 0.05$ shown by *.*

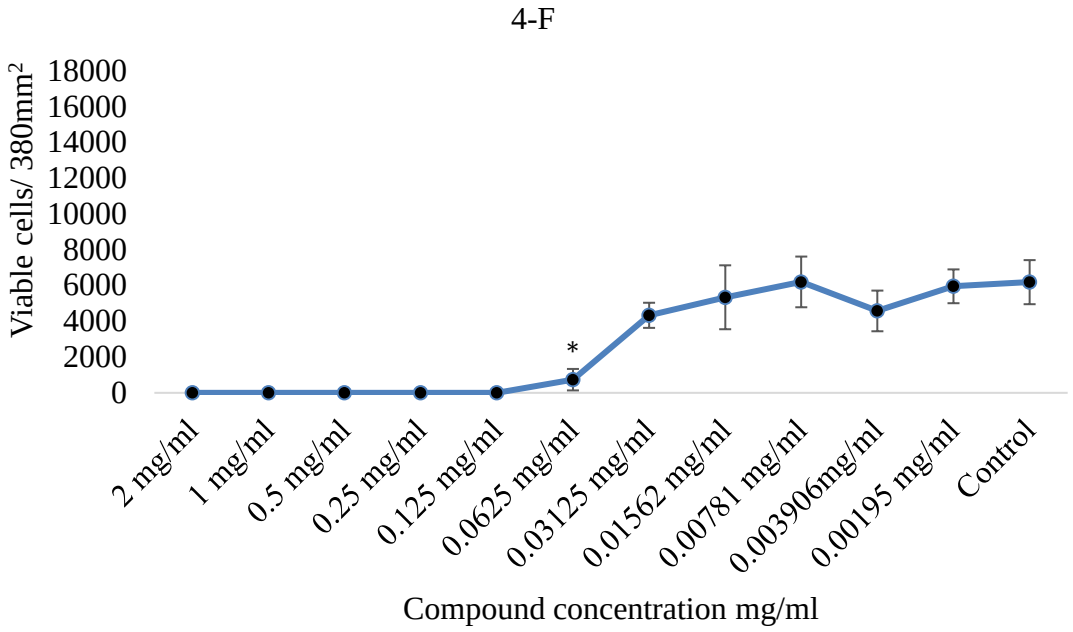

*Figure 15: Cell viability assay of 4-F on U-87MG glioblastoma cells. Cytotoxicity of the drug was measured by counting the number of cells per well for the 11 different concentrations and control. The error bars show the standard error, n =3 independent experiments. The lowest concentration significantly different from control is 0.0625mg/ml, $p \leq 0.05$ shown by *.*

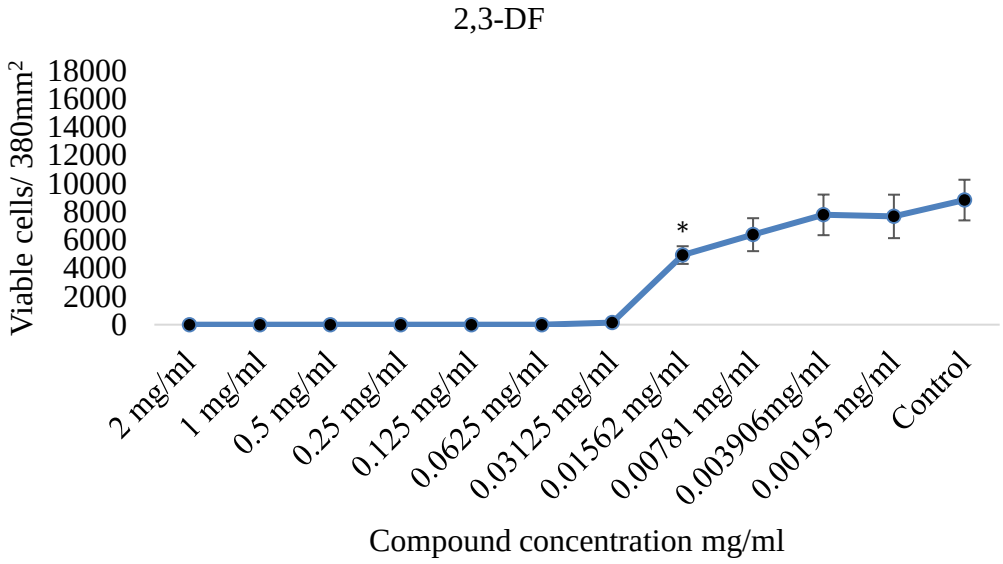

*Figure 16: Cell viability assay of 2,3-DF on U-87MG glioblastoma cells. Cytotoxicity of the drug was measured by counting the number of cells per well for the 11 different concentrations and control. The error bars show the standard error, n =3 independent experiments. The lowest concentration significantly different from control is 0.01562mg/ml, $p \leq 0.05$ shown by *.*

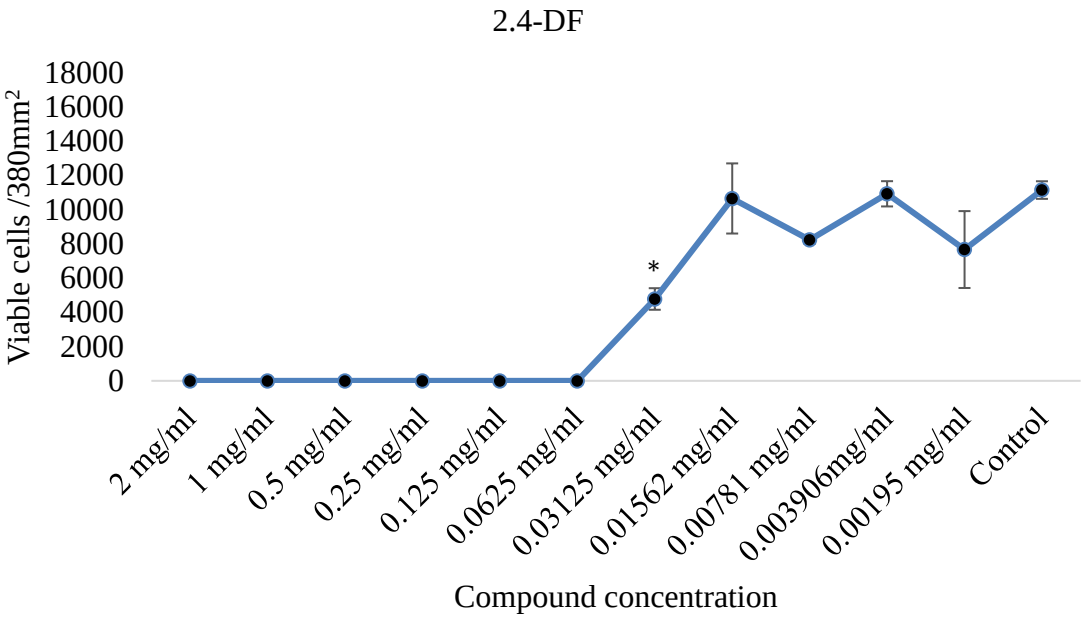

*Figure 17: Cell viability assay of 2,4-DF on U-87MG glioblastoma cells. Cytotoxicity of the drug was measured by counting the number of cells per well for the 11 different concentrations and control. The error bars show the standard error, n =3 independent experiments. The lowest concentration significantly different from control is 0.03125mg/ml, $p \leq 0.05$ shown by *.*

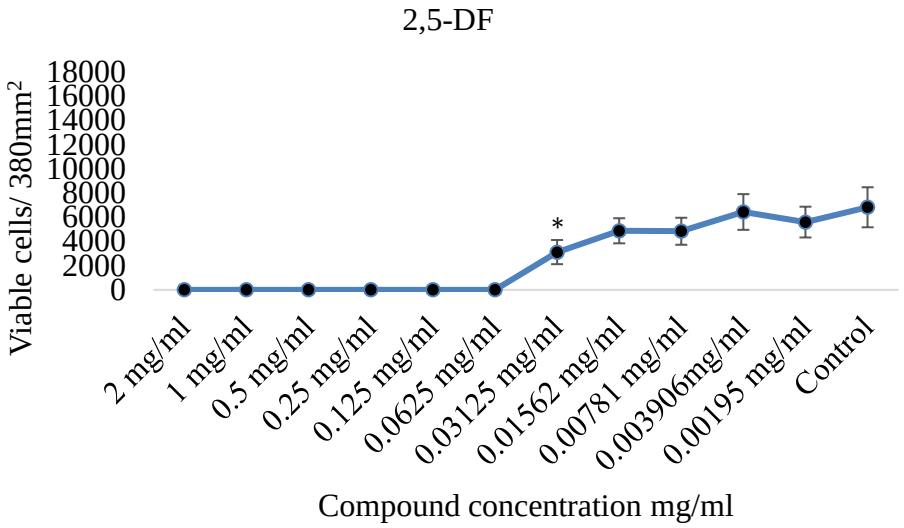

*Figure 18: Cell viability assay of 2,5-DF on U-87MG glioblastoma cells. Cytotoxicity of the drug was measured by counting the number of cells per well for the 11 different concentrations and control. The error bars show the standard error, n =3 independent experiments. The lowest concentration significantly different from control is 0.03125mg/ml, $p \leq 0.05$ shown by *.*

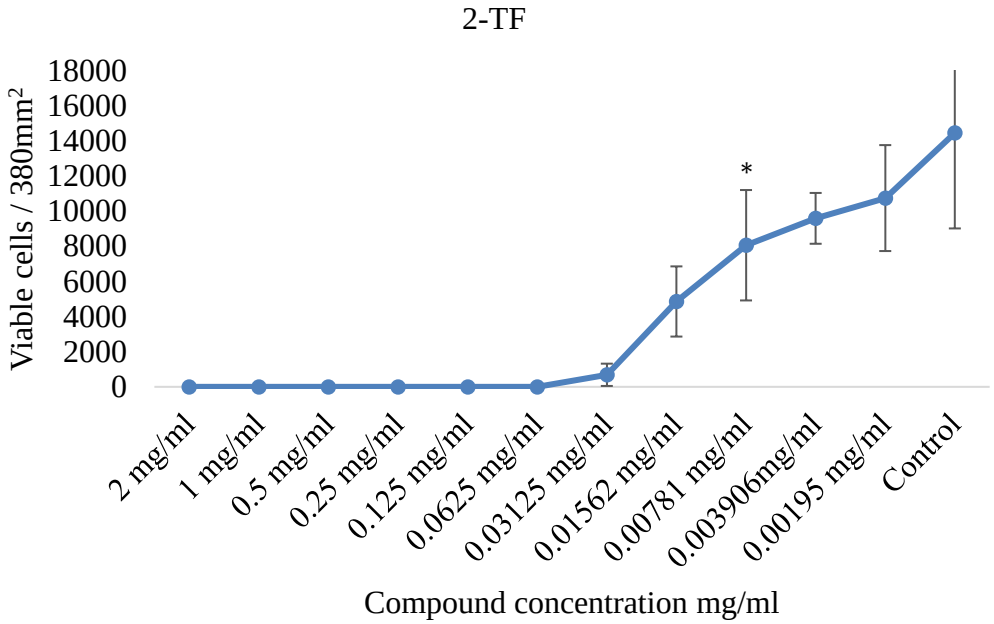

*Figure 19: Cell viability assay of 2-TF on U-87MG glioblastoma cells. Cytotoxicity of the drug was measured by counting the number of cells per well for the 11 different concentrations and control. The error bars show the standard error, n =3 independent experiments. The lowest concentration significantly different from control is 0.00781mg/ml, p≤ 0.05 shown by *.*

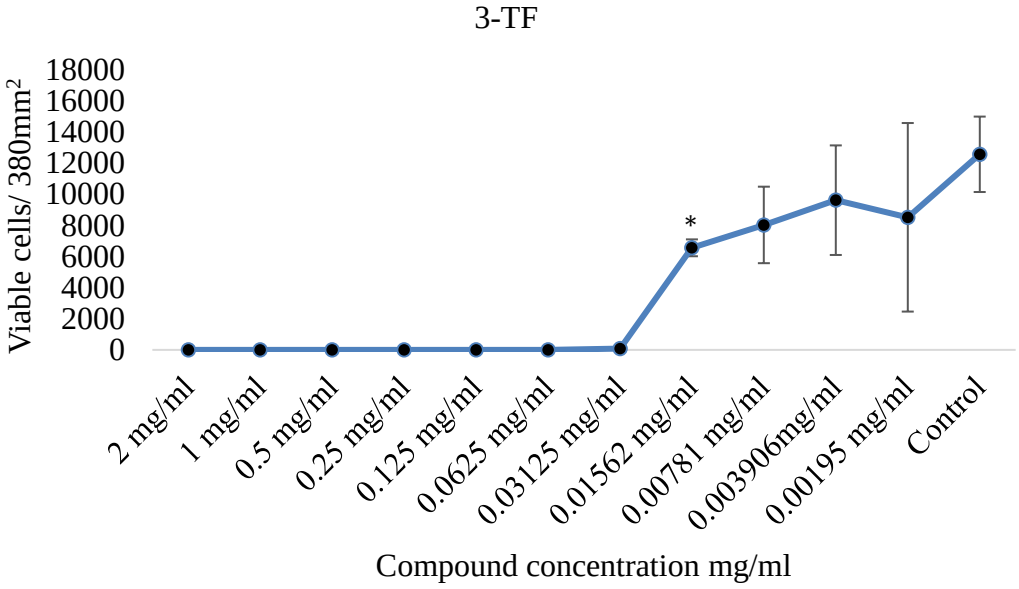

*Figure 20: Cell viability assay of 3-TF on U-87MG glioblastoma cells. Cytotoxicity of the drug was measured by counting the number of cells per well for the 11 different concentrations and control. The error bars show the standard error, n =3 independent experiments. The lowest concentration significantly different from control is 0.01562mg/ml, p≤ 0.05 shown by *.*

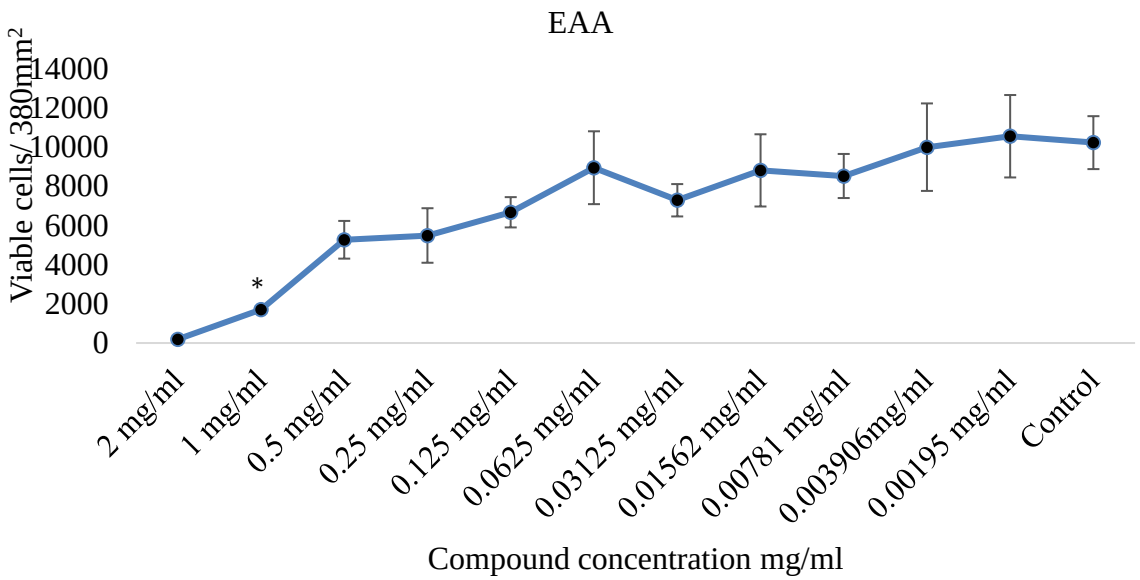

*Figure 21: Cell viability assay of EAA on U-87MG glioblastoma cells. Cytotoxicity of this starting material was measured by counting the number of cells per well for the 11 sdifferent concentrations and control. The error bars show the standard error, n =3 independent experiments. The lowest concentration significantly different from control is 1 mg/ml, $p \leq 0.05$ shown by *.*

Linear regression was used to calculate the LC_{50} of the novel dihydropyridines and the starting material (EAA). Table 2 shows the calculated values of the LC_{50}.

Table 2: LC_{50} values (μM) for the 14 compounds and EAA calculated through linear regression.

Compound	**LC_{50} mg/ml**	**LC_{50} µM**
2-TF	0.00550	13.84
3-TF	0.00757	19.04
4-F	0.00987	28
2-F	0.01253	50.89
3-F	0.01768	50.89
2,3-DF	0.01438	39.35
4-Cl	0.01954	42.32
3-Cl	0.02155	42.32
2,4-DF	0.02450	67.05
2,5-DF	0.02252	61.63
3-FPB	0.05625	150.71
4-FPB	0.05781	154.80
2-Q	0.05781	151.95
5-P	0.08875	267.82
EAA	0.2107	208.54

Figure 22-24 shows the average number of viable cells for the LC_{50} confirmation (n=9).

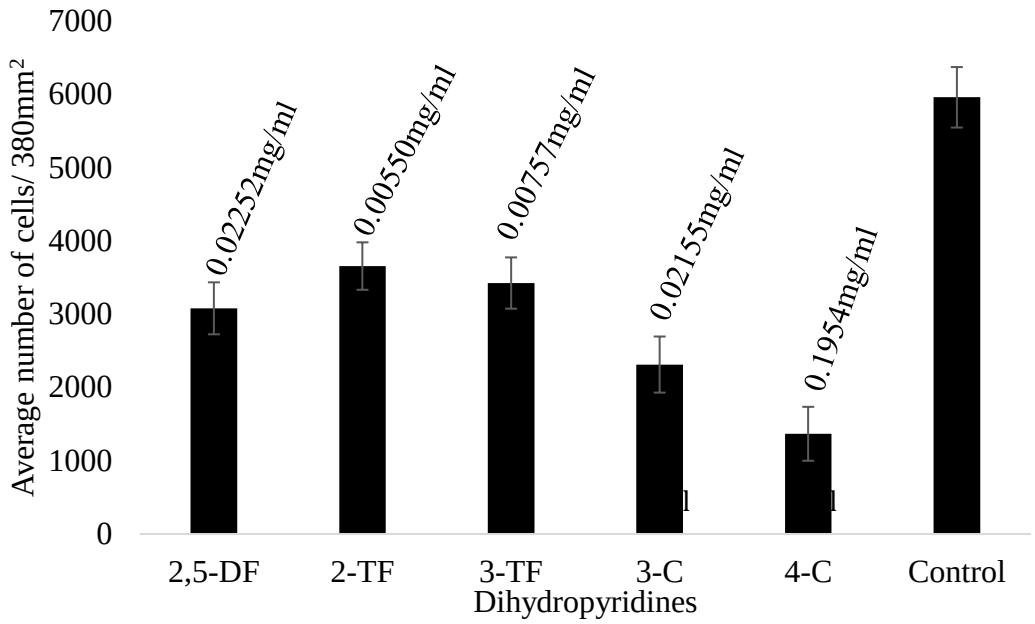

Figure 22: LC_{50} value confirmation through testing the cells with the LC_{50} concentration, n = 9. Error bars indicate standard error. 4-Cl has the average survival of 24% which is below 50 %.

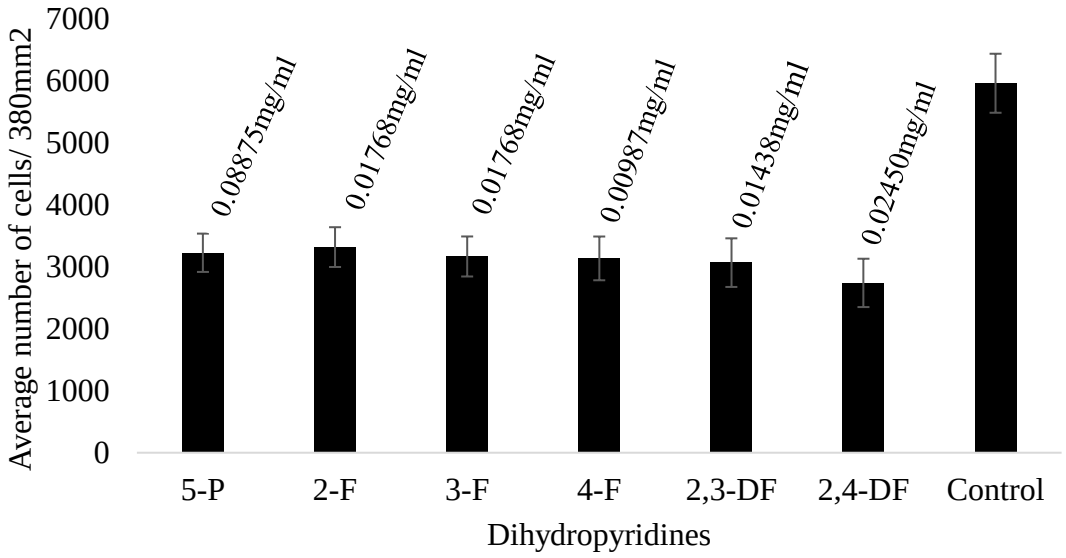

Figure 23: LC_{50} value confirmation through testing the cells with the LC_{50} concentration, n = 9. Error bars indicate standard error.

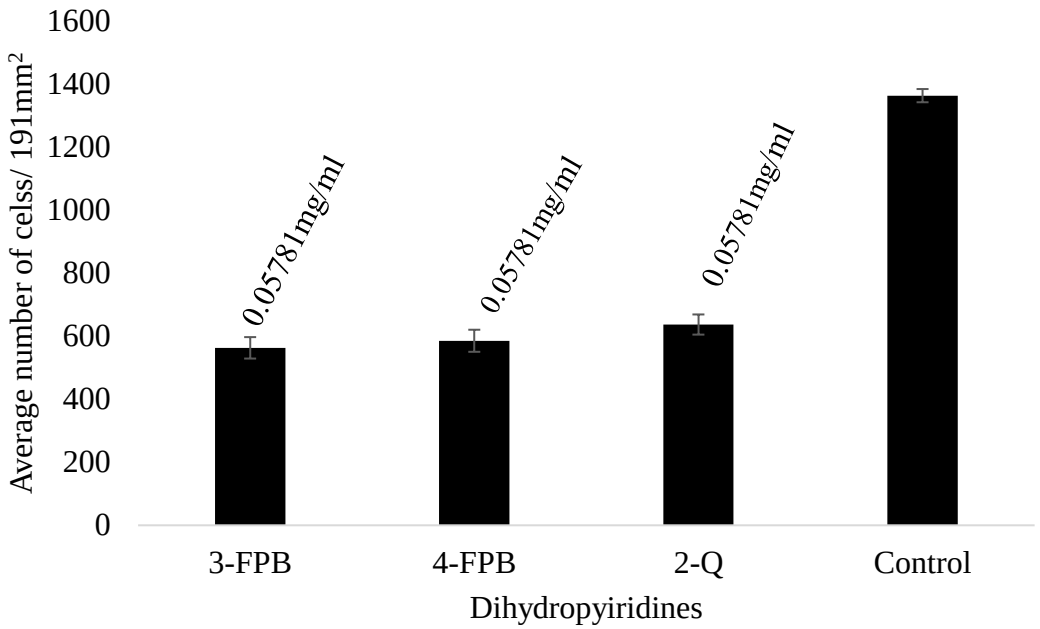

Figure 24: LC_{50} value confirmation through testing the cells with the LC_{50} concentration, n = 9. Error bars indicate standard error.

Discussion

The heteroaromatic dihydropyridines (2-Q and 5-P; figure 9 and 10) had the least potency compared to the rest of the compounds which had aromatic groups. Variability was also noticed within the substituted aromatic dihydropyridine group's activities. Contrary to speculation boronic acid pharmacophores were not as potent which leads to a conclusion that at least they are not compatible with dihydropyridines as hybrid compounds to treat glioblastoma cancer. Although the synthesis of dihydropyridines with boronic acids have been found in the literature, there is no information on these compound's biological activities making this research important for understanding the ability of dihydropyridine hybrid drugs to function as anti-cancer and/or anti-invasive drugs.

The hybrid dihydropyridines showed varied cytotoxicity effects on the glioblastoma cells which resulted in reduced numbers of viable cells after the drug was introduced. Eleven concentrations were used to establish the LC_{50} concentration which was used to identify compounds that had greater potency (lower concentration of LC_{50}) as well as provide the lowest tested concentration for each compound which would provide working concentrations to test other parameters such as phenotypic changes, neurosphere changes, cell mobility, and invasive potential.

The compounds that were tested had LC_{50} concentrations verified that ranged from 0.00550mg/ml-0.08875mg/ml. Further refinement of the LC_{50} concentration was needed for compound 4-Cl. The 11-concentration assay was modified by reducing the highest concentration to 0.5mg/ml from 2mg/ml. This changed the LC_{50} from 0.01945mg/ml to 0.0127mg/ml, which is a much lower and therefore a more promising LC_{50} for this compound. These LC_{50} values were comparable to those of cancer drugs that are FDA approved, especially temozolomide which had the LC_{50} more than 100µM (Holbeck et al., 2010). The published LC_{50} of cancer drugs showed that drugs containing boronic acid for example bortezomib had lower LC_{50} 3.6µM (Holbeck et al., 2010), which could be caused by the synergistic effects of the hybrid pharmacophores.

The starting material EAA was tested for its effect on cell viability resulting in a LC_{50} value of 208.54µM. This value was higher than the novel dihydropyridines except for compound 5-P indicating that this starting material is less inhibitory as compared to the synthesized drugs. The LC_{50} values showed that heteroaromatic substituted dihydropyridine compounds 2-Q and 5-P (151.95µM and 267.82µM) had the highest

concentration needed to kill 50% of the cells compared to the aromatic substituted dihydropyridines making these compounds less potent compared to the rest of the group.

The aromatic substituted dihydropyridines were more potent but within this group some variability was observed. The boronic acid substituted dihydropyridines 3-FPB and 4-FBP 0.05625mg/ml and 0.05781mg/ml (150.71µM and 154.80µM) were the least potent in this group. The published LC_{50} value of cancer drug bortezomib which has a boronic acid pharmacophore was 3.6µM which is very low compared to boronic acid containing hybrid dihydropyridines. It is possible that the addition of fluorine (bortezomib does not have fluorine) on the compound is causing a higher LC_{50} concentration is possible and needs exploration, but this seems unlikely as fluorine has been shown to enhance cytotoxicity. Boronic acid pharmacophores are known for drug delivery (Zhang et al., 2018) and have been shown to induce apoptosis and reduce autophagy. For example, bortezomib is one of the few glioblastoma drugs on the market (Zhang et al., 2014).

The electron withdrawing group substituted dihydropyridines were more potent with the trifluomethyl 2-TF and 3-TF having the lowest LC_{50} of 0.00550mg/ml and 0.00757mg.ml (13.84µM and 19.04µM) values followed by di-fluorides with LC_{50} values ranging from 0.00987mg/ml-0.01768mg/ml (28µM -50.89µM). The singly substituted fluoro- and chloro- compounds were within the same range. Incorporation of fluorine and chlorine in drugs has been shown to increase the potency of the compounds by increasing cytotoxicity through DNA fragmentation (Ren et al., 1998) and inducing apoptosis (Cattaneo-Pangrazzi et al., 2000). The data shows that the compounds reduced the viability of U-87 MG cells, therefore, I do not reject the hypothesis. The data

however does not indicate the mode of action for these drugs. Further investigations need to be performed to establish the mode of action such as an activated caspase ELISA which would indicate if the drugs are activating apoptosis which is one of the main hallmarks of cancer. More experiments were carried out to investigate the effects of the compounds on glioblastoma by utilizing the concentration that resembled control to test whether the compounds affected cell mobility as well as their ability to invade.

Scratch Assay

This assay was performed to test the effects of novel dihydropyridines on the motility of U-87MG glioblastoma cancer cells. This characteristic could impact the ability of these cells to invade as migration is part of the process involved in cancer cell invasion. The lowest drug concentration used in the cell viability assay (0.00195mg/ml) was used to test for this variable. The following compounds were tested: 2-TF; 3-TF; 3-Cl; 4-Cl; 2-F; 3-F; 4-F; 2,3-DF; 2,4-DF; 2,5-DF. These compounds were selected for their lower LC_{50} concentrations.

Experimental Procedure

U-87MG glioblastoma cells were used to perform this experiment. 100,000 cells were introduced into 60 mm cell culture dishes (Falcon) and allowed to grow to full confluency. These cells were maintained with 3 ml of minimum essential media in a humidified 37 °C and 5% carbon dioxide incubator until they reached full confluency.

Media was removed and 3 ml novel dihydropyridines at 0.00195mg/ml concentration diluted in media were introduced to the dishes. Using a sterile toothpick, a

scratch was made at the bottom of the well and pictures taken under the microscope to note the cell filling of the scratch. Pictures were taken on three consecutive days to compare cell filling of the scratch in compound treated dishes compared to control dishes.

Results

The scratch assay helped establish the effects of the drugs on cell filling of the scratch. No difference was noted in cell filling between all compound tested cells and control. Figure 25 is a representative example of the cell filling for all compounds tested.

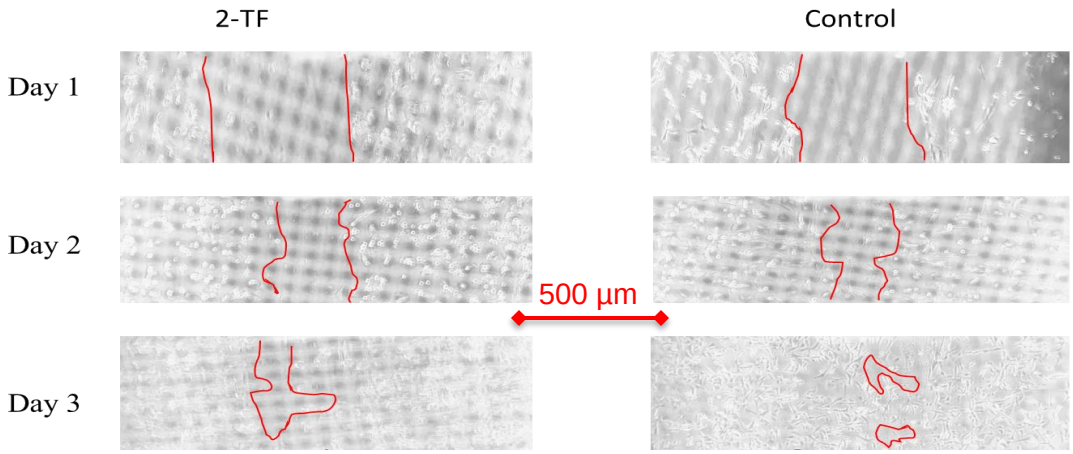

Figure 25: Scratch assay photos taken on consecutive days after introduction of compounds to cells, magnification 100X. The marked places show the area of the scratch. Compound 2-TF is shown as a representative all compounds tested.

Discussion

The results for the scratch assay showed no differences in cell filling of the scratch between the untreated cells (control) and the hybrid dihydropyridine treated cells for all the tested compounds. These results suggest that the novel hybrid compounds have no effect on cell movement. I therefore reject my hypothesis that the novel

dihydropyridines would reduce the motility of the glioblastoma cells therefore reducing their ability to invade new tissue. The compounds may have no effect on ADAM proteins which are involved in motility (Nakamura et al. 2004), which could be determined by further experiments such as ELISA and/or western blots.

The lack of noticeable differences may have been caused by the low concentration of the drugs used. An increased concentration of the compounds could have an effect on the migration and should be examined. Another possible reason for the lack of differences between the treatment and control could be the time intervals. The cells were photographed every 24 hours which could have been too long to notice any difference. Reducing this interval may show differences.

Invasion Assay

The novel dihydropyridines were screened for their effects on the invasiveness of U-87MG glioblastoma cells. One of the main steps towards invasion is the ability for cells to cross the basement membrane as they migrate away from the primary tumor. A drug that reduces this ability has great potential for reducing invasion in glioblastoma cancer after surgical removal of the cancer. The specific compounds used for this procedure were 2-TF; 3-TF; 2-F; 3-F; 4-F and were selected for their low LC_{50} concentrations.

Experimental Procedure

The experiment was performed using the Cell Invasion Assay Kit and protocol (Cell Biolabs CytoSelect), which is a 24-well plate consisting of inner Boyden chambers

with the basement membrane bases. The invasion chamber with the basement membrane inserts was warmed up to room temperature and rehydrated using serum free MEM media. 50,000 cells were added in serum free MEM media containing novel dihydropyridines at the concentration of 0.00195mg/ml. In the outer chamber MEM media containing fetal bovine serum (10%) was added to encourage cells to migrate. The plates were incubated for 24 hours in a humidified, 37 °C, 5% carbon dioxide incubator. After incubation, the media was removed from the Boyden chamber and using cotton-tipped swabs the noninvasive cells were removed from the inside of the Boyden chamber. The basement membrane of the Boyden chamber was stained. Cells that passed through the membrane were stained dark purple and were counted under the microscope (Cell Biolabs CytoSelect).

Results

Figure 26 shows the average number of cells that passed through the basement membrane of the invasion chamber. These results were obtained from an average of two well cell count in 3 independent experimental trials.

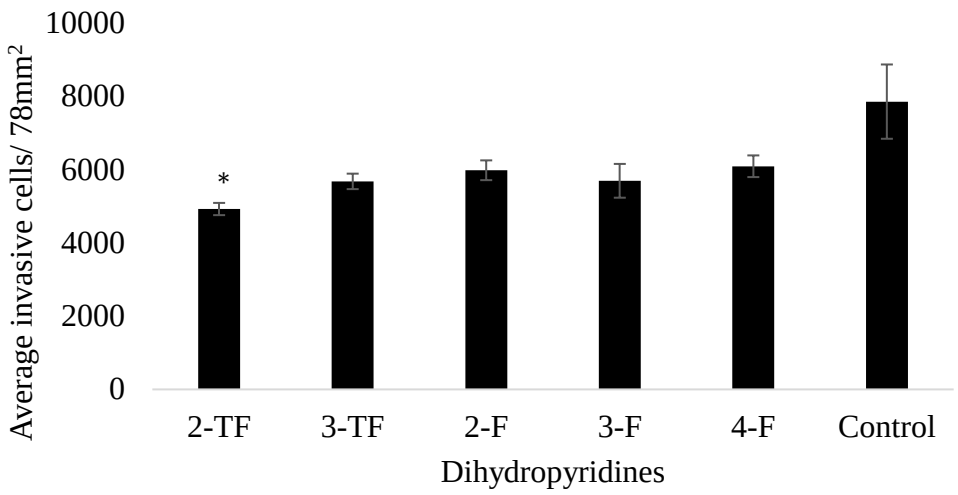

Figure 26: The effects of substituted aromatic novel dihydropyridines on cell invasion in U-87MG glioblastoma cells. 2-TF is the only one statistically significant from the control $p \leq 0.05$ (ANOVA and Post hoc). The error bars indicate standard error, n = 3 independent experiments using an average of two wells in each experiment.

Cell treated by 2-TF compound had a statistically significant reduction in number of invasive cells when compared to the control. The remaining compounds had no statistical difference when compared to control.

Discussion

The treated cells were able to invade the basement membrane with only the 2-TF treated cells showing significant reduction in invasiveness. I therefore reject the hypothesis that the novel dihydropyridines would reduce the rate of invasion on glioblastoma cells except for 2-TF. The drug lercanidipine, a dihydropyridine has also been shown to reduce MMP-2 activity which is one of the proteins involved in invasion (Martinez et al., 2008). The compound 2-TF may be using the same mechanism to reduce invasion.

These results, however, support the scratch test results in which the compound-treated cells were mobile and able to fill the scratch the same as the control. More verification assays may be performed in the future, for example, the use of the modified U-87MG cells that are selective for invasion (Lu et al., 2004) will be necessary to perform these experiments. The results showed only 2-TF having anti-invasive properties, which will be necessary to investigate its effects on invasion proteins such as MMP-2 and MMP-9 to give more insight on its targets.

Neurosphere Assay

Neurospheres are noticeable *in vitro* and they may have an effect in the formation of new tumors. The dihydropyridines synthesized may have effects on neurosphere development, size and number which could be a therapeutic target to reduce the risk of recurrence in glioblastoma.

Experimental Procedure

The experiment was performed following an assay developed by Dr. D. Smith. 5000 cells per well were introduced into a 24-well plate and incubated in a humidified 37 °C, 5% carbon dioxide incubator for 24 hours. Compounds were used at the LC_{50} concentration and at 0.00195mg/ml which is the lowest hybrid drug concentration used in the viability assay (3 drugs per plate plus a control). The cells were incubated for 24 hours and the wells for day 1 (2 wells per compound LC_{50} concentration and 0.00195mg/ml concentration as well as 1 well for control) were fixed using methanol for five minutes and stained for five minutes using crystal violet. Excess stain was removed

by washing with water. The plates were incubated for additional 48 hours and the wells for day 3 were fixed, stained and washed as above, then an additional 48-hour incubation for day 6 followed by fixing, staining and washing as above. The number of neurospheres formed was counted, and the sizes estimated. Morphological features in terms of neurosphere size and number were observed.

Results

The neurospheres were observed for size and presence in a qualitative data collection. Table 3 shows the total number of neurospheres for 3 independent experimental set ups was recorded. The neurospheres were described as small (S), for starting to develop with a lot of U-87MG cells gathering around and large (L) for already developed with a solid material at the center and U-87MG cells protruding from the neurosphere or a lot of circular cells grouped together (Fig. 27).

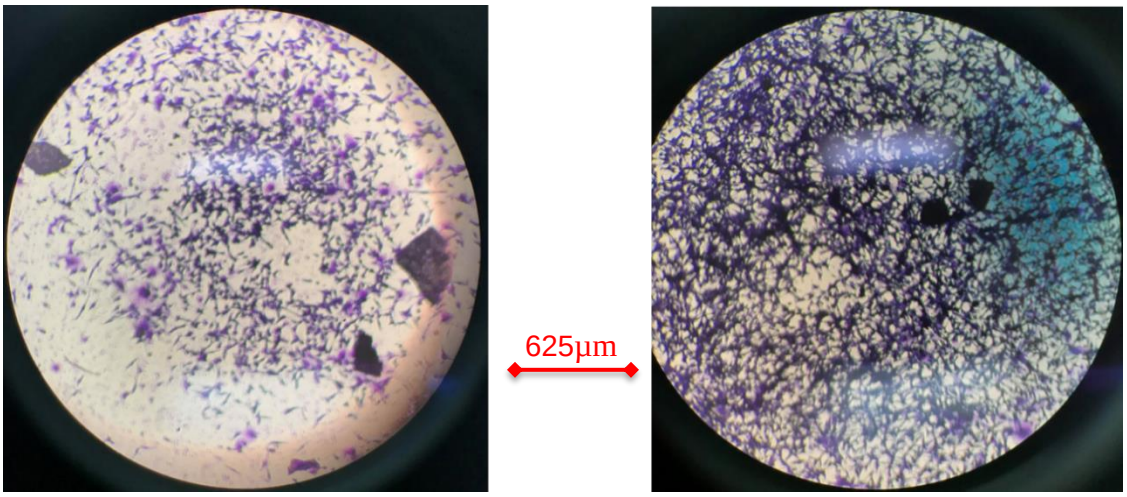

Figure 27: Images of neurospheres with the small starting (S) on the left and a large neurosphere (L) on the right.

Table 3: Total number of neurosphere counted and their sizes, n = 3.

Compound		Day 1	Day 3	Day 6
3-FPB	**0.00195**	3S	5S	3 L
	LC_{50}	0	1S	2 S
4-FPB	**0.00195**	1L, 1 S	2 S, 1 L	2 L, 4 S
	LC_{50}	1 S	0	1 S
2-Q	**0.00195**	1 S	2 S, 1 L	2 L, 2 S
	LC_{50}	1 S	1 S	1 S, 1 L
Control		2 S	2 S, 1L	3 S, 4 L

Compound		Day 1	Day 3	Day 6
5-P	**0.00195**	2 S	3 S, 1 L	5 S, 3 L
	LC_{50}	3S	3 S	1 S, 4 L
2-F	**0.00195**	2 S	2 S, 2 L	3 L
	LC_{50}	1 S	2 S	1 S, 2 L
3-F	**0.00195**	2 S	3 S	6 S
	LC_{50}	1 S	3 S	3 S, 3 L
Control		3 S	2 S, 3 L	4 S, 2 L

Compound		Day 1	Day 3	Day 6
4-F	**0.00195**	2 S	3 S	3 L
	LC_{50}	2 S	3 S	2 S, 2 L
2,3- DF	**0.00195**	3 S	2 S	2 S, 3 L

	LC_{50}	1 S	2 S	2 S, 3 L
2,4-DF	**0.00195**	2 S	2 S, 2 L	2 S,2 L
	LC_{50}	0	0	2 S
Control		6 S	3 S, 2 L	3 S, 3 L
[redacted]				

Compound	Day 1	Day 3	Day 6

2,5-DF	**0.00195**	2 S	3 S	3 L
	LC_{50}	0	2 S	2 S, 1 L
2-TF	**0.00195**	2 S	3 L, 1 S	1 S, 3 L
	LC_{50}	2 S	3 S	1 S, 3 L
3-TF	**0.00195**	2 S	3 S	2 S, 2 L
	LC_{50}	1 S	2 S	2 L
Control		3 S	3 S, 2 L	1 S, 3 L
[redacted]				

3-Cl	**0.00195**	3 S	2 S, 1 L	3 L
	LC_{50}	0	1 S	2 S
4-Cl	**0.00195**	3 S	3 S, 1 L	3 L
	LC_{50}	0	0	0
Control		3 S	3 L	2 S, 3 L

Substituted boronic acid compounds 3-FPB and 4-FPB gave a large number of neurospheres higher than control at concentration 0.00195 mg/ml for days 1 and 3 and had lower neurospheres at LC_{50} concentration. The substituted heteroaromatics (2-Q and 5-P) developed neurospheres at both concentrations. The substituents fluorine and chlorines also developed neurospheres at concentration 0.00195 mg/ml and did not have many neurospheres at the LC_{50} concentration and in most cases the LC_{50} concentration resulted in delayed onset of neurospheres.

Discussion

The introduction of drugs did not terminate the development of neurospheres, even at the LC_{50} concentration. However, neurospheres from day one and day three were small and still developing with normal U-87MG cell morphology which seemed to indicate the compounds did slow development down. Day six neurospheres, however, presented as a large circle in the middle with cells protruding from them. The compounds at LC_{50} concentration reduced the number, the size or the onset of neurospheres depending on the drug used. Temozolomide and carmustine cancer drugs have been shown to block neurosphere formation (Mihaliak et al. 2010).

Substituted boronic acid compounds 3-FPB and 4-FPB presented a large number of neurospheres at the 0.00195 mg/ml concentration and appeared much like control while the LC_{50} concentration did seem to delay formation which suggest an inhibitory role in neurosphere formation.

Compounds 3-Cl, 4-Cl, 2,4-DF and 2,5-DF showed low numbers in neurosphere development at the LC_{50} concentration, which is what was expected of all the drugs.

These compounds may have an effect on reducing neurosphere formation which could have a positive effect towards treating glioblastoma. Further investigations may need to be performed using selective neurosphere models to see the mode of action and results. Of all compounds tested, 4-Cl was the most promising for impacting development of neurospheres.

The substituted heterocyclic dihydropyridines 2-Q and 5-P had neurospheres developing from day one in both the concentrations, although small. Quinolone derivatives have been shown to reduce the formation of neurospheres in glioblastoma (Kwak et al., 2018), contrary to 2-Q, which had as many neurospheres as the control between the 2 concentrations. Available literature has yet to present the effects of dihydropyridines on neurospheres.

Although most of the drugs tested had neurospheres developing when introduced to the cells, a more robust assay could be used to test the effects of the drugs on already developed neurospheres (Galli et al., 2004). Some of the targets for neurosphere development may be tested in the future, for example, mitochondrial proteins (Jung et al. 2018) and neurosphere kinase enzyme (Wilson et al. 2016).

CHAPTER 4

CONCLUSION

The synthesis of substituted aromatic and substituted heteroaromatic novel hybrid dihydropyridines using the classic Hantzsch reaction was possible with the use of boric acid as a catalyst and water/ethanol as a solvent. The substituted styrl group was not successfully synthesized as a result of unavailability of cinnamaldehydes commercially and the impracticality of the products formed because of the heavy pigmentation and stickiness of the products.

Cheminformatics was used to predict the biological activities of the synthesized drugs, which showed all the compounds to be lipophilic, hydrophobic and passable according to Lipinski's rules of oral bioavailability. These predictions also suggested that the synthesized dihydropyridines may pass through the blood-brain barrier which would be necessary when treating glioblastoma.

The cell viability assay established the LC_{50} of the compounds, a pharmacological value needed when investigating the toxicity of a drug. This assay also helped establish the highest concentration which the cells were growing the same as control, which in this case turned out to be 0.00195 mg/ml for all the synthesized and tested (14 compounds) dihydropyridine compounds. This concentration was used in invasion, scratch and neurosphere assays which investigated the effects of synthesized compounds on cells phenotypically, not just their toxicity.

One of the major objectives of this project was to investigate the effects of the synthesized dihydropyridines on glioblastoma invasion. The compounds (2-TF, 3-TF, 2-F, 3-F, and 4-F) were used to test invasion as they had the lowest LC_{50} concentration. This investigation showed 2-TF to have effects on invasion as it had significantly lower invasive cell numbers when compared to the control. The rest of the tested compounds although they had lower numbers, they did not significantly reduce invasion. These results support the scratch assay in which all the drugs seemed to affect cell proliferation to the same extent as control. This assay can be improved though to provide quantifiable data, which would be useful in performing statistical analysis.

The 2-TF compound appears to be effective in all the assays, with the lowest LC_{50} value showing that it had high cytotoxicity effects, lowered the invasion significantly and had lower number of neurospheres developing when treated with 0.00195 mg/ml concentration and close to none when treated with LC_{50}. There is a need to further investigate the effects of this compound at a molecular level to identify molecular targets.

When U-87MG cells were treated with LC_{50} concentration of 3-Cl and 4-CL compounds during neurosphere assay, there was nearly no neurosphere developing. These two compounds would be good candidates for further investigations targeting proteins involved in neurosphere development.

Although most of the compounds, did not show effects on reducing invasion, they showed cytotoxicity effects through the cell viability test. Further investigation into the mode of action of the drugs to establish their molecular targets should be investigated further. Novel hybrid dihydropyridines have a cytotoxicity effect on U-87MG

glioblastoma cells and have a great potential of being used in the future after further research.

REFERENCES

Berube G. 2016. An overview of molecular hybrids in drug discovery. Expert Opin Drug Discov. 11(3):281-305.

Bray F, Ferlay J, Soerjomataram I, Siegel RL, Torre LA, Jemal A. 2018. Global cancer statistics 2018: Globocan estimates of incidence and mortality worldwide for 36 cancers in 185 countries. CA: a cancer journal for clinicians. 68(6):394-424.

Castro BA, Aghi MK. 2014. Bevacizumab for glioblastoma: Current indications, surgical implications, and future directions. Neurosurgical focus. 37(6):E9.

Cattaneo-Pangrazzi RM, Schott H, Wunderli-Allenspach H, Rothen-Rutishauser B, Guenthert M, Schwendener RA. 2000. Cell-cycle arrest and p53-independent induction of apoptosis in vitro by the new anticancer drugs 5-fdurd-p-fdcydoct and dcydpam-p-fdurd in du-145 human prostate cancer cells. J Cancer Res Clin Oncol. 126(5):247-256.

Cavalli A, Bolognesi ML. 2009. Neglected tropical diseases: Multi-target-directed ligands in the search for novel lead candidates against trypanosoma and leishmania. J Med Chem. 52(23):7339-7359.

Chang L, Zhao D, Liu HB, Wang QS, Zhang P, Li CL, Du WZ, Wang HJ, Liu X, Zhang ZR. 2015. Activation of sonic hedgehog signaling enhances cell migration and invasion by induction of matrix metalloproteinase-2 and-9 via the phosphoinositide-3 kinase/akt signaling pathway in glioblastoma corrigendum in/mmr/12/5/7815. Molecular medicine reports. 12(5):6702-6710.

Da Fonseca CO, Simao M, Lins IR, Caetano RO, Futuro D, Quirico-Santos T. 2011. Efficacy of monoterpene perillyl alcohol upon survival rate of patients with recurrent glioblastoma. Journal of cancer research and clinical oncology. 137(2):287-293.

Demirayak S, Kayagil I, Yurttas L. 2011. Microwave supported synthesis of some novel 1, 3-diarylpyrazino [1, 2-a] benzimidazole derivatives and investigation of their anticancer activities. European journal of medicinal chemistry. 46(1):411-416.

Demuth T, Berens ME. 2004. Molecular mechanisms of glioma cell migration and invasion. Journal of neuro-oncology. 70(2):217-228.

Egeblad M, Werb Z. 2002. New functions for the matrix metalloproteinases in cancer progression. Nature reviews cancer. 2(3):161.

Firuzi O, Javidnia K, Mansourabadi E, Saso L, Mehdipour AR, Miri R. 2013. Reversal of multidrug resistance in cancer cells by novel asymmetrical 1,4-dihydropyridines. Archives of pharmacal research. 36(11):1392-1402.

Gallego O. 2015. Nonsurgical treatment of recurrent glioblastoma. Current oncology. 22(4):e273.

Galli R, Binda E, Orfanelli U, Cipelletti B, Gritti A, De Vitis S, Fiocco R, Foroni C, Dimeco F, Vescovi A. 2004. Isolation and characterization of tumorigenic, stem-like neural precursors from human glioblastoma. Cancer research. 64(19):7011-7021.

Gandalovičová A, Rosel D, Fernandes M, Veselý P, Heneberg P, Čermák V, Petruželka L, Kumar S, Sanz-Moreno V, Brábek J. 2017. Migrastatics—anti-metastatic and anti-invasion drugs: Promises and challenges. Trends in cancer. 3(6):391-406.

Gediya LK, Njar VC. 2009. Promise and challenges in drug discovery and development of hybrid anticancer drugs. Expert opinion on drug discovery. 4(11):1099-1111.

Giese A, Bjerkvig R, Berens M, Westphal M. 2003. Cost of migration: Invasion of malignant gliomas and implications for treatment. Journal of clinical oncology. 21(8):1624-1636.

Gilbert CA, Ross AH. 2009. Cancer stem cells: Cell culture, markers and targets for new therapies. Journal of cellular biochemistry. 108(5):1031-1038.

Holbeck SL, Collins JM, Doroshow JH. 2010. Analysis of food and drug administration-approved anticancer agents in the nci60 panel of human tumor cell lines. Molecular cancer therapeutics. 9(5):1451-1460.

Huang H, Hara A, Homma T, Yonekawa Y, Ohgaki H. 2005. Altered expression of immune defense genes in pilocytic astrocytomas. Journal of Neuropathology & Experimental Neurology. 64(10):891-901.

Issa F, Kassiou M, Rendina LM. 2011. Boron in drug discovery: Carboranes as unique pharmacophores in biologically active compounds. Chemical reviews. 111(9):5701-5722.

Jung N, Kwon HJ, Jung HJ. 2018. Downregulation of mitochondrial uqcrb inhibits cancer stem cell-like properties in glioblastoma. International journal of oncology. 52(1):241-251.

Kaplan MS, Hinds JW. 1977. Neurogenesis in the adult rat: Electron microscopic analysis of light radioautographs. Science. 197(4308):1092-1094.

Kim S-S, Pirollo KF, Chang EH. 2015. Isolation and culturing of glioma cancer stem cells. Current protocols in cell biology / editorial board, Juan S Bonifacino [et al]. 67:23.10.21-23.10.10.

Kleihues P, Ohgaki H. 1999. Primary and secondary glioblastomas: From concept to clinical diagnosis. Neuro-oncology. 1(1):44-51.

Kodama T, Ikeda E, Okada A, Ohtsuka T, Shimoda M, Shiomi T, Yoshida K, Nakada M, Ohuchi E, Okada Y. 2004. Adam12 is selectively overexpressed in human glioblastomas and is associated with glioblastoma cell proliferation and shedding of heparin-binding epidermal growth factor. The American journal of pathology. 165(5):1743-1753.

Kong D-X, Li X-J, Zhang H-Y. 2009. Where is the hope for drug discovery? Let history tell the future. Drug discovery today. 14(3-4):115-119.

Kwak SH, Shin S, Lee JH, Shim JK, Kim M, Lee SD, Lee A, Bae J, Park JH, Abdelrahman A et al. 2018. Synthesis and structure-activity relationships of quinolinone and quinoline-based p2x7 receptor antagonists and their anti-sphere formation activities in glioblastoma cells. European journal of medicinal chemistry. 151:462-481.

Lara-Velazquez M, Al-Kharboosh R, Jeanneret S, Vazquez-Ramos C, Mahato D, Tavanaiepour D, Rahmathulla G, Quinones-Hinojosa A. 2017. Advances in brain tumor surgery for glioblastoma in adults. Brain sciences. 7(12):166.

Lashinger LM, Zhu K, Williams SA, Shrader M, Dinney CP, McConkey DJ. 2005. Bortezomib abolishes tumor necrosis factor-related apoptosis-inducing ligand resistance via a p21-dependent mechanism in human bladder and prostate cancer cells. Cancer research. 65(11):4902-4908.

Lu KV, Jong KA, Rajasekaran AK, Cloughesy TF, Mischel PS. 2004. Upregulation of tissue inhibitor of metalloproteinases (timp)-2 promotes matrix metalloproteinase (mmp)-2 activation and cell invasion in a human glioblastoma cell line. Laboratory investigation. 84(1):8.

Martinez ML, Rizzi E, Castro MM, Fernandes K, Bendhack LM, Gerlach RF, Tanus-Santos JE. 2008. Lercanidipine decreases vascular matrix metalloproteinase-2 activity and protects against vascular dysfunction in diabetic rats. European journal of pharmacology. 599(1-3):110-116.

Meunier B. 2008. Hybrid molecules with a dual mode of action: Dream or reality? Accounts of chemical research. 41(1):69-77.

Micheal B. 2017. Design of hybrid molecules for drug development.

Mihaliak, A. M., Gilbert, C. A., Li, L., Daou, M. C., Moser, R. P., Reeves, A.,Ross, A. H. (2010). Clinically relevant doses of chemotherapy agents reversibly block formation of glioblastoma neurospheres. *Cancer letters*, *296*(2), 168–177. doi:10.1016/j.canlet.2010.04.005

Morgan E, Norman A, Laing K, Seal M. 2017. Treatment and outcomes for glioblastoma in elderly compared with non-elderly patients: A population-based study. Current Oncology. 24(2):e92.

Muregi FW, Ishih A. 2010. Next-generation antimalarial drugs: Hybrid molecules as a new strategy in drug design. Drug Development Research. 71(1):20-32.

Nakamura H, Suenaga N, Taniwaki K, Matsuki H, Yonezawa K, Fujii M, Okada Y, Seiki M. 2004. Constitutive and induced cd44 shedding by adam-like proteases and membrane-type 1 matrix metalloproteinase. Cancer research. 64(3):876-882.

Naziroglu M, Cig B, Blum W, Vizler C, Buhala A, Marton A, Katona R, Josvay K, Schwaller B, Olah Z et al. 2017. Targeting breast cancer cells by mrs1477, a positive allosteric modulator of trpv1 channels. PLoS One. 12(6):e0179950.

Niklasson M, Maddalo G, Sramkova Z, Mutlu E, Wee S, Sekyrova P, Schmidt L, Fritz N, Dehnisch I, Kyriatzis G et al. 2017. Membrane-depolarizing channel blockers induce selective glioma cell death by impairing nutrient transport and unfolded protein/amino acid responses. Cancer research. 77(7):1741-1752.

Ohgaki H, Dessen P, Jourde B, Horstmann S, Nishikawa T, Di Patre P-L, Burkhard C, Schüler D, Probst-Hensch NM, Maiorka PC. 2004. Genetic pathways to glioblastoma: A population-based study. Cancer research. 64(19):6892-6899.

Paris D, Bachmeier C, Patel N, Quadros A, Volmar C-H, Laporte V, Ganey J, Beaulieu-Abdelahad D, Ait-Ghezala G, Crawford F et al. 2011. Selective antihypertensive dihydropyridines lower aβ accumulation by targeting both the production and the clearance of aβ across the blood-brain barrier. Molecular Medicine. 17(3-4):149-162.

Pastrana E, Silva-Vargas V, Doetsch F. 2011. Eyes wide open: A critical review of sphere-formation as an assay for stem cells. Cell stem cell. 8(5):486-498.

Ramachandran RK, Sørensen MD, Aaberg-Jessen C, Hermansen SK, Kristensen BW. 2017. Expression and prognostic impact of matrix metalloproteinase-2 (mmp-2) in astrocytomas. PLoS One. 12(2):e0172234.

Ramsay RR, Popovic-Nikolic MR, Nikolic K, Uliassi E, Bolognesi ML. 2018. A perspective on multi-target drug discovery and design for complex diseases. Clinical and Translational Medicine. 7:3.

Ren Q, Kao V, Grem JL. 1998. Cytotoxicity and DNA fragmentation associated with sequential gemcitabine and 5-fluoro-2'-deoxyuridine in ht-29 colon cancer cells. Clinical cancer research : an official journal of the American Association for Cancer Research. 4(11):2811-2818.

Reynolds BA, Tetzlaff W, Weiss S. 1992. A multipotent egf-responsive striatal embryonic progenitor cell produces neurons and astrocytes. Journal of Neuroscience. 12(11):4565-4574.

Reynolds BA, Weiss S. 1992. Generation of neurons and astrocytes from isolated cells of the adult mammalian central nervous system. science. 255(5052):1707-1710.

Ritz B, Rhodes SL, Qian L, Schernhammer E, Olsen JH, Friis S. 2010. L-type calcium channel blockers and parkinson disease in denmark. Annals of neurology. 67(5):600-606.

Sarkar S, Nuttall RK, Liu S, Edwards DR, Yong VW. 2006. Tenascin-c stimulates glioma cell invasion through matrix metalloproteinase-12. Cancer research. 66(24):11771-11780.

Scarano W, Duong HT, Lu H, De Souza PL, Stenzel MH. 2013. Folate conjugation to polymeric micelles via boronic acid ester to deliver platinum drugs to ovarian cancer cell lines. Biomacromolecules. 14(4):962-975.

Scotti L, Mendonca Junior FJ, Ishiki HM, Ribeiro FF, Singla RK, Barbosa Filho JM, Da Silva MS, Scotti MT. 2017. Docking studies for multi-target drugs. Current drug targets. 18(5):592-604.

Stupp R, Mason WP, Van Den Bent MJ, Weller M, Fisher B, Taphoorn MJ, Belanger K, Brandes AA, Marosi C, Bogdahn U. 2005. Radiotherapy plus concomitant and adjuvant temozolomide for glioblastoma. New England Journal of Medicine. 352(10):987-996.

Takamune Y, Ikebe T, Nagano O, Shinohara M. 2008. Involvement of nf-κb-mediated maturation of adam-17 in the invasion of oral squamous cell carcinoma. Biochemical and biophysical research communications. 365(2):393-398.

Velena A, Zarkovic N, Gall Troselj K, Bisenieks E, Krauze A, Poikans J, Duburs G. 2016. 1,4-dihydropyridine derivatives: Dihydronicotinamide analogues-model compounds targeting oxidative stress. Oxid Med Cell Longev. 2016:1892412-1892412.

Verkhratsky A, Butt A. 2013. Glial physiology and pathophysiology. John Wiley & Sons.

Wilson TJ, Zamler DB, Doherty R, Castro MG, Lowenstein PR. 2016. Reversibility of glioma stem cells' phenotypes explains their complex in vitro and in vivo

behavior: Discovery of a novel neurosphere-specific enzyme, cgmp-dependent protein kinase 1, using the genomic landscape of human glioma stem cells as a discovery tool. Oncotarget. 7(39):63020.

Woods N, Trevino J, Coppola D, Chellappan S, Yang S, Padmanabhan J. 2015. Fendiline inhibits proliferation and invasion of pancreatic cancer cells by interfering with adam10 activation and β-catenin signaling. Oncotarget. 6(34):35931-35948.

Zarrin A, Mehdipour AR, Miri R. 2010. Dihydropyridines and multidrug resistance: Previous attempts, present state, and future trends. Chemical biology & drug design. 76(5):369-381.

Zhang X, Alves DS, Lou J, Hill SD, Barrera FN, Best MD. 2018. Boronic acid liposomes for cellular delivery and content release driven by carbohydrate binding. Chemical communications (Cambridge, England). 54(48):6169-6172.

Zhang X, Li W, Wang C, Leng X, Lian S, Feng J, Li J, Wang H. 2014. Inhibition of autophagy enhances apoptosis induced by proteasome inhibitor bortezomib in human glioblastoma u87 and u251 cells. Molecular and cellular biochemistry. 385(1-2):265-275.

Zhou XF, Yang X, Wang Q, Coburn RA, Morris ME. 2005. Effects of dihydropyridines and pyridines on multidrug resistance mediated by breast cancer resistance protein: In vitro and in vivo studies. Drug metabolism and disposition: the biological fate of chemicals. 33(8):1220-1228.

Zong H, Verhaak RG, Canoll P. 2012. The cellular origin for malignant glioma and prospects for clinical advancements. Expert review of molecular diagnostics. 12(4):383-394.

APPENDIX A

Multiple Comparisons 3-PFB

Dependent Variable: average cells

Dunnett t (2-sided)[a]

(I) drugconcentration	(J) drugconcentration	Mean Difference (I-J)	Std. Error	Sig.	95% Confidence Interval	
					Lower Bound	Upper Bound
2	control	-138.33333*	21.33981	.000	-201.6636	-75.0030
1	control	-138.33333*	21.33981	.000	-201.6636	-75.0030
0.5	control	-138.33333*	21.33981	.000	-201.6636	-75.0030
0.25	control	-138.33333*	21.33981	.000	-201.6636	-75.0030
0.125	control	-101.34333*	21.33981	.001	-164.6736	-38.0130
0.0625	control	-49.00000	21.33981	.192	-112.3303	14.3303
0.03125	control	-4.33333	21.33981	1.000	-67.6636	58.9970
0.01562	control	-13.66667	21.33981	.997	-76.9970	49.6636
0.00781	control	-40.22667	21.33981	.381	-103.5570	23.1036
0.003906	control	-34.00000	21.33981	.568	-97.3303	29.3303
0.00195	control	-2.00000	21.33981	1.000	-65.3303	61.3303

*. The mean difference is significant at the 0.05 level.

a. Dunnett t-tests treat one group as a control, and compare all other groups against it.

Dependent Variable: averagecells

Multiple Comparisons 4-FPB

Dunnett t (2-sided)[a]

(I) drugconcentration	(J) drugconcentration	Mean Difference (I-J)	Std. Error	Sig.	95% Confidence Interval	
					Lower Bound	Upper Bound
2	control	-148.33333*	15.57902	.000	-194.5673	-102.0994
1	control	-148.33333*	15.57902	.000	-194.5673	-102.0994
0.5	control	-148.33333*	15.57902	.000	-194.5673	-102.0994
0.25	control	-148.33333*	15.57902	.000	-194.5673	-102.0994
0.125	control	-130.77778*	15.57902	.000	-177.0117	-84.5438
0.0625	control	-64.66667*	15.57902	.003	-110.9006	-18.4327
0.03125	control	-17.11111	15.57902	.889	-63.3451	29.1228
0.01562	control	-28.22222	15.57902	.424	-74.4562	18.0117
0.00781	control	-4.66667	15.57902	1.000	-50.9006	41.5673
0.003906	control	-7.66667	15.57902	1.000	-53.9006	38.5673
0.00195	control	-.77778	15.57902	1.000	-47.0117	45.4562

*. The mean difference is significant at the 0.05 level.

a. Dunnett t-tests treat one group as a control, and compare all other groups against it.

Multiple Comparisons- 2Q

Dependent Variable: averagecells

Dunnett t (2-sided)[a]

(I) drugconcentration	(J) drugconcentration	Mean Difference (I-J)	Std. Error	Sig.	95% Confidence Interval	
					Lower Bound	Upper Bound
2	control	-153.55556*	32.57596	.001	-250.2314	-56.8797
1	control	-153.55556*	32.57596	.001	-250.2314	-56.8797
0.5	control	-117.33333*	32.57596	.012	-214.0092	-20.6575
0.25	control	-107.00000*	32.57596	.025	-203.6759	-10.3241
0.125	control	-67.22222	32.57596	.287	-163.8981	29.4537
0.0625	control	-59.77778	32.57596	.410	-156.4537	36.8981
0.03125	control	-34.88889	32.57596	.901	-131.5648	61.7870
0.01562	control	-16.66667	32.57596	.999	-113.3425	80.0092
0.00781	control	-16.11111	32.57596	1.000	-112.7870	80.5648
0.003906	control	-12.11111	32.57596	1.000	-108.7870	84.5648
0.00195	control	-36.89361	32.57596	.871	-133.5695	59.7823

*. The mean difference is significant at the 0.05 level.

a. Dunnett t-tests treat one group as a control, and compare all other groups against it.

Multiple Comparisons 5-P

Dependent Variable: averagecells

Dunnett t (2-sided)[a]

(I) drugconcentration	(J) drugconcentration	Mean Difference (I-J)	Std. Error	Sig.	95% Confidence Interval	
					Lower Bound	Upper Bound
2	control	-132.88889*	26.85190	.000	-212.5775	-53.2003
1	control	-132.88889*	26.85190	.000	-212.5775	-53.2003
0.5	control	-119.77778*	26.85190	.001	-199.4663	-40.0892
0.25	control	-87.55556*	26.85190	.026	-167.2441	-7.8670
0.125	control	-68.44444	26.85190	.119	-148.1330	11.2441
0.0625	control	-58.77778	26.85190	.232	-138.4663	20.9108
0.03125	control	-49.44444	26.85190	.406	-129.1330	30.2441
0.01562	control	-36.77778	26.85190	.725	-116.4663	42.9108
0.00781	control	-41.77778	26.85190	.594	-121.4663	37.9108
0.003906	control	-19.11111	26.85190	.992	-98.7997	60.5775
0.00195	control	-4.00000	26.85190	1.000	-83.6886	75.6886

*. The mean difference is significant at the 0.05 level.

a. Dunnett t-tests treat one group as a control, and compare all other groups against it.

Multiple Comparisons 2-F

Dependent Variable: averagecells

Dunnett t (2-sided)[a]

(I) drugconcentration	(J) drugconcentration	Mean Difference (I-J)	Std. Error	Sig.	95% Confidence Interval	
					Lower Bound	Upper Bound
2	control	-70.11111*	14.82310	.001	-114.1017	-26.1205
1	control	-70.11111*	14.82310	.001	-114.1017	-26.1205
0.5	control	-70.11111*	14.82310	.001	-114.1017	-26.1205
0.25	control	-70.11111*	14.82310	.001	-114.1017	-26.1205
0.125	control	-70.11111*	14.82310	.001	-114.1017	-26.1205
0.0625	control	-69.88889*	14.82310	.001	-113.8795	-25.8983
0.03125	control	-51.22222*	14.82310	.017	-95.2128	-7.2316
0.01562	control	-33.11111	14.82310	.214	-77.1017	10.8795
0.00781	control	-20.22222	14.82310	.729	-64.2128	23.7684
0.003906	control	-16.11111	14.82310	.894	-60.1017	27.8795
0.00195	control	-17.44444	14.82310	.847	-61.4351	26.5462

*. The mean difference is significant at the 0.05 level.

a. Dunnett t-tests treat one group as a control, and compare all other groups against it.

Multiple Comparisons 3-F

Dependent Variable: averagecells

Dunnett t (2-sided)[a]

(I) drugconcentration	(J) drugconcentration	Mean Difference (I-J)	Std. Error	Sig.	95% Confidence Interval	
					Lower Bound	Upper Bound
2	control	-55.44444*	10.53235	.000	-86.7014	-24.1875
1	control	-55.44444*	10.53235	.000	-86.7014	-24.1875
0.5	control	-55.44444*	10.53235	.000	-86.7014	-24.1875
0.25	control	-55.44444*	10.53235	.000	-86.7014	-24.1875
0.125	control	-55.44444*	10.53235	.000	-86.7014	-24.1875
0.0625	control	-55.44444*	10.53235	.000	-86.7014	-24.1875
0.03125	control	-32.77778*	10.53235	.036	-64.0347	-1.5209
0.01562	control	-22.77778	10.53235	.243	-54.0347	8.4791
0.00781	control	-8.55556	10.53235	.980	-39.8125	22.7014
0.003906	control	-4.77778	10.53235	1.000	-36.0347	26.4791
0.00195	control	-18.54578	10.53235	.456	-49.8027	12.7111

*. The mean difference is significant at the 0.05 level.

a. Dunnett t-tests treat one group as a control, and compare all other groups against it.

Multiple Comparisons 4-F

Dependent Variable: averagecells

Dunnett t (2-sided)[a]

(I) drugconcentration	(J) drugconcentration	Mean Difference (I-J)	Std. Error	Sig.	95% Confidence Interval	
					Lower Bound	Upper Bound
2	control	-50.44444*	12.75731	.005	-88.3044	-12.5845
1	control	-50.44444*	12.75731	.005	-88.3044	-12.5845
0.5	control	-50.44444*	12.75731	.005	-88.3044	-12.5845
0.25	control	-50.44444*	12.75731	.005	-88.3044	-12.5845
0.125	control	-50.44444*	12.75731	.005	-88.3044	-12.5845
0.0625	control	-44.44444*	12.75731	.016	-82.3044	-6.5845
0.03125	control	-15.11111	12.75731	.843	-52.9711	22.7488
0.01562	control	-6.88889	12.75731	.999	-44.7488	30.9711
0.00781	control	.11111	12.75731	1.000	-37.7488	37.9711
0.003906	control	-13.11111	12.75731	.920	-50.9711	24.7488
0.00195	control	-1.88889	12.75731	1.000	-39.7488	35.9711

*. The mean difference is significant at the 0.05 level.

a. Dunnett t-tests treat one group as a control, and compare all other groups against it.

Multiple Comparisons 2,3-DF

Dependent Variable: averagecells

Dunnett t (2-sided)[a]

(I) drugconcentration	(J) drugconcentration	Mean Difference (I-J)	Std. Error	Sig.	95% Confidence Interval	
					Lower Bound	Upper Bound
2	control	-72.00000*	11.76056	.000	-106.9019	-37.0981
1	control	-72.00000*	11.76056	.000	-106.9019	-37.0981
0.5	control	-72.00000*	11.76056	.000	-106.9019	-37.0981
0.25	control	-72.00000*	11.76056	.000	-106.9019	-37.0981
0.125	control	-72.00000*	11.76056	.000	-106.9019	-37.0981
0.0625	control	-72.00000*	11.76056	.000	-106.9019	-37.0981
0.03125	control	-70.77778*	11.76056	.000	-105.6797	-35.8759
0.01562	control	-31.77778	11.76056	.087	-66.6797	3.1241
0.00781	control	-20.00000	11.76056	.495	-54.9019	14.9019
0.003906	control	-8.55556	11.76056	.991	-43.4574	26.3463
0.00195	control	-9.44444	11.76056	.982	-44.3463	25.4574

*. The mean difference is significant at the 0.05 level.

a. Dunnett t-tests treat one group as a control, and compare all other groups against it.

Multiple Comparisons 2,4-DF

Dependent Variable: averagecells

Dunnett t (2-sided)[a]

(I) drugconcentration	(J) drugconcentration	Mean Difference (I-J)	Std. Error	Sig.	95% Confidence Interval	
					Lower Bound	Upper Bound
2	control	-90.88889*	13.23619	.000	-130.1700	-51.6078
1	control	-90.88889*	13.23619	.000	-130.1700	-51.6078
0.5	control	-90.88889*	13.23619	.000	-130.1700	-51.6078
0.25	control	-90.88889*	13.23619	.000	-130.1700	-51.6078
0.125	control	-90.88889*	13.23619	.000	-130.1700	-51.6078
0.0625	control	-90.88889*	13.23619	.000	-130.1700	-51.6078
0.03125	control	-51.88889*	13.23619	.006	-91.1700	-12.6078
0.01562	control	-4.00000	13.23619	1.000	-43.2811	35.2811
0.00781	control	-23.77778	13.23619	.434	-63.0589	15.5033
0.003906	control	-1.77778	13.23619	1.000	-41.0589	37.5033
0.00195	control	-28.33351	13.23619	.252	-67.6146	10.9476

*. The mean difference is significant at the 0.05 level.

a. Dunnett t-tests treat one group as a control, and compare all other groups against it.

Multiple Comparisons 2,5-DF

Dependent Variable: averagecells

Dunnett t (2-sided)[a]

(I) drugconcentration	(J) drugconcentration	Mean Difference (I-J)	Std. Error	Sig.	95% Confidence Interval	
					Lower Bound	Upper Bound
2	control	-112.77778*	12.80842	.000	-150.7894	-74.7662
1	control	-112.77778*	12.80842	.000	-150.7894	-74.7662
0.5	control	-112.77778*	12.80842	.000	-150.7894	-74.7662
0.25	control	-112.77778*	12.80842	.000	-150.7894	-74.7662
0.125	control	-112.77778*	12.80842	.000	-150.7894	-74.7662
0.0625	control	-112.77778*	12.80842	.000	-150.7894	-74.7662
0.03125	control	-61.22222*	12.80842	.001	-99.2338	-23.2106
0.01562	control	-32.11111	12.80842	.129	-70.1227	5.9005
0.00781	control	-32.77778	12.80842	.116	-70.7894	5.2338
0.003906	control	-6.44444	12.80842	1.000	-44.4561	31.5672
0.00195	control	-20.22222	12.80842	.578	-58.2338	17.7894

*. The mean difference is significant at the 0.05 level.

a. Dunnett t-tests treat one group as a control, and compare all other groups against it.

Multiple Comparisons- 2-TF

Dependent Variable: averagecells

Dunnett t (2-sided)[a]

(I) drugconcentration	(J) drugconcentration	Mean Difference (I-J)	Std. Error	Sig.	95% Confidence Interval	
					Lower Bound	Upper Bound
2	control	-239.22222*	30.29288	.000	-329.1226	-149.3219
1	control	-239.22222*	30.29288	.000	-329.1226	-149.3219
0.5	control	-239.22222*	30.29288	.000	-329.1226	-149.3219
0.25	control	-239.22222*	30.29288	.000	-329.1226	-149.3219
0.125	control	-239.22222*	30.29288	.000	-329.1226	-149.3219
0.0625	control	-239.22222*	30.29288	.000	-329.1226	-149.3219
0.03125	control	-227.88889*	30.29288	.000	-317.7893	-137.9885
0.01562	control	-158.77778*	30.29288	.000	-248.6781	-68.8774
0.00781	control	-105.77778*	30.29288	.015	-195.6781	-15.8774
0.003906	control	-80.44444	30.29288	.096	-170.3448	9.4559
0.00195	control	-61.33333	30.29288	.306	-151.2337	28.5670

*. The mean difference is significant at the 0.05 level.

a. Dunnett t-tests treat one group as a control, and compare all other groups against it.

Multiple Comparisons 2-TF

Dependent Variable: averagecells

Dunnett t (2-sided)[a]

(I) drugconcentration	(J) drugconcentration	Mean Difference (I-J)	Std. Error	Sig.	95% Confidence Interval	
					Lower Bound	Upper Bound
2	control	-208.00000*	31.98698	.000	-302.9280	-113.0720
1	control	-208.00000*	31.98698	.000	-302.9280	-113.0720
0.5	control	-208.00000*	31.98698	.000	-302.9280	-113.0720
0.25	control	-208.00000*	31.98698	.000	-302.9280	-113.0720
0.125	control	-208.00000*	31.98698	.000	-302.9280	-113.0720
0.0625	control	-208.00000*	31.98698	.000	-302.9280	-113.0720
0.03125	control	-206.55556*	31.98698	.000	-301.4835	-111.6276
0.01562	control	-99.44444*	31.98698	.037	-194.3724	-4.5165
0.00781	control	-75.11111	31.98698	.174	-170.0391	19.8168
0.003906	control	-48.77778	31.98698	.616	-143.7057	46.1502
0.00195	control	-66.98245	31.98698	.273	-161.9104	27.9455

*. The mean difference is significant at the 0.05 level.

a. Dunnett t-tests treat one group as a control, and compare all other groups against it.

Multiple Comparisons 3-Cl

Dependent Variable: averagecells

Dunnett t (2-sided)[a]

(I) drugconcentration	(J) drugconcentration	Mean Difference (I-J)	Std. Error	Sig.	95% Confidence Interval	
					Lower Bound	Upper Bound
2	control	-230.44444*	42.83299	.000	-357.5602	-103.3287
1	control	-230.44444*	42.83299	.000	-357.5602	-103.3287
0.5	control	-230.44444*	42.83299	.000	-357.5602	-103.3287
0.25	control	-230.44444*	42.83299	.000	-357.5602	-103.3287
0.125	control	-230.44444*	42.83299	.000	-357.5602	-103.3287
0.0625	control	-230.44444*	42.83299	.000	-357.5602	-103.3287
0.03125	control	-195.11111*	42.83299	.001	-322.2268	-67.9954
0.01562	control	-96.88889	42.83299	.204	-224.0046	30.2268
0.00781	control	-75.88889	42.83299	.449	-203.0046	51.2268
0.003906	control	-28.88889	42.83299	.995	-156.0046	98.2268
0.00195	control	38.77778	42.83299	.961	-88.3379	165.8935

*. The mean difference is significant at the 0.05 level.

a. Dunnett t-tests treat one group as a control, and compare all other groups against it.

Multiple Comparisons 4-Cl

Dependent Variable: averagecells

Dunnett t (2-sided)[a]

(I) drugconcentration	(J) drugconcentration	Mean Difference (I-J)	Std. Error	Sig.	95% Confidence Interval	
					Lower Bound	Upper Bound
2	control	-227.66667*	33.44814	.000	-326.9309	-128.4024
1	control	-227.66667*	33.44814	.000	-326.9309	-128.4024
0.5	control	-227.66667*	33.44814	.000	-326.9309	-128.4024
0.25	control	-227.66667*	33.44814	.000	-326.9309	-128.4024
0.125	control	-227.66667*	33.44814	.000	-326.9309	-128.4024
0.0625	control	-227.66667*	33.44814	.000	-326.9309	-128.4024
0.03125	control	-223.55556*	33.44814	.000	-322.8198	-124.2913
0.01562	control	-84.22222	33.44814	.126	-183.4865	15.0420
0.00781	control	-38.33333	33.44814	.864	-137.5976	60.9309
0.003906	control	-22.44444	33.44814	.995	-121.7087	76.8198
0.00195	control	.33333	33.44814	1.000	-98.9309	99.5976

*. The mean difference is significant at the 0.05 level.

a. Dunnett t-tests treat one group as a control, and compare all other groups against it.

Multiple Comparisons EAA

Dependent Variable: averagecells

Dunnett t (2-sided)[a]

(I) drugconcentration	(J) drugconcentration	Mean Difference (I-J)	Std. Error	Sig.	95% Confidence Interval	
					Lower Bound	Upper Bound
2	control	-81.88889*	19.81416	.003	-140.6915	-23.0863
1	control	-69.55556*	19.81416	.015	-128.3582	-10.7530
0.5	control	-40.44444	19.81416	.298	-99.2470	18.3582
0.25	control	-38.66667	19.81416	.344	-97.4693	20.1359
0.125	control	-29.00000	19.81416	.660	-87.8026	29.8026
0.0625	control	-10.44444	19.81416	.999	-69.2470	48.3582
0.03125	control	-24.00000	19.81416	.827	-82.8026	34.8026
0.01562	control	-11.55556	19.81416	.998	-70.3582	47.2470
0.00781	control	-13.88889	19.81416	.993	-72.6915	44.9137
0.003906	control	-1.88889	19.81416	1.000	-60.6915	56.9137
0.00195	control	2.66667	19.81416	1.000	-56.1359	61.4693

*. The mean difference is significant at the 0.05 level.

a. Dunnett t-tests treat one group as a control, and compare all other groups against it.

Invasion

(I) compound	(J) compound	Mean Difference (I-J)	Std. Error	Sig.	95% Confidence Interval	
					Lower Bound	Upper Bound
2-TF	3-TF	-754.19333	684.39633	1.000	-3251.4798	1743.0931
	2-F	-1057.99667	684.39633	1.000	-3555.2831	1439.2898
	3-F	-769.70333	684.39633	1.000	-3266.9898	1727.5831
	4-F	-1167.26333	684.39633	1.000	-3664.5498	1330.0231
	control	-2931.59000*	684.39633	.016	-5428.8764	-434.3036
3-TF	2-TF	754.19333	684.39633	1.000	-1743.0931	3251.4798
	2-F	-303.80333	684.39633	1.000	-2801.0898	2193.4831
	3-F	-15.51000	684.39633	1.000	-2512.7964	2481.7764
	4-F	-413.07000	684.39633	1.000	-2910.3564	2084.2164
	control	-2177.39667	684.39633	.118	-4674.6831	319.8898
2-F	2-TF	1057.99667	684.39633	1.000	-1439.2898	3555.2831
	3-TF	303.80333	684.39633	1.000	-2193.4831	2801.0898
	3-F	288.29333	684.39633	1.000	-2208.9931	2785.5798
	4-F	-109.26667	684.39633	1.000	-2606.5531	2388.0198
	control	-1873.59333	684.39633	.270	-4370.8798	623.6931
3-F	2-TF	769.70333	684.39633	1.000	-1727.5831	3266.9898
	3-TF	15.51000	684.39633	1.000	-2481.7764	2512.7964
	2-F	-288.29333	684.39633	1.000	-2785.5798	2208.9931
	4-F	-397.56000	684.39633	1.000	-2894.8464	2099.7264
	control	-2161.88667	684.39633	.124	-4659.1731	335.3998
4-F	2-TF	1167.26333	684.39633	1.000	-1330.0231	3664.5498
	3-TF	413.07000	684.39633	1.000	-2084.2164	2910.3564
	2-F	109.26667	684.39633	1.000	-2388.0198	2606.5531
	3-F	397.56000	684.39633	1.000	-2099.7264	2894.8464
	control	-1764.32667	684.39633	.363	-4261.6131	732.9598
control	2-TF	2931.59000*	684.39633	.016	434.3036	5428.8764

	3-TF	2177.39667	684.39633	.118	-319.8898	4674.6831
	2-F	1873.59333	684.39633	.270	-623.6931	4370.8798
	3-F	2161.88667	684.39633	.124	-335.3998	4659.1731
	4-F	1764.32667	684.39633	.363	-732.9598	4261.6131

APPENDIX B

3-FPB

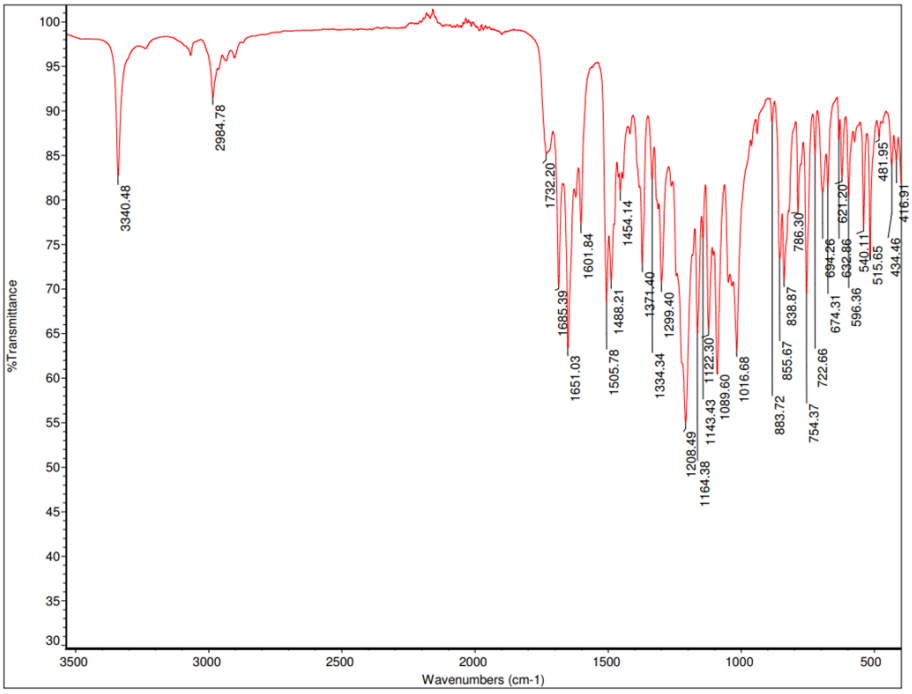

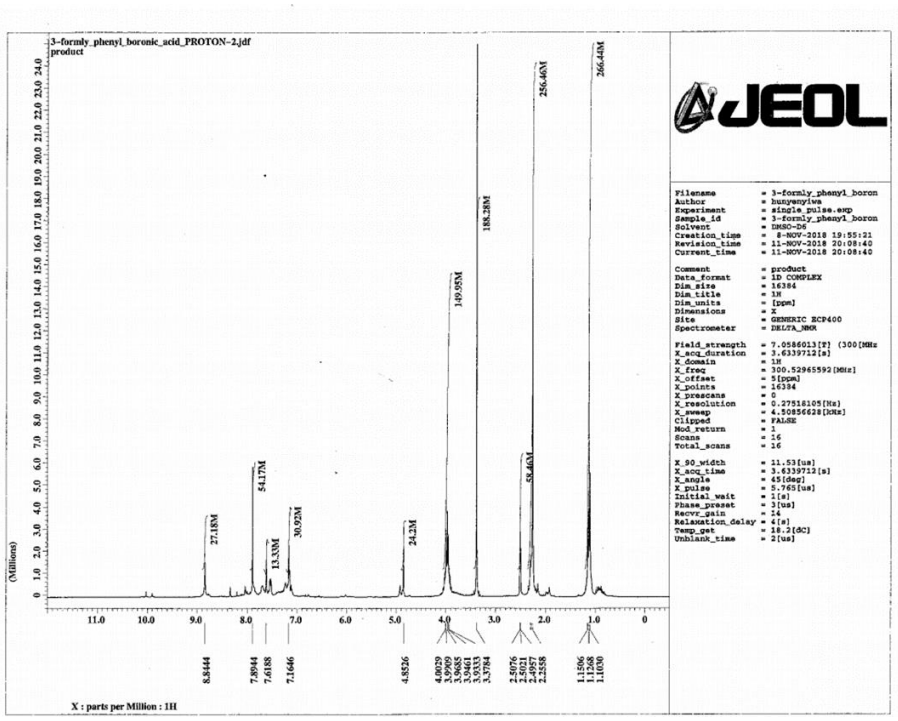

4-FPB

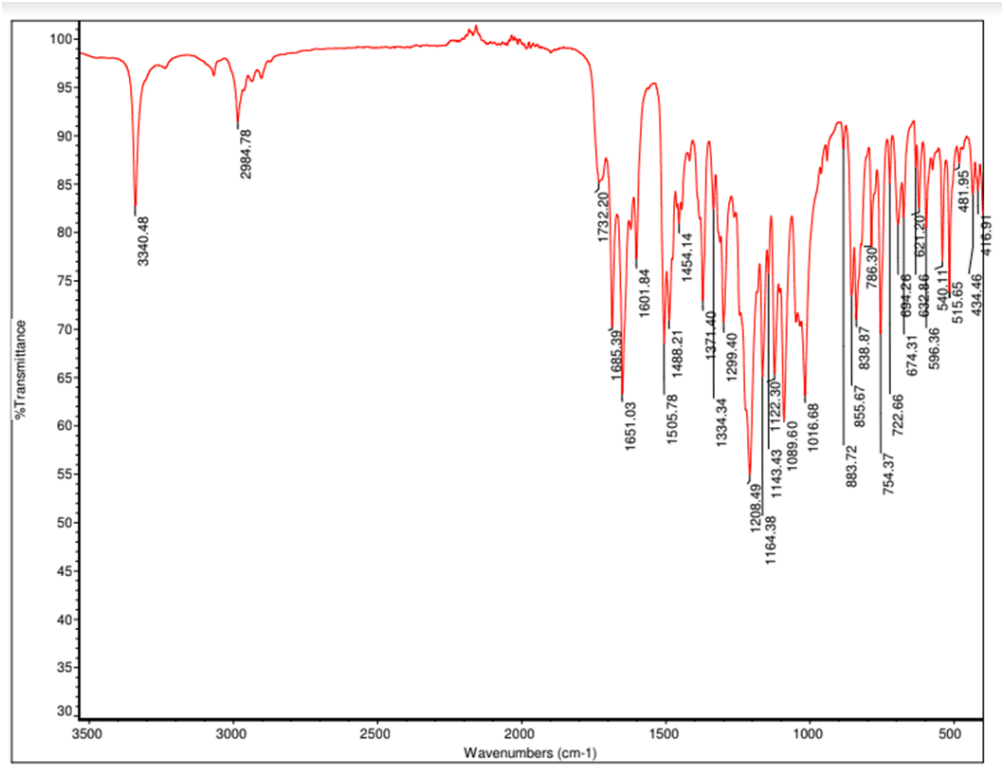
%Transmittance
Wavenumbers (cm-1)
3340.48
2984.78
1732.20
1685.39
1651.03
1601.84
1505.78
1488.21
1454.14
1371.40
1334.34
1299.40
1208.49
1164.38
1143.43
1122.30
1089.60
1016.68
883.72
855.67
838.87
786.30
754.37
722.66
674.31
694.26
632.86
621.20
596.36
540.11
515.65
481.95
434.46
416.91

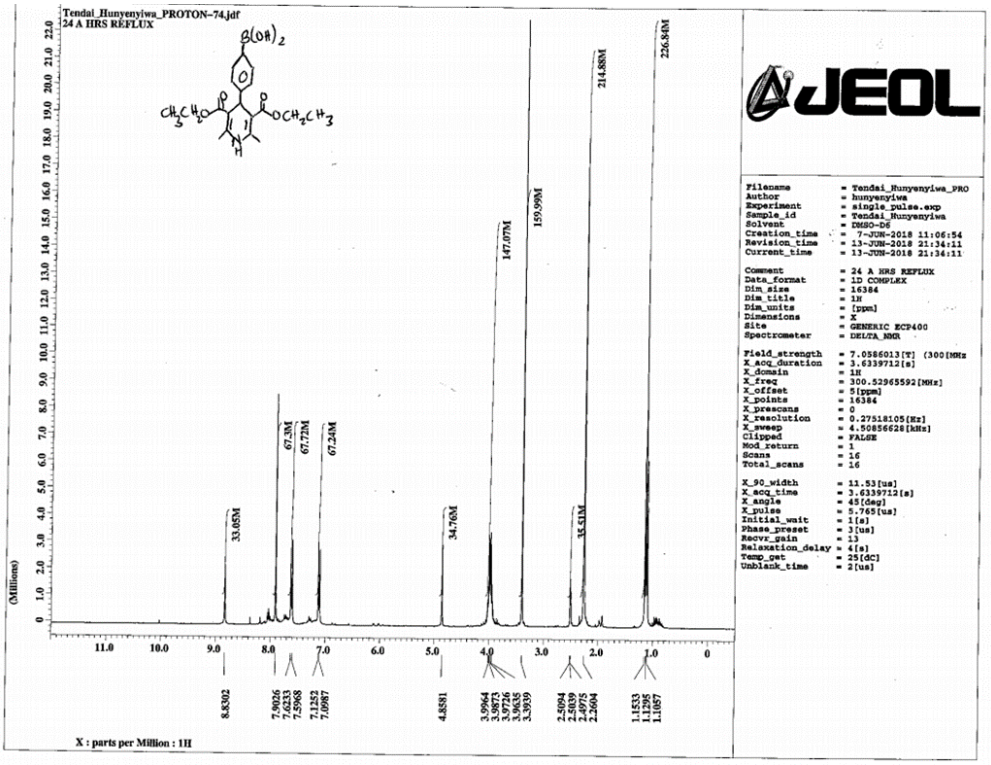
Tendai_Hunyenyiwa_PROTON-74.jdf
24 A HRS REFLUX
JEOL
X : parts per Million : 1H
(Millions)
33.065M
67.38M
67.72M
67.24M
34.76M
147.07M
159.99M
35.51M
214.88M
226.84M
Filename = Tendai_Hunyenyiwa_PRO
Author = hunyenyiwa
Experiment = single_pulse.exp
Sample_id = Tendai_Hunyenyiwa
Solvent = DMSO-D6
Creation_time = 7-JUN-2018 11:06:54
Revision_time = 13-JUN-2018 21:34:11
Current_time = 13-JUN-2018 21:34:11
Comment = 24 A HRS REFLUX
Data_format = 1D COMPLEX
Dim_size = 16384
Dim_title = 1H
Dim_units = [ppm]
Dimensions = X
Site = GENERIC ECP400
Spectrometer = DELTA_NMR
Field_strength = 7.0586013[T] (300[MHz
X_acq_duration = 3.6339712[s]
X_domain = 1H
X_freq = 300.52965592[MHz]
X_offset = 5[ppm]
X_points = 16384
X_prescans = 0
X_resolution = 0.27518105[Hz]
X_sweep = 4.50856628[kHz]
Clipped = FALSE
Mod_return = 1
Scans = 16
Total_scans = 16
X_90_width = 11.53[us]
X_acq_time = 3.6339712[s]
X_angle = 45[deg]
X_pulse = 5.765[us]
Initial_wait = 1[s]
Phase_preset = 3[us]
Recvr_gain = 13
Relaxation_delay = 4[s]
Temp_get = 25[dC]
Unblank_time = 2[us]

2-Q

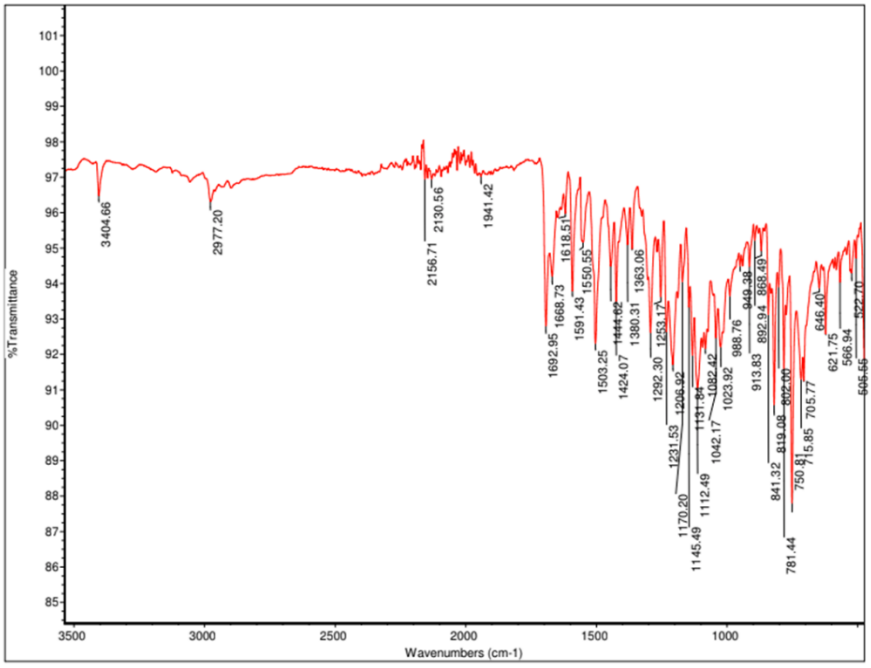
%Transmittance
Wavenumbers (cm-1)
3404.66
2977.20
2156.71
2130.56
1941.42
1692.95
1668.73
1618.51
1591.43
1550.55
1503.25
1424.07
1380.31
1363.06
1292.30
1253.17
1231.53
1208.92
1170.20
1145.49
1131.84
1112.49
1082.42
1042.17
1023.92
988.76
949.38
913.83
892.94
868.49
841.32
819.08
802.00
781.44
750.81
715.85
705.77
646.40
621.75
566.94
522.70
505.65

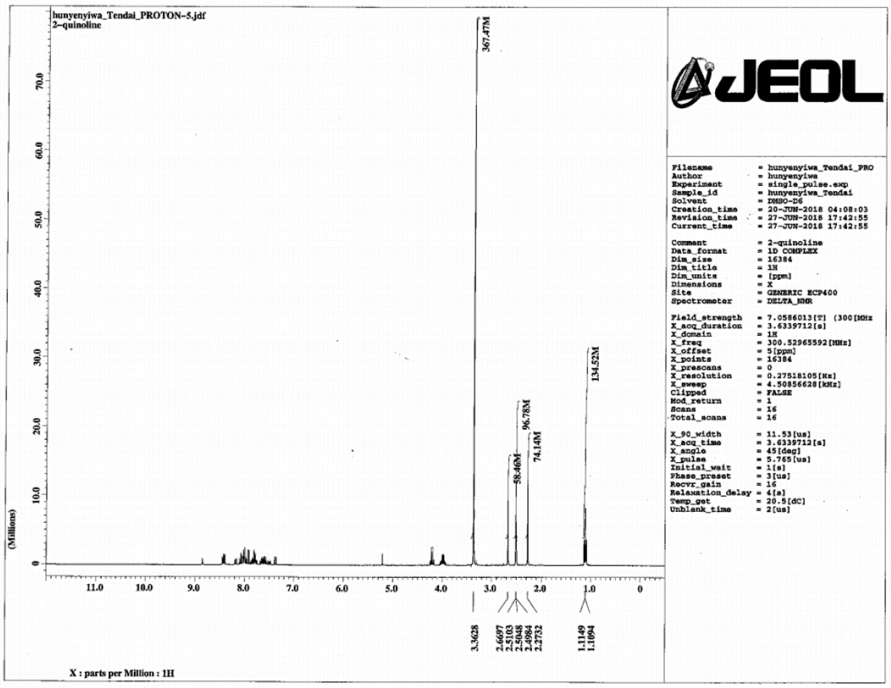
hunyenyiwa_Tendai_PROTON-5.jdf
2-quinoline
367.47M
134.52M
96.78M
74.14M
58.46M
(Millions)
X : parts per Million : 1H
JEOL
Filename = hunyenyiwa_Tendai_PRO
Author = hunyenyiwa
Experiment = single_pulse.exp
Sample_id = hunyenyiwa_Tendai
Solvent = DMSO-D6
Creation_time = 20-JUN-2018 04:08:03
Revision_time = 27-JUN-2018 17:42:55
Current_time = 27-JUN-2018 17:42:55
Comment = 2-quinoline
Data_format = 1D COMPLEX
Dim_size = 16384
Dim_title = 1H
Dim_units = [ppm]
Dimensions = X
Site = GEMINIC BCP400
Spectrometer = DELTA_NMR
Field_strength = 7.0586013[T] (300[MHz
X_acq_duration = 3.6339712[s]
X_domain = 1H
X_freq = 300.52965592[MHz]
X_offset = 5[ppm]
X_points = 16384
X_prescans = 0
X_resolution = 0.27518105[Hz]
X_sweep = 4.50856628[kHz]
Clipped = FALSE
Mod_return = 1
Scans = 16
Total_scans = 16
X_90_width = 11.53[us]
X_acq_time = 3.6339712[s]
X_angle = 45[deg]
X_pulse = 5.765[us]
Initial_wait = 1[s]
Phase_preset = 3[us]
Recvr_gain = 16
Relaxation_delay = 4[s]
Temp_get = 20.5[dC]
Unblank_time = 2[us]

5-P

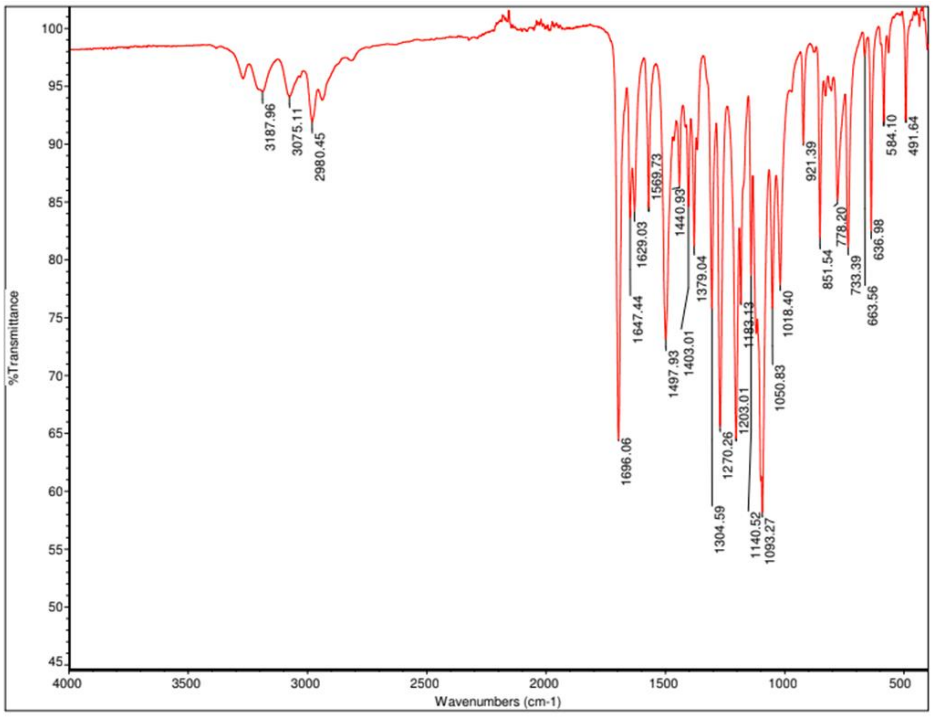
%Transmittance
Wavenumbers (cm-1)
3187.96
3075.11
2980.45
1696.06
1647.44
1629.03
1569.73
1497.93
1440.93
1403.01
1379.04
1304.59
1270.26
1203.01
1183.13
1140.52
1093.27
1050.83
1018.40
921.39
851.54
778.20
733.39
663.56
636.98
584.10
491.64

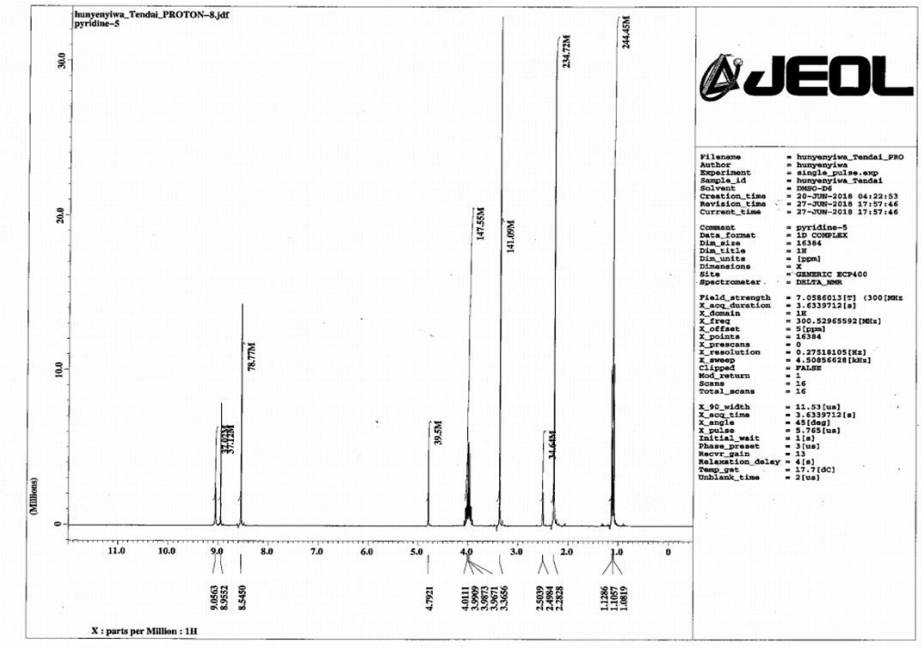
hunyenyiwa_Tendai_PROTON-8.jdf
pyridine-5
JEOL
X : parts per Million : 1H

2-F

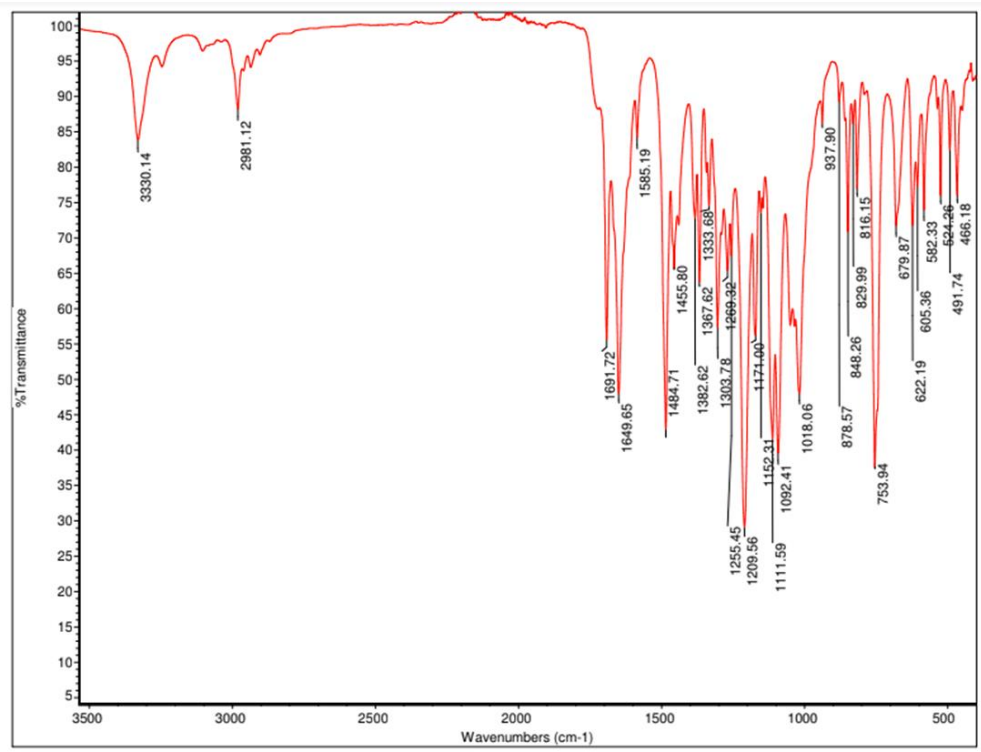
%Transmittance
Wavenumbers (cm-1)
3330.14
2981.12
1691.72
1649.65
1585.19
1484.71
1455.80
1382.62
1367.62
1333.68
1303.78
1269.32
1255.45
1209.56
1171.00
1152.31
1111.59
1092.41
1018.06
937.90
878.57
848.26
829.99
816.15
753.94
679.87
622.19
605.36
582.33
524.26
491.74
466.18

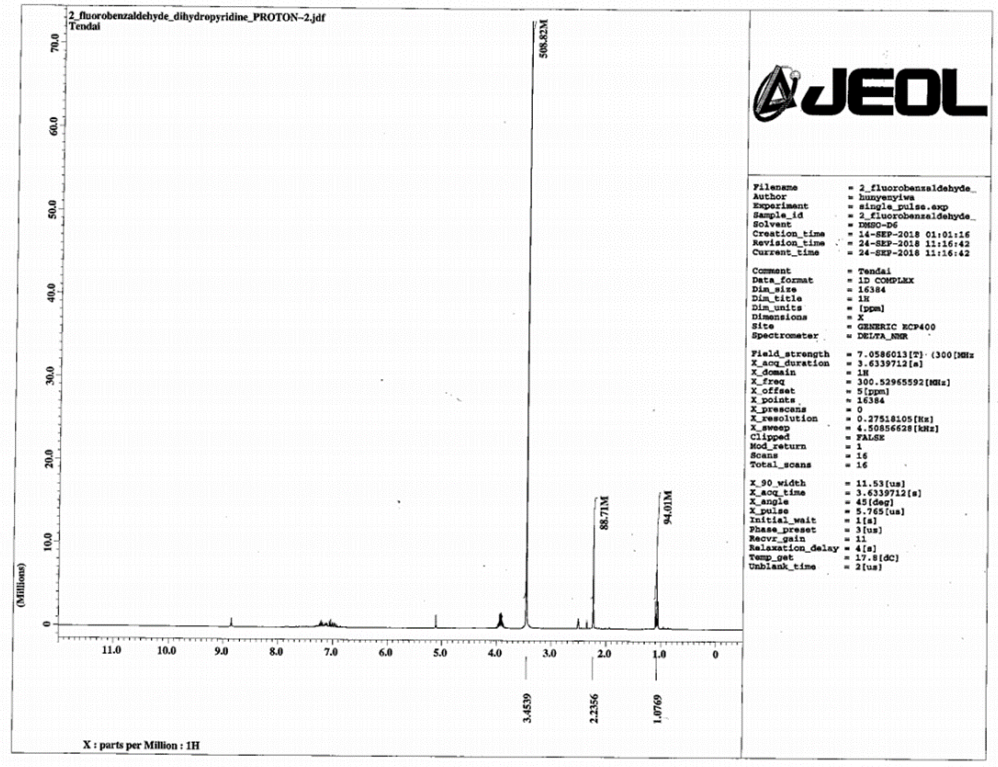
2_fluorobenzaldehyde_dihydropyridine_PROTON--2.jdf
Tendai
JEOL
508.82M
88.71M
94.01M
3.4539
2.2356
1.0769
X : parts per Million : 1H
(Millions)
Filename = 2_fluorobenzaldehyde_
Author = hunyenyiwa
Experiment = single_pulse.exp
Sample_id = 2_fluorobenzaldehyde_
Solvent = DMSO-D6
Creation_time = 14-SEP-2018 01:01:16
Revision_time = 24-SEP-2018 11:16:42
Current_time = 24-SEP-2018 11:16:42
Comment = Tendai
Data_format = 1D COMPLEX
Dim_size = 16384
Dim_title = 1H
Dim_units = [ppm]
Dimensions = X
Site = GENERIC ECP400
Spectrometer = DELTA_NMR
Field_strength = 7.0586013[T] (300[MHz
X_acq_duration = 3.6339712[s]
X_domain = 1H
X_freq = 300.52965592[MHz]
X_offset = 5[ppm]
X_points = 16384
X_prescans = 0
X_resolution = 0.27518105[Hz]
X_sweep = 4.50856628[kHz]
Clipped = FALSE
Mod_return = 1
Scans = 16
Total_scans = 16
X_90_width = 11.53[us]
X_acq_time = 3.6339712[s]
X_angle = 45[deg]
X_pulse = 5.765[us]
Initial_wait = 1[s]
Phase_preset = 3[us]
Recvr_gain = 11
Relaxation_delay = 4[s]
Temp_get = 17.8[dC]
Unblank_time = 2[us]

3-F

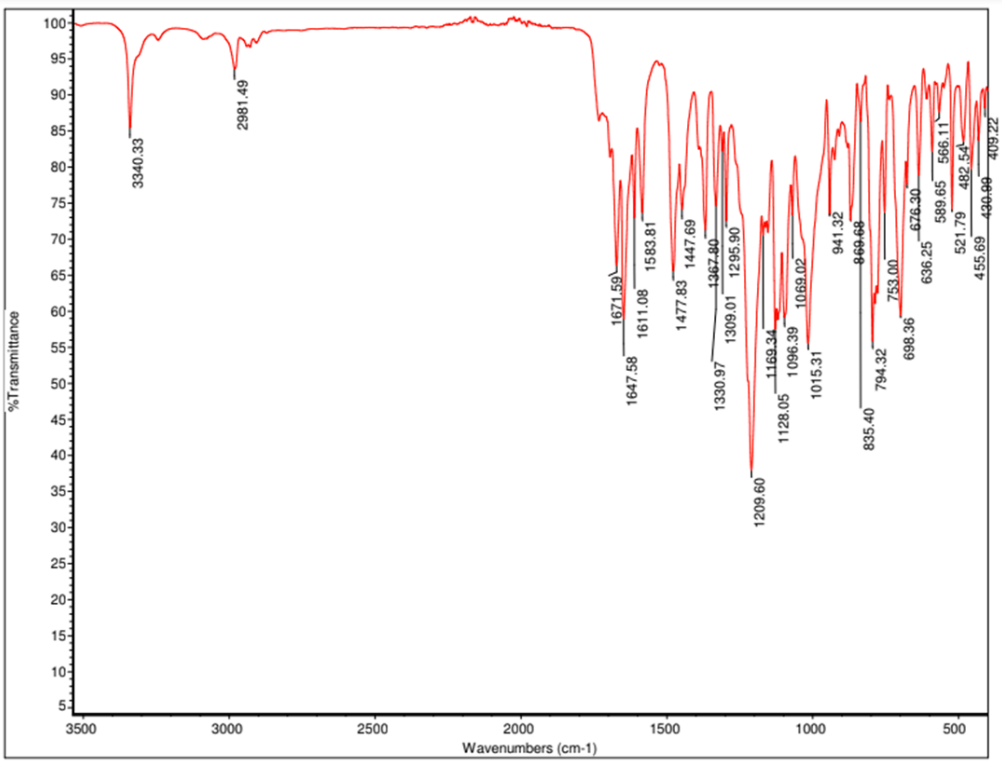
%Transmittance
Wavenumbers (cm-1)
3340.33
2981.49
1671.59
1647.58
1611.08
1583.81
1477.83
1447.69
1367.80
1330.97
1309.01
1295.90
1209.60
1169.34
1128.05
1096.39
1069.02
1015.31
941.32
868.68
835.40
794.32
753.00
698.36
676.30
636.25
589.65
566.11
521.79
482.54
455.69
430.80
409.22

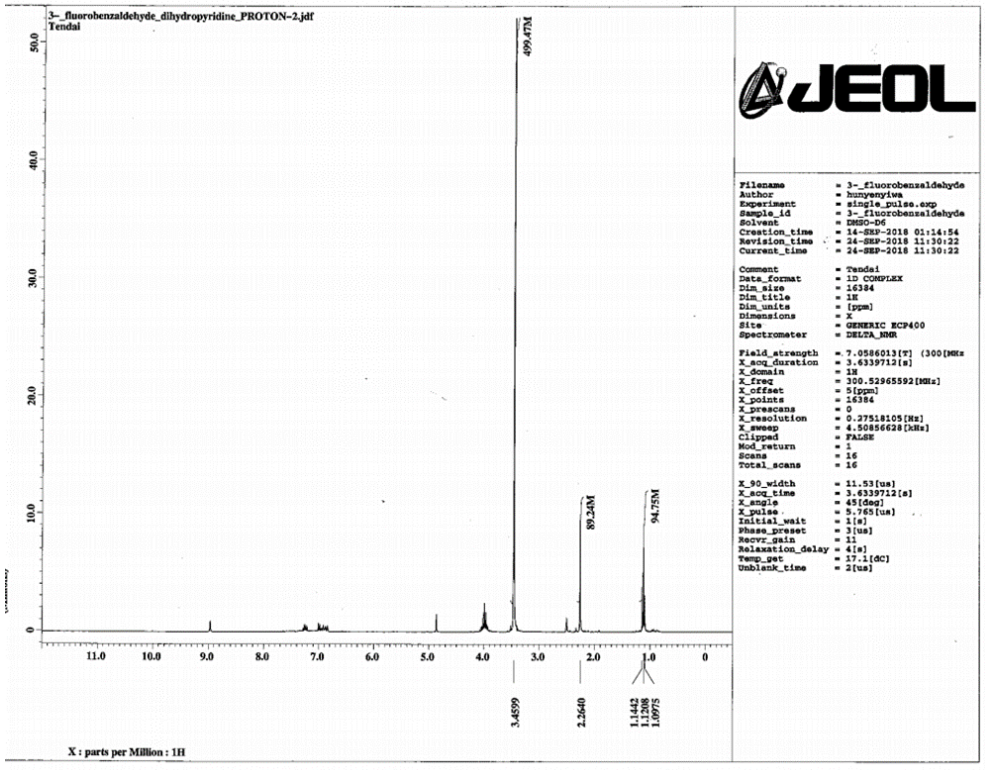
3-_fluorobenzaldehyde_dihydropyridine_PROTON-2.jdf
Tendai
499.47M
89.24M
94.75M
3.4599
2.2640
1.1442
1.1208
1.0975
X : parts per Million : 1H
JEOL
Filename = 3-_fluorobenzaldehyde
Author = hunyenyiwa
Experiment = single_pulse.exp
Sample_id = 3-_fluorobenzaldehyde
Solvent = DMSO-D6
Creation_time = 14-SEP-2018 01:14:54
Revision_time = 24-SEP-2018 11:30:22
Current_time = 24-SEP-2018 11:30:22
Comment = Tendai
Data_format = 1D COMPLEX
Dim_size = 16384
Dim_title = 1H
Dim_units = [ppm]
Dimensions = X
Site = GENERIC ECP400
Spectrometer = DELTA_NMR
Field_strength = 7.0586013[T] (300[MHz
X_acq_duration = 3.6339712[s]
X_domain = 1H
X_freq = 300.52965592[MHz]
X_offset = 5[ppm]
X_points = 16384
X_prescans = 0
X_resolution = 0.27518105[Hz]
X_sweep = 4.50856628[kHz]
Clipped = FALSE
Mod_return = 1
Scans = 16
Total_scans = 16
X_90_width = 11.53[us]
X_acq_time = 3.6339712[s]
X_angle = 45[deg]
X_pulse = 5.765[us]
Initial_wait = 1[s]
Phase_preset = 3[us]
Recvr_gain = 11
Relaxation_delay = 4[s]
Temp_get = 17.1[dC]
Unblank_time = 2[us]

4-F

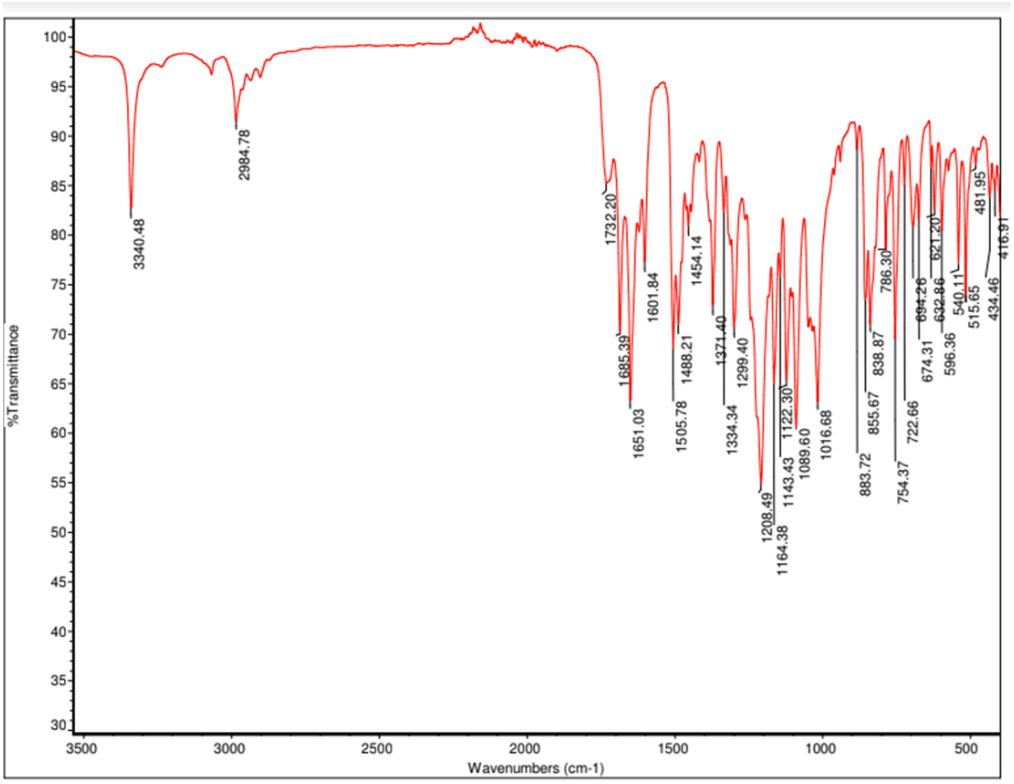
%Transmittance
Wavenumbers (cm-1)
3340.48
2984.78
1732.20
1685.39
1651.03
1601.84
1505.78
1488.21
1454.14
1371.40
1334.34
1299.40
1208.49
1164.38
1143.43
1122.30
1089.60
1016.68
883.72
855.67
838.87
786.30
754.37
722.66
674.31
694.26
632.86
621.20
596.36
540.11
515.65
481.95
434.46
416.91

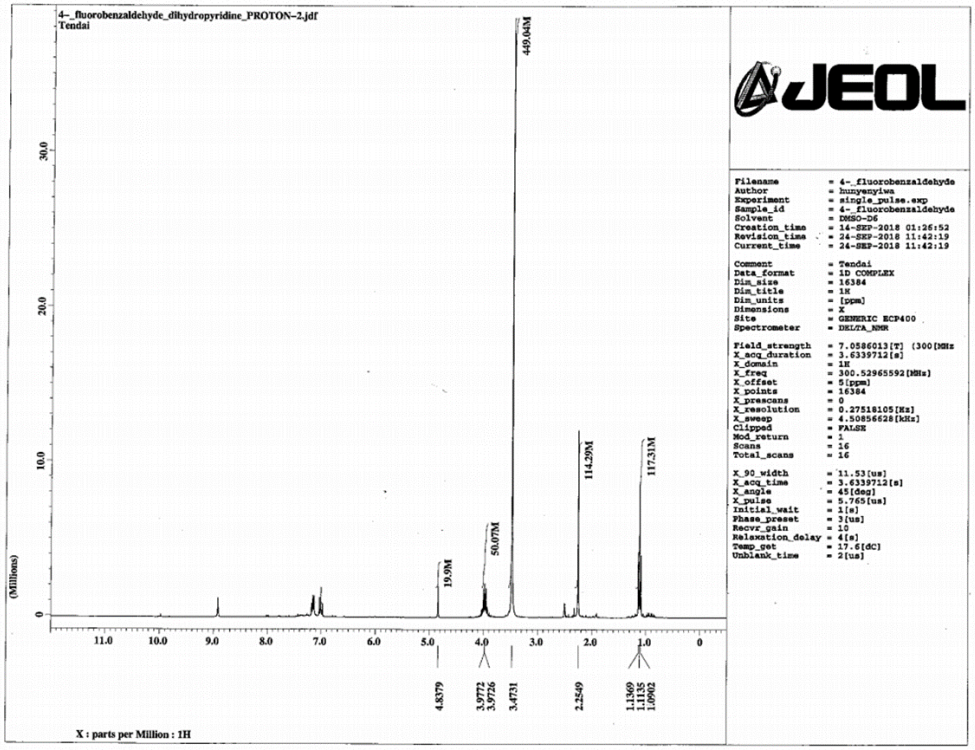
4-_fluorobenzaldehyde_dihydropyridine_PROTON-2.jdf
Tendai
449.04M
114.29M
117.31M
50.07M
19.99M
(Millions)
X : parts per Million : 1H
4.8379
3.9772
3.9726
3.4731
2.2549
1.1369
1.1135
1.0962
JEOL
Filename = 4-_fluorobenzaldehyde
Author = kuzyemyiwa
Experiment = single_pulse.exp
Sample_id = 4-_fluorobenzaldehyde
Solvent = DMSO-D6
Creation_time = 14-SEP-2018 01:26:52
Revision_time = 24-SEP-2018 11:42:19
Current_time = 24-SEP-2018 11:42:19
Comment = Tendai
Data_format = 1D COMPLEX
Dim_size = 16384
Dim_title = 1H
Dim_units = [ppm]
Dimensions = X
Site = GENERIC ECP400
Spectrometer = DELTA_NMR
Field_strength = 7.0586013[T] (300[MHz
X_acq_duration = 3.6339712[s]
X_domain = 1H
X_freq = 300.52965592[MHz]
X_offset = 5[ppm]
X_points = 16384
X_prescans = 0
X_resolution = 0.27518105[Hz]
X_sweep = 4.50856628[kHz]
Clipped = FALSE
Mod_return = 1
Scans = 16
Total_scans = 16
X_90_width = 11.53[us]
X_acq_time = 3.6339712[s]
X_angle = 45[deg]
X_pulse = 5.765[us]
Initial_wait = 1[s]
Phase_preset = 3[us]
Recvr_gain = 10
Relaxation_delay = 4[s]
Temp_get = 17.6[dC]
Unblank_time = 2[us]

2,3-DF

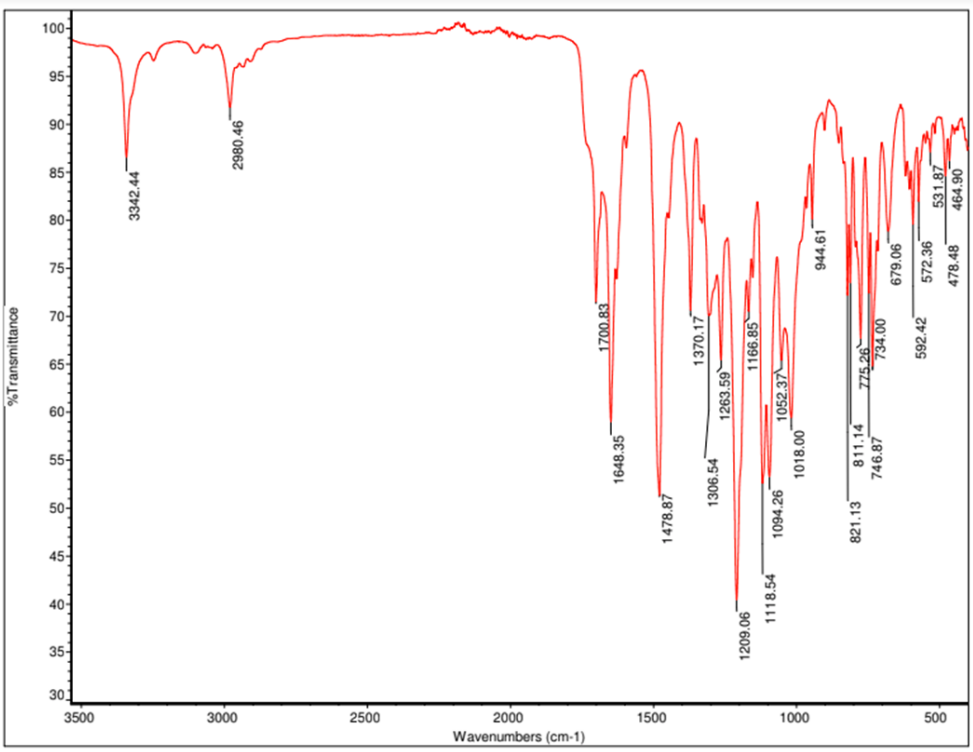
%Transmittance
Wavenumbers (cm-1)
3342.44
2980.46
1700.83
1648.35
1478.87
1370.17
1306.54
1263.59
1209.06
1166.85
1118.54
1094.26
1052.37
1018.00
944.61
821.13
811.14
775.26
746.87
734.00
679.06
592.42
572.36
531.87
478.48
464.90

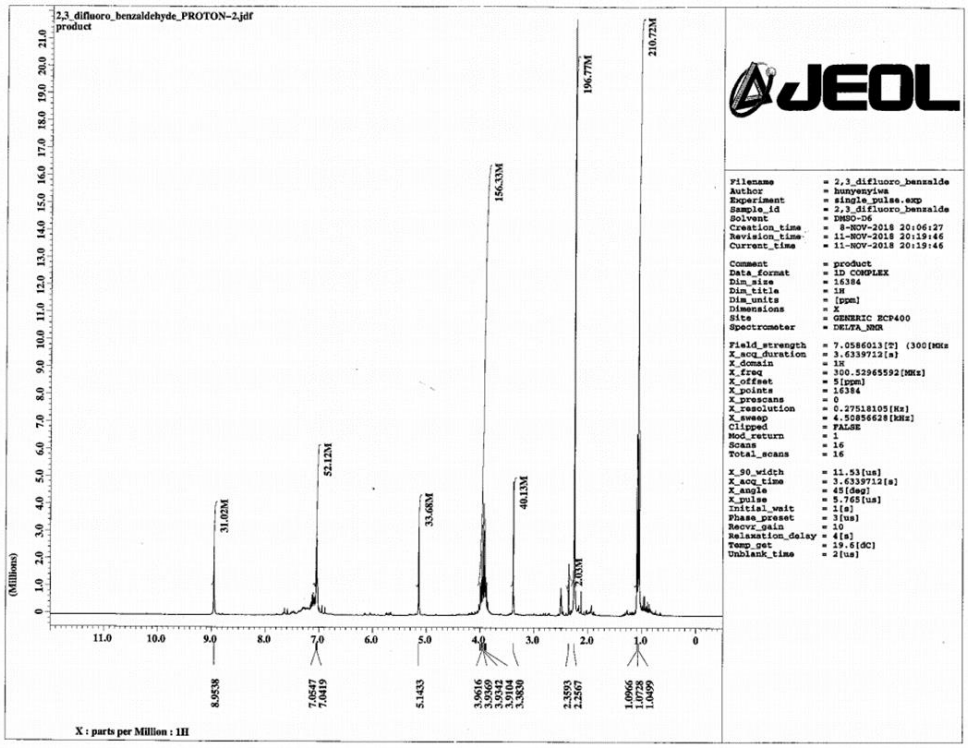
2,3_difluoro_benzaldehyde_PROTON-2.jdf
product
(Millions)
X : parts per Million : 1H
31.02M
52.12M
33.68M
156.33M
40.13M
196.77M
2.03M
210.72M
JEOL
Filename = 2,3_difluoro_benzalde
Author = hunyenyiwa
Experiment = single_pulse.exp
Sample_id = 2,3_difluoro_benzalde
Solvent = DMSO-D6
Creation_time = 8-NOV-2018 20:06:27
Revision_time = 11-NOV-2018 20:19:46
Current_time = 11-NOV-2018 20:19:46
Comment = product
Data_format = 1D COMPLEX
Dim_size = 16384
Dim_title = 1H
Dim_units = [ppm]
Dimensions = X
Site = GENERIC ECP400
Spectrometer = DELTA_NMR
Field_strength = 7.0586013[T] (300[MHz
X_acq_duration = 3.6339712[s]
X_domain = 1H
X_freq = 300.52965592[MHz]
X_offset = 5[ppm]
X_points = 16384
X_prescans = 0
X_resolution = 0.27518105[Hz]
X_sweep = 4.50856628[kHz]
Clipped = FALSE
Mod_return = 1
Scans = 16
Total_scans = 16
X_90_width = 11.53[us]
X_acq_time = 3.6339712[s]
X_angle = 45[deg]
X_pulse = 5.765[us]
Initial_wait = 1[s]
Phase_preset = 3[us]
Recvr_gain = 10
Relaxation_delay = 4[s]
Temp_get = 19.6[dC]
Unblank_time = 2[us]

2,4-DF

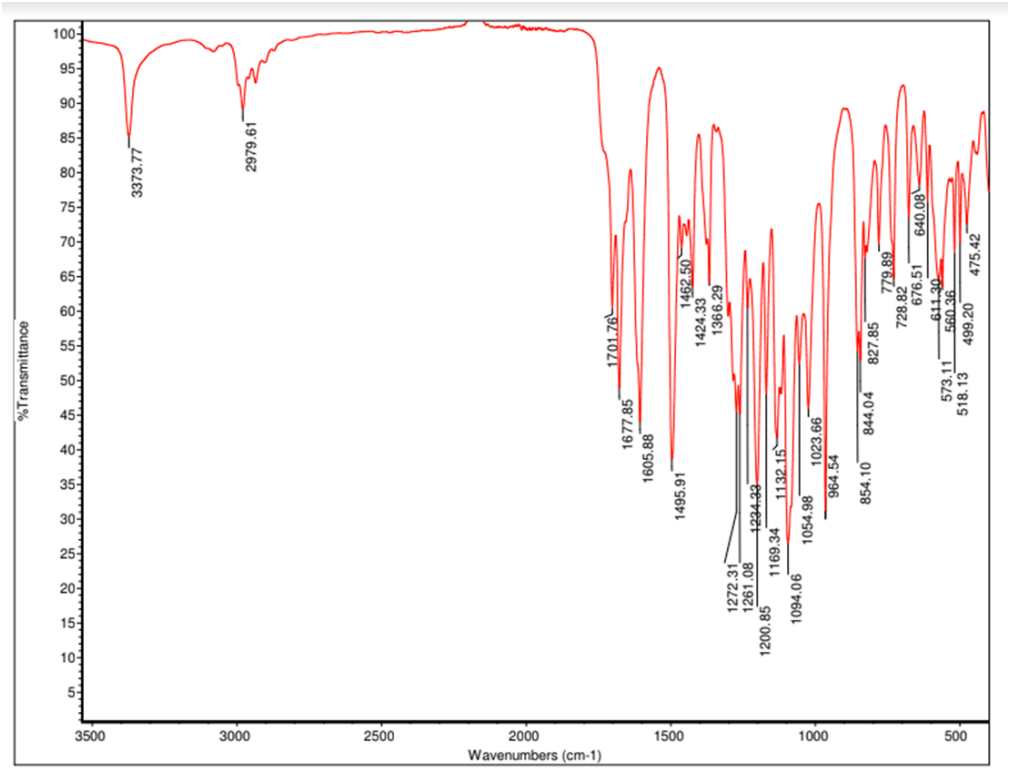
%Transmittance
Wavenumbers (cm-1)
3373.77
2979.61
1701.76
1677.85
1605.88
1495.91
1462.50
1424.33
1366.29
1272.31
1261.08
1224.33
1200.85
1169.34
1132.15
1094.06
1054.98
1023.66
964.54
854.10
844.04
827.85
779.89
728.82
676.51
640.08
611.30
573.11
560.36
518.13
499.20
475.42

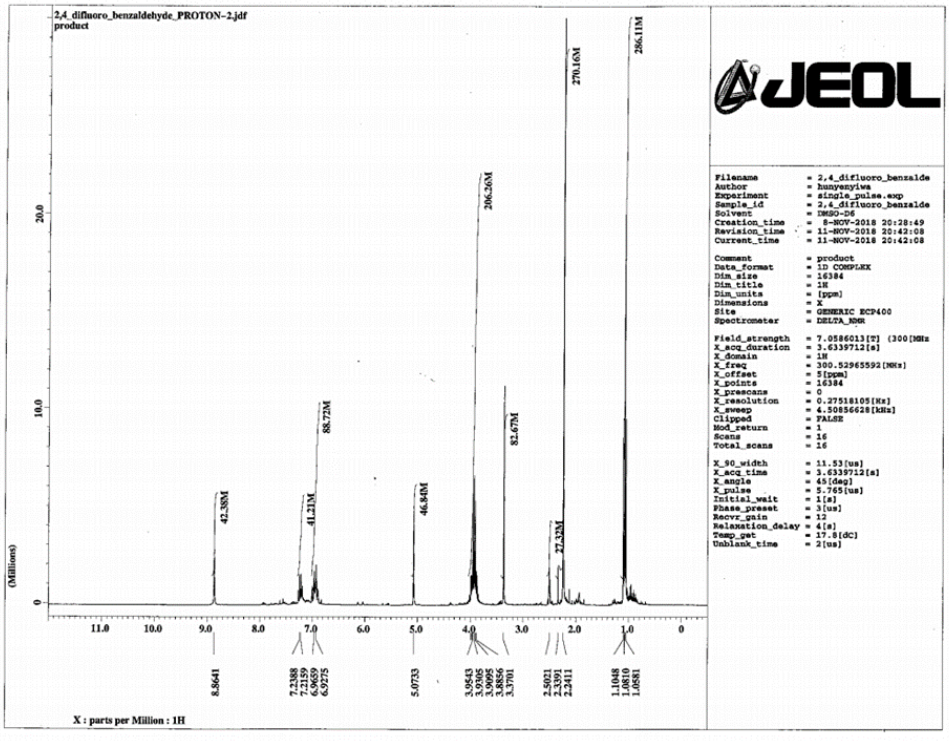
2,4_difluoro_benzaldehyde_PROTON-2.jdf
product
JEOL
Filename = 2,4_difluoro_benzalde
Author = hunyenyiwa
Experiment = single_pulse.exp
Sample_id = 2,4_difluoro_benzalde
Solvent = DMSO-D6
Creation_time = 8-NOV-2018 20:28:49
Revision_time = 11-NOV-2018 20:42:08
Current_time = 11-NOV-2018 20:42:08
Comment = product
Data_format = 1D COMPLEX
Dim_size = 16384
Dim_title = 1H
Dim_units = [ppm]
Dimensions = X
Site = GENERIC RCP400
Spectrometer = DELTA_NMR
Field_strength = 7.0586013[T] (300[MHz
X_acq_duration = 3.6339712[s]
X_domain = 1H
X_freq = 300.52965592[MHz]
X_offset = 5[ppm]
X_points = 16384
X_prescans = 0
X_resolution = 0.27518105[Hz]
X_sweep = 4.50856628[kHz]
Clipped = FALSE
Mod_return = 1
Scans = 16
Total_scans = 16
X_90_width = 11.53[us]
X_acq_time = 3.6339712[s]
X_angle = 45[deg]
X_pulse = 5.765[us]
Initial_wait = 1[s]
Phase_preset = 3[us]
Recvr_gain = 12
Relaxation_delay = 4[s]
Temp_get = 17.8[dC]
Unblank_time = 2[us]
42.38M
41.21M
88.72M
46.84M
206.26M
82.67M
27.32M
270.16M
286.11M
(Millions)
X : parts per Million : 1H

2,5-DF

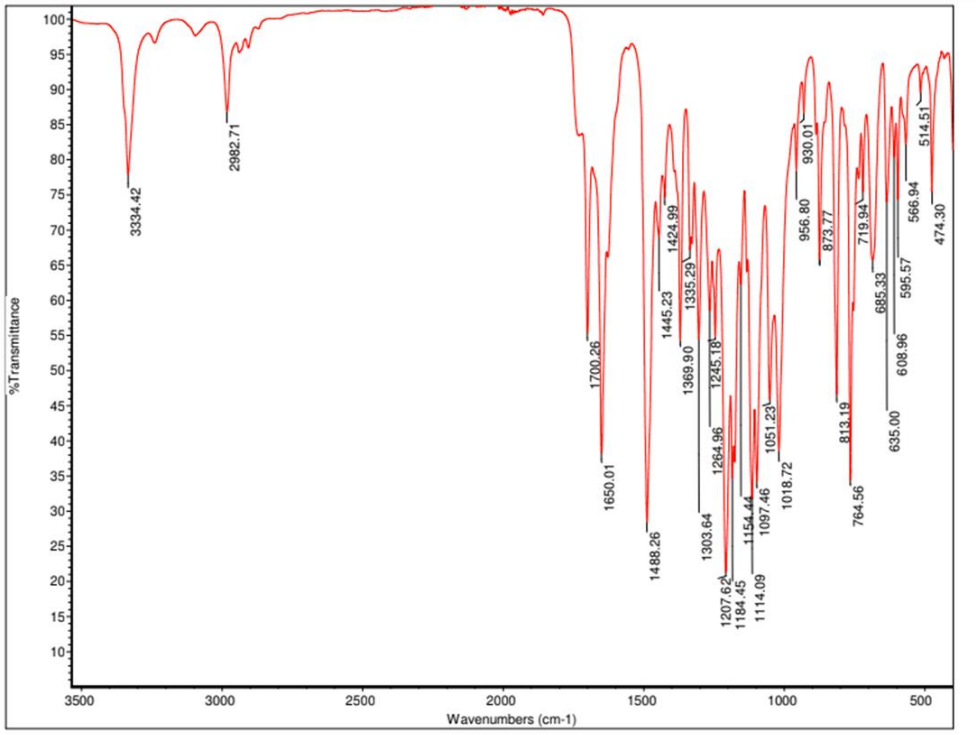
%Transmittance
Wavenumbers (cm-1)
3334.42
2982.71
1700.26
1650.01
1488.26
1445.23
1424.99
1369.90
1335.29
1303.64
1264.96
1245.18
1207.62
1184.45
1154.44
1114.09
1097.46
1051.23
1018.72
956.80
930.01
873.77
813.19
764.56
719.94
685.33
635.00
608.96
595.57
566.94
514.51
474.30

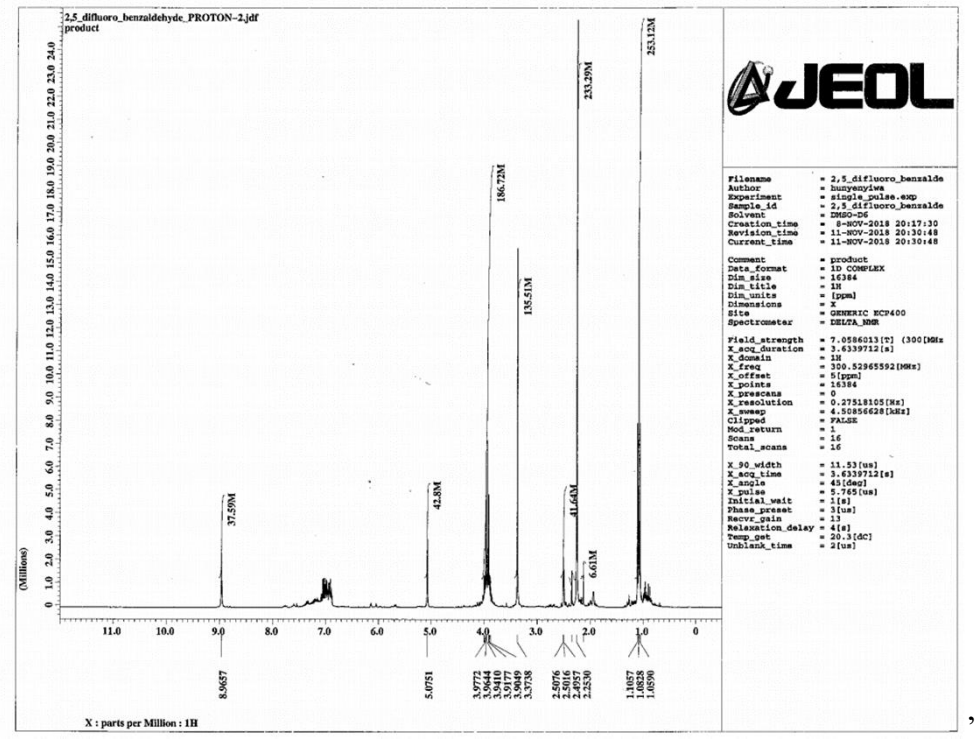
2,5_difluoro_benzaldehyde_PROTON-2.jdf
product
JEOL
X : parts per Million : 1H
Filename = 2,5_difluoro_benzalde
Author = bunyenjwa
Experiment = single_pulse.exp
Sample_id = 2,5_difluoro_benzalde
Solvent = DMSO-D6
Creation_time = 8-NOV-2018 20:17:30
Revision_time = 11-NOV-2018 20:30:48
Current_time = 11-NOV-2018 20:30:48
Comment = product
Data_format = 1D COMPLEX
Dim_size = 16384
Dim_title = 1H
Dim_units = [ppm]
Dimensions = X
Site = GENERIC ECP400
Spectrometer = DELTA_NMR
Field_strength = 7.0586013[T] (300[MHz
X_acq_duration = 3.6339712[s]
X_domain = 1H
X_freq = 300.52965592[MHz]
X_offset = 5[ppm]
X_points = 16384
X_prescans = 0
X_resolution = 0.27518105[Hz]
X_sweep = 4.50856628[kHz]
Clipped = FALSE
Mod_return = 1
Scans = 16
Total_scans = 16
X_90_width = 11.53[us]
X_acq_time = 3.6339712[s]
X_angle = 45[deg]
X_pulse = 5.765[us]
Initial_wait = 1[s]
Phase_preset = 3[us]
Recvr_gain = 13
Relaxation_delay = 4[s]
Temp_get = 20.3[dC]
Unblank_time = 2[us]

,

2-TF

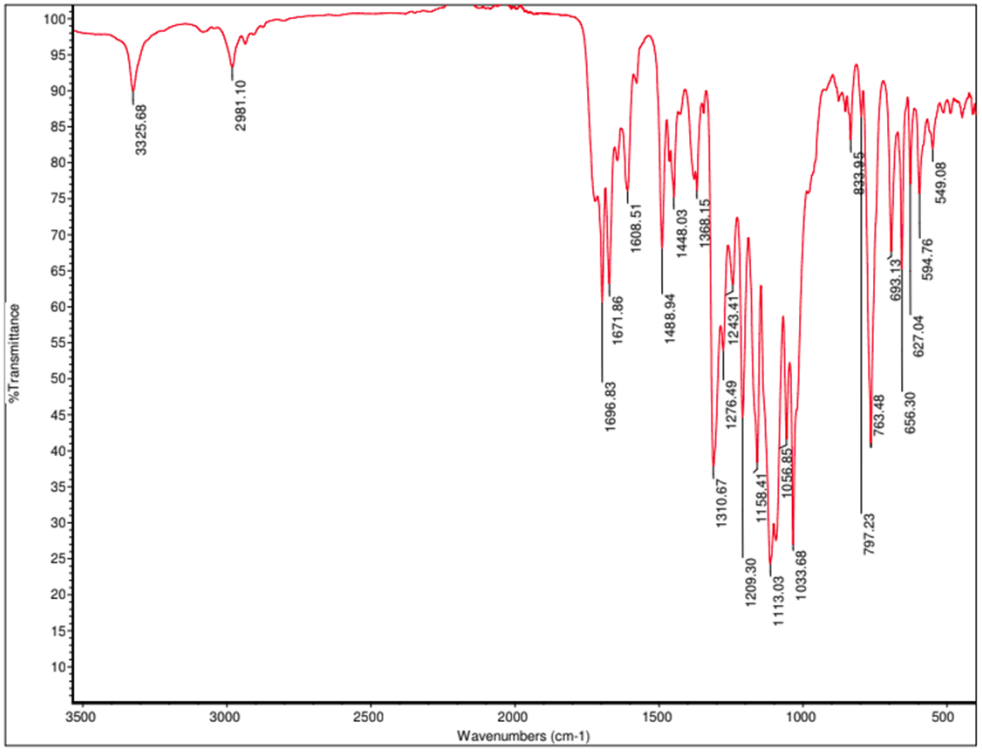
%Transmittance
Wavenumbers (cm-1)
3325.68
2981.10
1696.83
1671.86
1608.51
1488.94
1448.03
1368.15
1310.67
1276.49
1243.41
1209.30
1158.41
1113.03
1056.85
1033.68
933.95
797.23
763.48
693.13
656.30
627.04
594.76
549.08

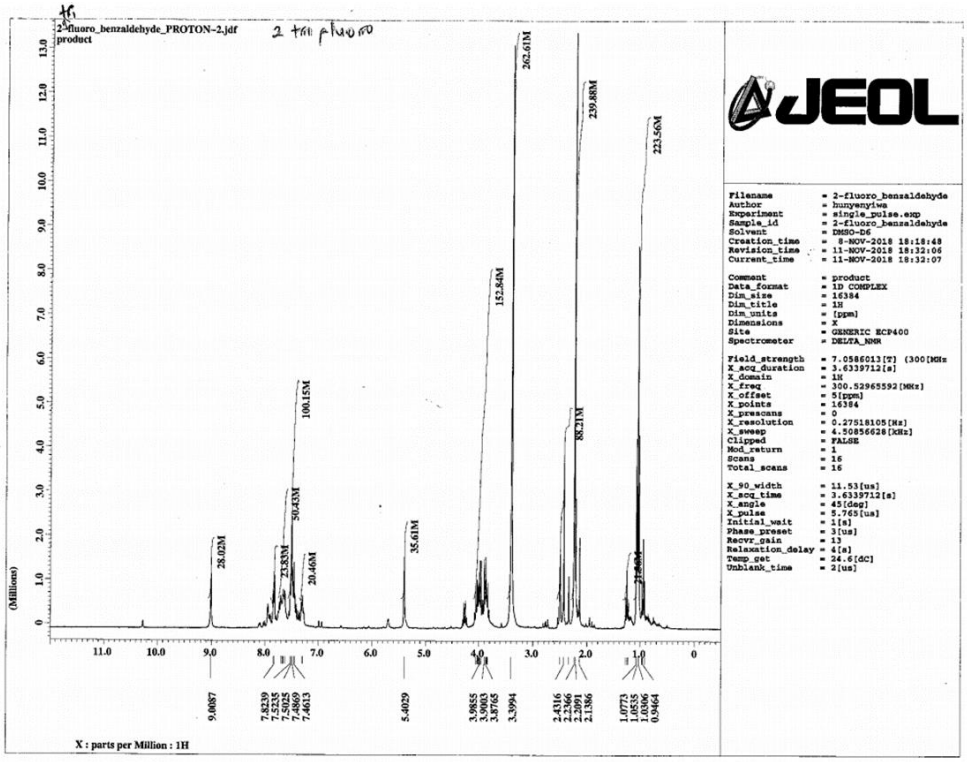
2-fluoro_benzaldehyde_PROTON-2.jdf
product
2 tan fluoro
X : parts per Million : 1H
JEOL
Filename = 2-fluoro_benzaldehyde
Author = hunyenyiwa
Experiment = single_pulse.exp
Sample_id = 2-fluoro_benzaldehyde
Solvent = DMSO-D6
Creation_time = 8-NOV-2018 18:18:48
Revision_time = 11-NOV-2018 18:32:06
Current_time = 11-NOV-2018 18:32:07
Comment = product
Data_format = 1D COMPLEX
Dim_size = 16384
Dim_title = 1H
Dim_units = [ppm]
Dimensions = X
Site = GENERIC ECP400
Spectrometer = DELTA_NMR
Field_strength = 7.0586013[T] (300[MHz
X_acq_duration = 3.6339712[s]
X_domain = 1H
X_freq = 300.52965592[MHz]
X_offset = 5[ppm]
X_points = 16384
X_prescans = 0
X_resolution = 0.27518105[Hz]
X_sweep = 4.50856628[kHz]
Clipped = FALSE
Mod_return = 1
Scans = 16
Total_scans = 16
X_90_width = 11.53[us]
X_acq_time = 3.6339712[s]
X_angle = 45[deg]
X_pulse = 5.765[us]
Initial_wait = 1[s]
Phase_preset = 3[us]
Recvr_gain = 13
Relaxation_delay = 4[s]
Temp_get = 24.6[dC]
Unblank_time = 2[us]

3-TF

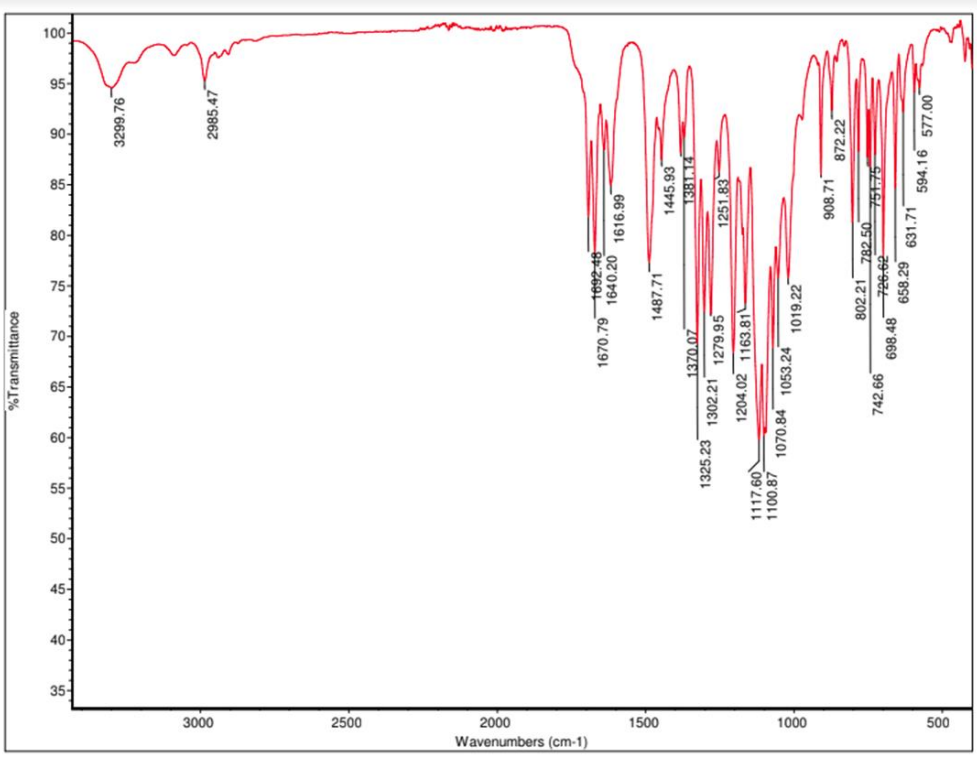
%Transmittance
Wavenumbers (cm-1)
3299.76
2985.47
1692.48
1670.79
1640.20
1616.99
1487.71
1445.93
1381.14
1370.07
1325.23
1302.21
1279.95
1251.83
1204.02
1163.81
1117.60
1100.87
1070.84
1053.24
1019.22
908.71
872.22
802.21
782.50
751.75
742.66
726.62
698.48
658.29
631.71
594.16
577.00

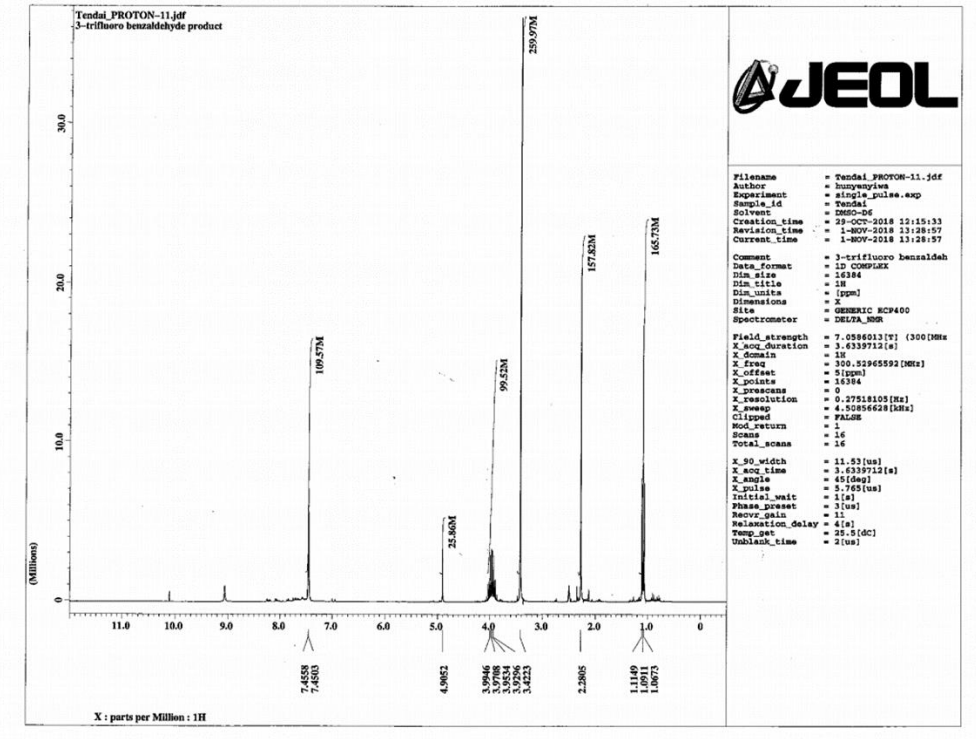
Tendai_PROTON-11.jdf
3-trifluoro benzaldehyde product
JEOL
(Millions)
X : parts per Million : 1H
109.57M
25.86M
99.52M
259.97M
157.82M
165.73M
Filename = Tendai_PROTON-11.jdf
Author = bunyanyiwa
Experiment = single_pulse.exp
Sample_id = Tendai
Solvent = DMSO-D6
Creation_time = 29-OCT-2018 12:15:33
Revision_time = 1-NOV-2018 13:28:57
Current_time = 1-NOV-2018 13:28:57
Comment = 3-trifluoro benzaldeh
Data_format = 1D COMPLEX
Dim_size = 16384
Dim_title = 1H
Dim_units = [ppm]
Dimensions = X
Site = GENERIC RCP400
Spectrometer = DELTA_NMR
Field_strength = 7.0586013[T] (300[MHz
X_acq_duration = 3.6339712[s]
X_domain = 1H
X_freq = 300.52965592[MHz]
X_offset = 5[ppm]
X_points = 16384
X_prescans = 0
X_resolution = 0.27518105[Hz]
X_sweep = 4.50856628[kHz]
Clipped = FALSE
Mod_return = 1
Scans = 16
Total_scans = 16
X_90_width = 11.53[us]
X_acq_time = 3.6339712[s]
X_angle = 45[deg]
X_pulse = 5.765[us]
Initial_wait = 1[s]
Phase_preset = 3[us]
Recvr_gain = 11
Relaxation_delay = 4[s]
Temp_set = 25.5[dC]
Unblank_time = 2[us]

3-Cl

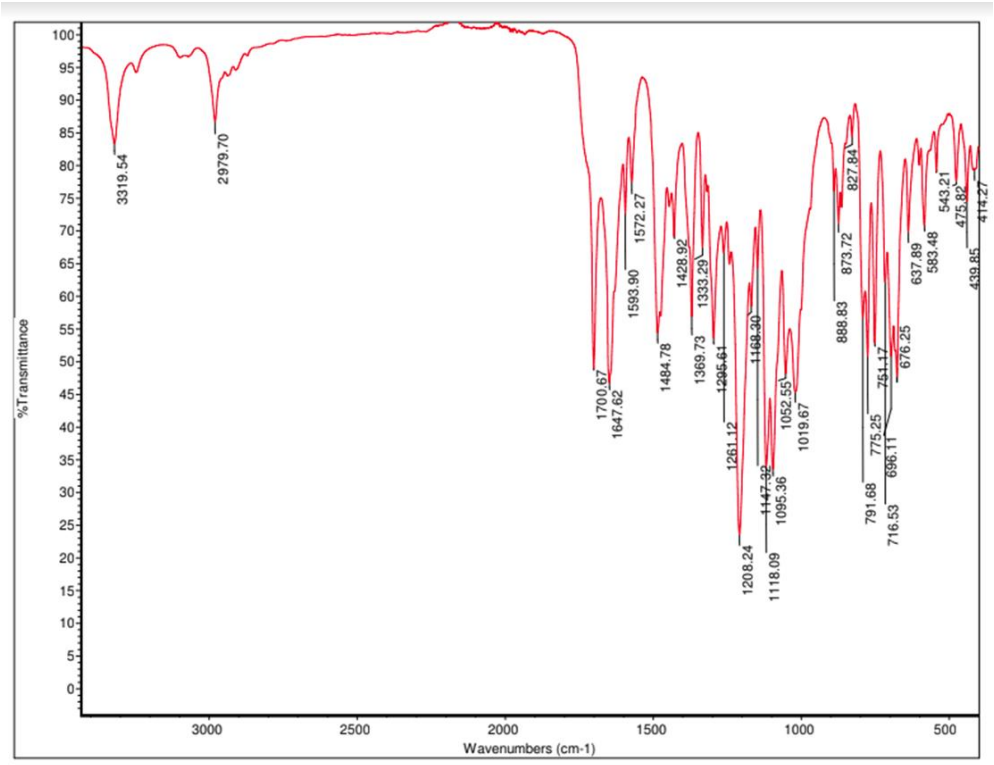
%Transmittance
Wavenumbers (cm-1)
3319.54
2979.70
1700.67
1647.62
1593.90
1572.27
1484.78
1428.92
1369.73
1333.29
1261.12
1208.24
1168.30
1147.32
1118.09
1095.36
1052.55
1019.67
888.83
873.72
827.84
791.68
775.25
751.17
716.53
696.11
676.25
637.89
583.48
543.21
475.82
439.85
414.27

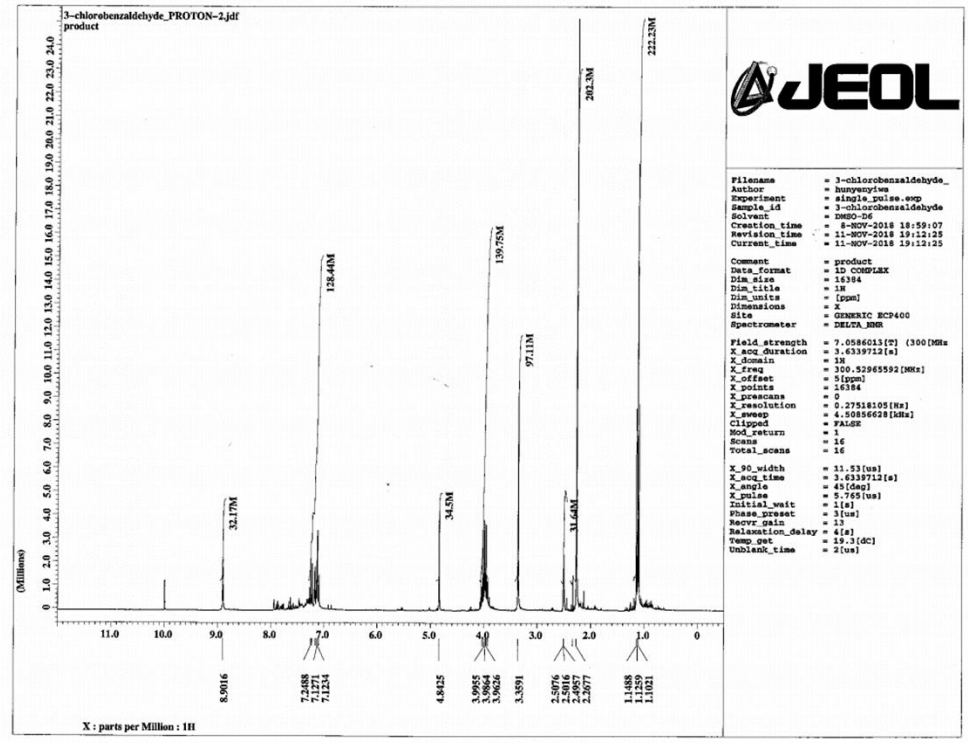
3-chlorobenzaldehyde_PROTON-2.jdf
product
JEOL
Filename = 3-chlorobenzaldehyde_
Author = hunyenyiwa
Experiment = single_pulse.exp
Sample_id = 3-chlorobenzaldehyde
Solvent = DMSO-D6
Creation_time = 8-NOV-2018 18:59:07
Revision_time = 11-NOV-2018 19:12:25
Current_time = 11-NOV-2018 19:12:25
Comment = product
Data_format = 1D COMPLEX
Dim_size = 16384
Dim_title = 1H
Dim_units = [ppm]
Dimensions = X
Site = GENERIC ECP400
Spectrometer = DELTA_NMR
Field_strength = 7.0586013[T] (300[MHz
X_acq_duration = 3.6339712[s]
X_domain = 1H
X_freq = 300.52965592[MHz]
X_offset = 5[ppm]
X_points = 16384
X_prescans = 0
X_resolution = 0.27518105[Hz]
X_sweep = 4.50856628[kHz]
Clipped = FALSE
Mod_return = 1
Scans = 16
Total_scans = 16
X_90_width = 11.53[us]
X_acq_time = 3.6339712[s]
X_angle = 45[deg]
X_pulse = 5.765[us]
Initial_wait = 1[s]
Phase_preset = 3[us]
Recvr_gain = 13
Relaxation_delay = 4[s]
Temp_get = 19.3[dC]
Unblank_time = 2[us]
32.17M
128.44M
139.75M
97.11M
34.53M
31.64M
203.3M
222.23M
8.9016
7.2488
7.1271
7.1234
4.8425
3.9955
3.9864
3.9626
3.3591
2.5976
2.5816
2.5657
2.2677
1.1488
1.1259
1.1021
X : parts per Million : 1H

4-Cl

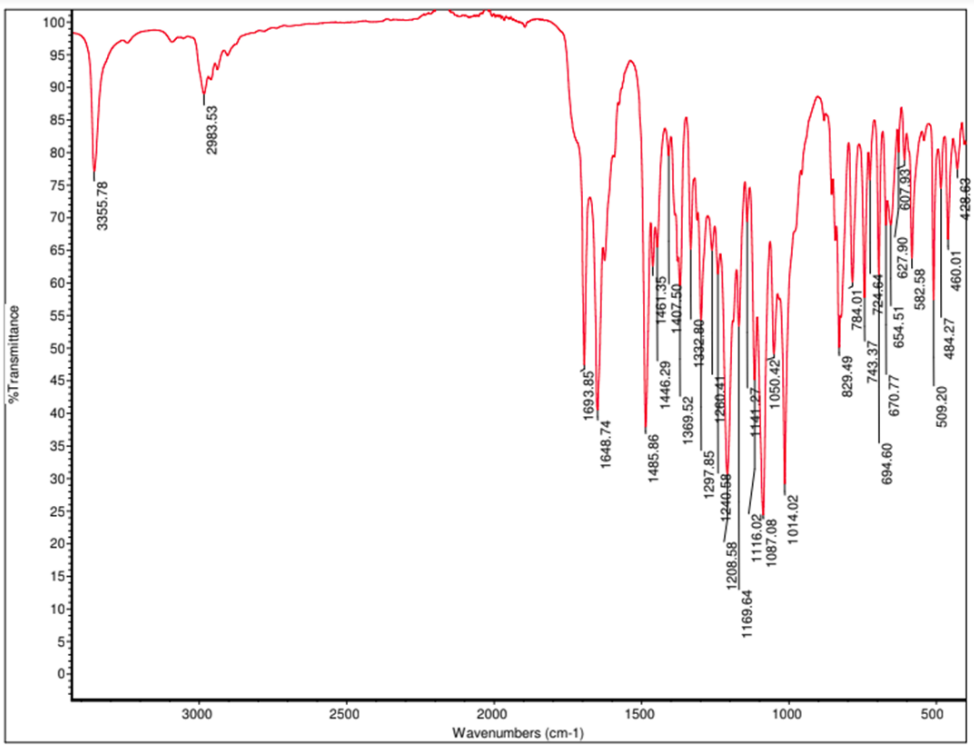
%Transmittance
Wavenumbers (cm-1)
3355.78
2983.53
1693.85
1648.74
1485.86
1446.29
1461.35
1407.50
1369.52
1332.80
1297.85
1260.41
1240.58
1208.58
1169.64
1141.27
1116.02
1087.08
1050.42
1014.02
829.49
784.01
743.37
724.64
694.60
670.77
654.51
627.90
607.93
582.58
509.20
484.27
460.01
428.63

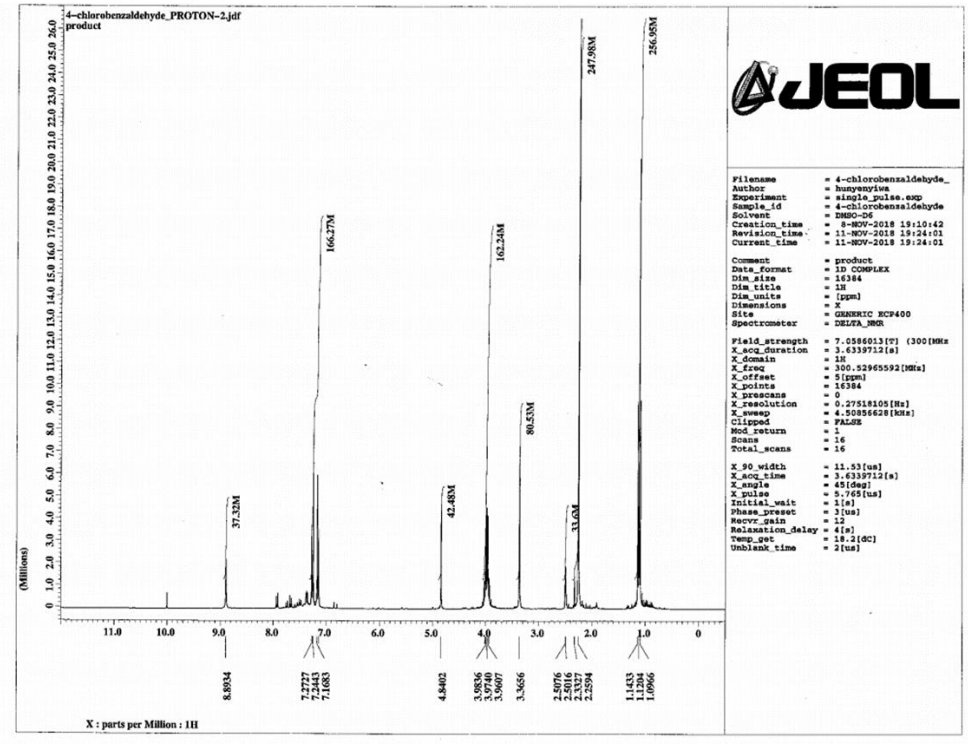
4-chlorobenzaldehyde_PROTON-2.jdf
product
JEOL
X : parts per Million : 1H
(Millions)
37.32M
166.27M
42.48M
162.24M
80.53M
33.43M
247.98M
256.95M
Filename = 4-chlorobenzaldehyde_
Author = hunyenyiwa
Experiment = single_pulse.exp
Sample_id = 4-chlorobenzaldehyde
Solvent = DMSO-D6
Creation_time = 8-NOV-2018 19:10:42
Revision_time = 11-NOV-2018 19:24:01
Current_time = 11-NOV-2018 19:24:01
Comment = product
Data_format = 1D COMPLEX
Dim_size = 16384
Dim_title = 1H
Dim_units = [ppm]
Dimensions = X
Site = GENERIC ECP400
Spectrometer = DELTA_NMR
Field_strength = 7.0586013[T] (300[MHz
X_acq_duration = 3.6339712[s]
X_domain = 1H
X_freq = 300.52965592[MHz]
X_offset = 5[ppm]
X_points = 16384
X_prescans = 0
X_resolution = 0.27518105[Hz]
X_sweep = 4.50856628[kHz]
Clipped = FALSE
Mod_return = 1
Scans = 16
Total_scans = 16
X_90_width = 11.53[us]
X_acq_time = 3.6339712[s]
X_angle = 45[deg]
X_pulse = 5.765[us]
Initial_wait = 1[s]
Phase_preset = 3[us]
Recvr_gain = 12
Relaxation_delay = 4[s]
Temp_get = 18.2[dC]
Unblank_time = 2[us]

4-Q

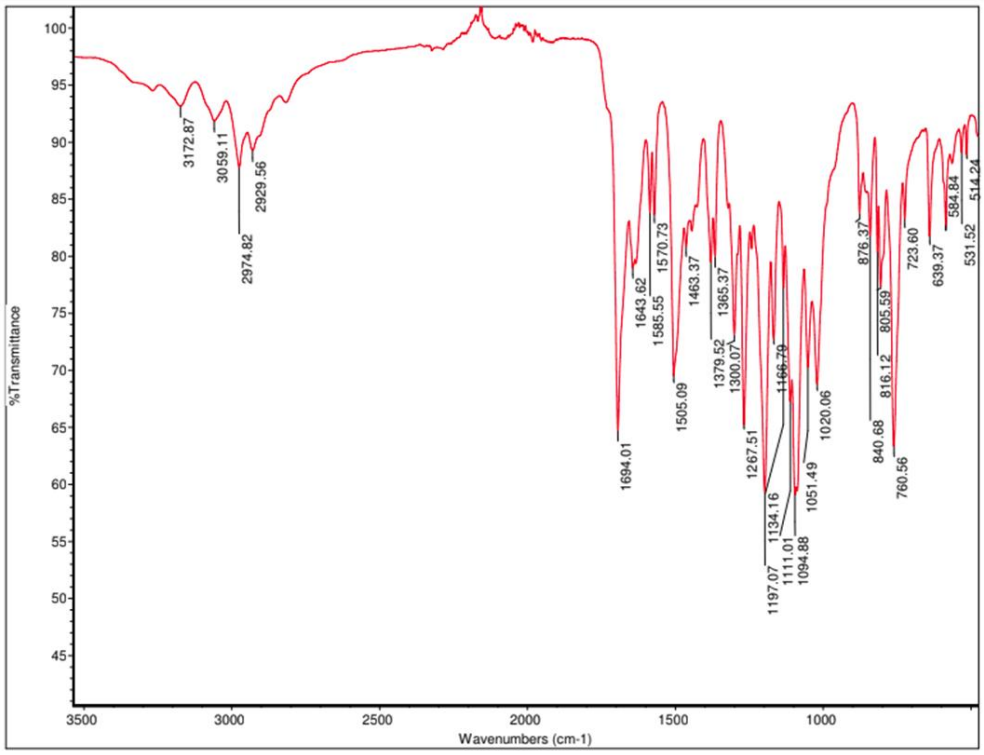
%Transmittance
Wavenumbers (cm-1)
3172.87
3059.11
2974.82
2929.56
1694.01
1643.62
1585.55
1570.73
1505.09
1463.37
1379.52
1365.37
1300.07
1267.51
1197.07
1166.79
1134.16
1111.01
1094.88
1051.49
1020.06
876.37
840.68
816.12
805.59
760.56
723.60
639.37
584.84
531.52
514.24

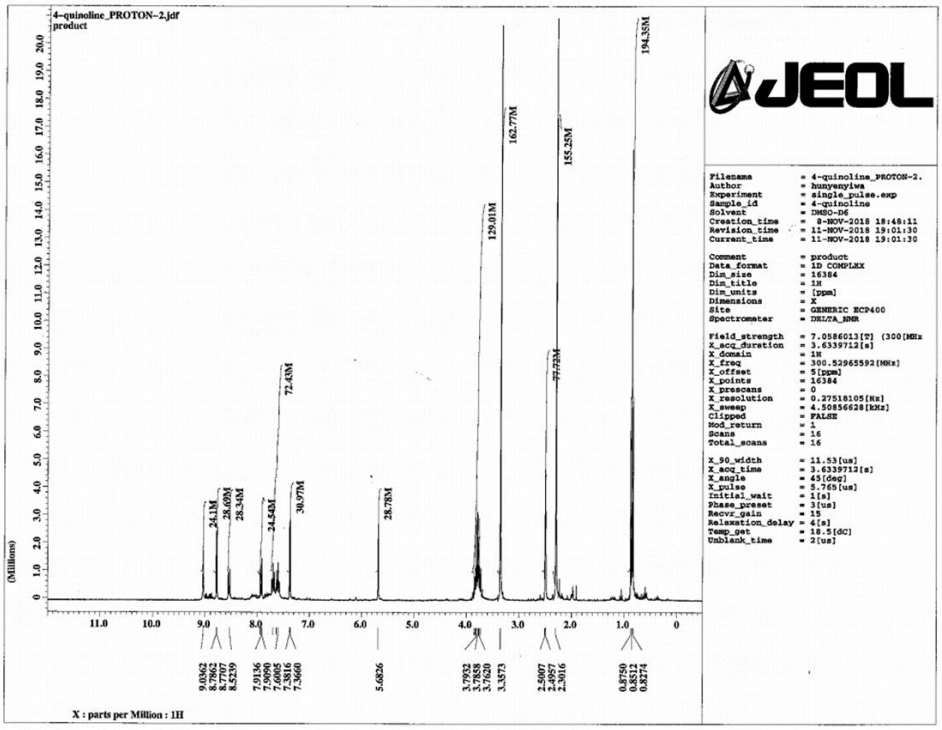
4-quinoline_PROTON-2.jdf
product
JEOL
194.38M
162.77M
155.25M
129.01M
77.73M
72.43M
30.97M
28.78M
28.40M
28.34M
24.54M
24.13M
X : parts per Million : 1H
Filename = 4-quinoline_PROTON-2.
Author = hunyenyiwa
Experiment = single_pulse.exp
Sample_id = 4-quinoline
Solvent = DMSO-D6
Creation_time = 8-NOV-2018 18:48:11
Revision_time = 11-NOV-2018 19:01:30
Current_time = 11-NOV-2018 19:01:30
Comment = product
Data_format = 1D COMPLEX
Dim_size = 16384
Dim_title = 1H
Dim_units = [ppm]
Dimensions = X
Site = GENERIC ECP400
Spectrometer = DELTA_NMR
Field_strength = 7.0586013[T] (300[MHz
X_acq_duration = 3.6339712[s]
X_domain = 1H
X_freq = 300.52965592[MHz]
X_offset = 5[ppm]
X_points = 16384
X_prescans = 0
X_resolution = 0.27518105[Hz]
X_sweep = 4.50856628[kHz]
Clipped = FALSE
Mod_return = 1
Scans = 16
Total_scans = 16
X_90_width = 11.53[us]
X_acq_time = 3.6339713[s]
X_angle = 45[deg]
X_pulse = 5.765[us]
Initial_wait = 1[s]
Phase_preset = 3[us]
Recvr_gain = 15
Relaxation_delay = 4[s]
Temp_get = 18.51[dC]
Unblank_time = 3[us]

5-M2F

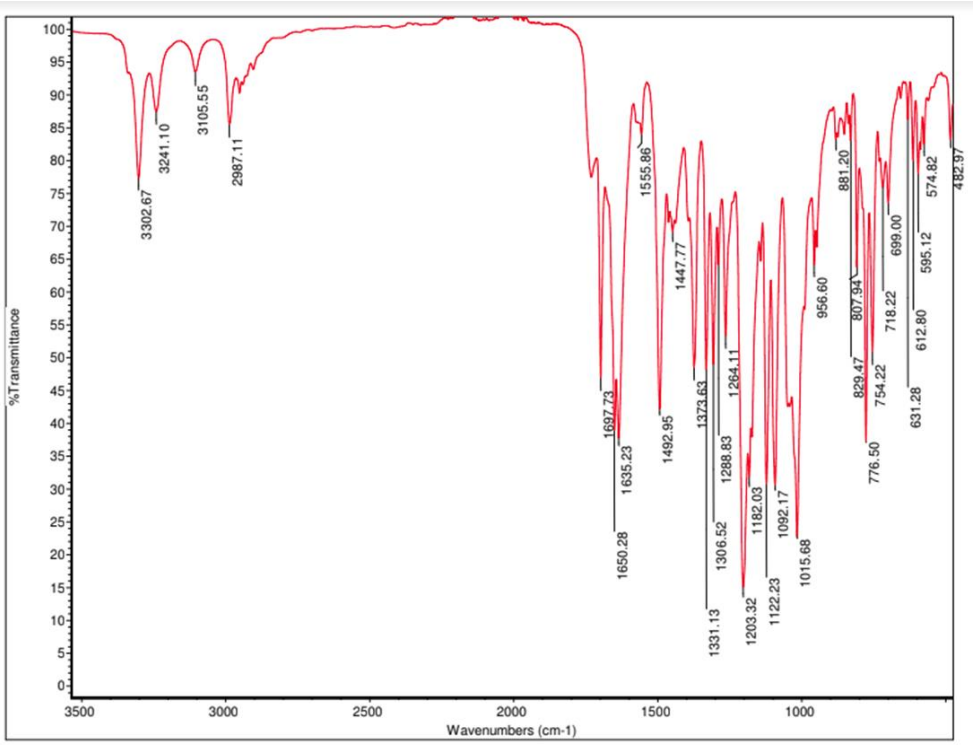
%Transmittance
Wavenumbers (cm-1)
3302.67
3241.10
3105.55
2987.11
1697.73
1650.28
1635.23
1555.86
1492.95
1447.77
1373.63
1331.13
1306.52
1288.83
1264.11
1203.32
1182.03
1122.23
1092.17
1015.68
956.60
881.20
829.47
807.94
776.50
754.22
718.22
699.00
631.28
612.80
595.12
574.82
482.97

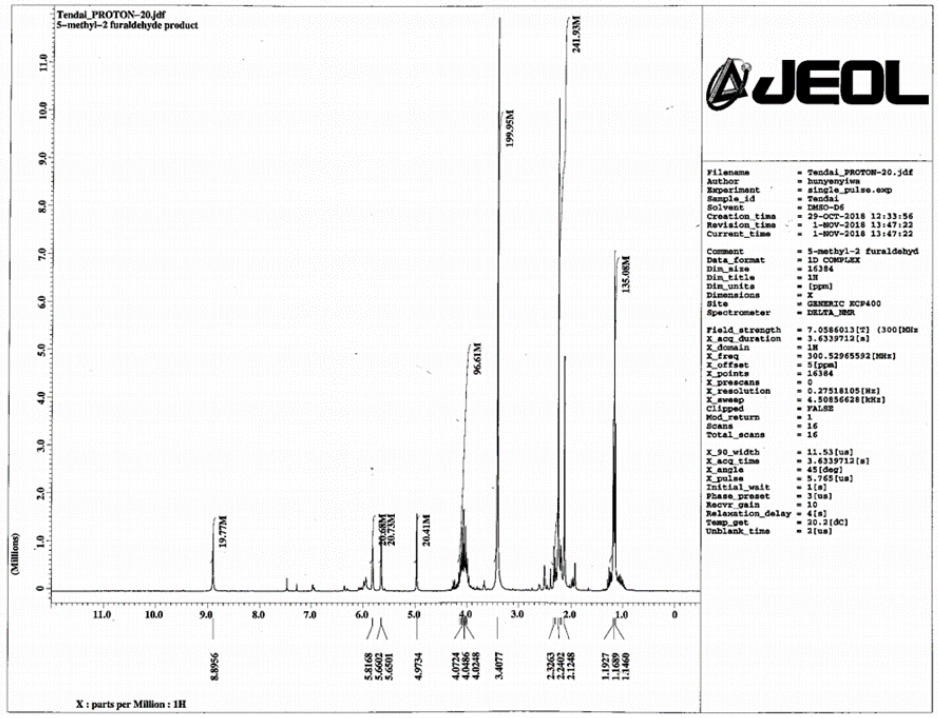
Tendai_PROTON-20.jdf
5-methyl-2 furaldehyde product
JEOL
Filename = Tendai_PROTON-20.jdf
Author = hunyenyiwa
Experiment = single_pulse.exp
Sample_id = Tendai
Solvent = DMSO-D6
Creation_time = 29-OCT-2018 12:33:56
Revision_time = 1-NOV-2018 13:47:22
Current_time = 1-NOV-2018 13:47:22
Comment = 5-methyl-2 furaldehyd
Data_format = 1D COMPLEX
Dim_size = 16384
Dim_title = 1H
Dim_units = [ppm]
Dimensions = X
Site = GENERIC ECP400
Spectrometer = DELTA_NMR
Field_strength = 7.0586013[T] (300[MHz
X_acq_duration = 3.6339712[s]
X_domain = 1H
X_freq = 300.52965592[MHz]
X_offset = 5[ppm]
X_points = 16384
X_prescans = 0
X_resolution = 0.27516105[Hz]
X_sweep = 4.50856626[kHz]
Clipped = FALSE
Mod_return = 1
Scans = 16
Total_scans = 16
X_90_width = 11.53[us]
X_acq_time = 3.6339712[s]
X_angle = 45[deg]
X_pulse = 5.765[us]
Initial_wait = 1[s]
Phase_preset = 3[us]
Recvr_gain = 10
Relaxation_delay = 4[s]
Temp_get = 20.2[dC]
Unblank_time = 2[us]
(Millions)
X : parts per Million : 1H

5-M2-TF

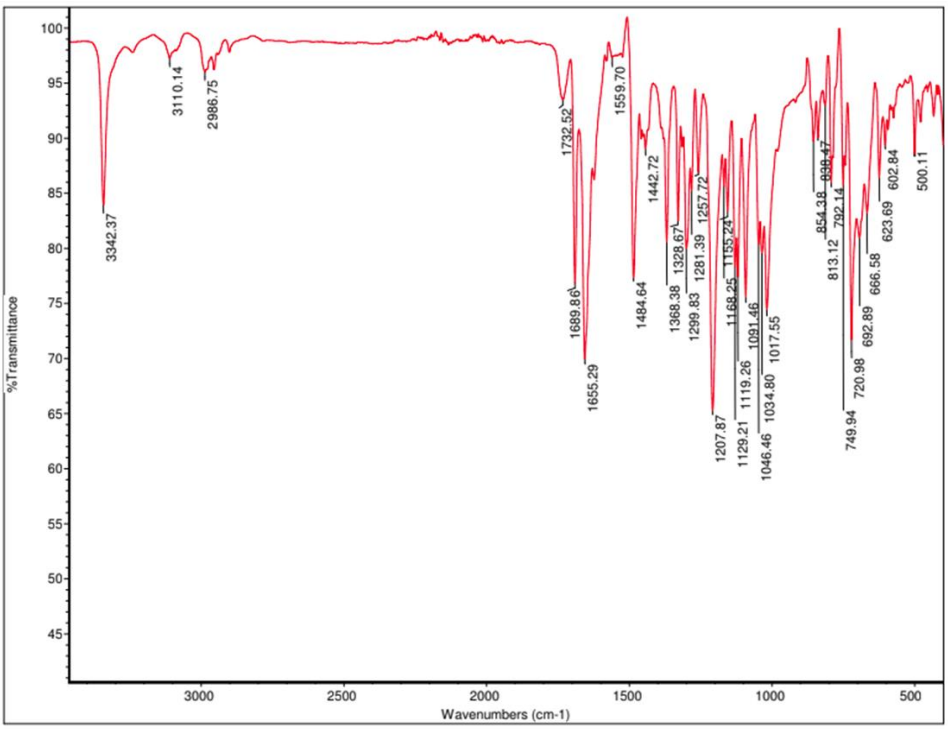
%Transmittance
Wavenumbers (cm-1)
3342.37
3110.14
2986.75
1732.52
1689.86
1655.29
1559.70
1484.64
1442.72
1368.38
1328.67
1299.83
1281.39
1257.72
1207.87
1168.25
1155.24
1129.21
1119.26
1091.46
1046.46
1034.80
1017.55
854.38
838.47
813.12
792.14
749.94
720.98
692.89
666.58
623.69
602.84
500.11

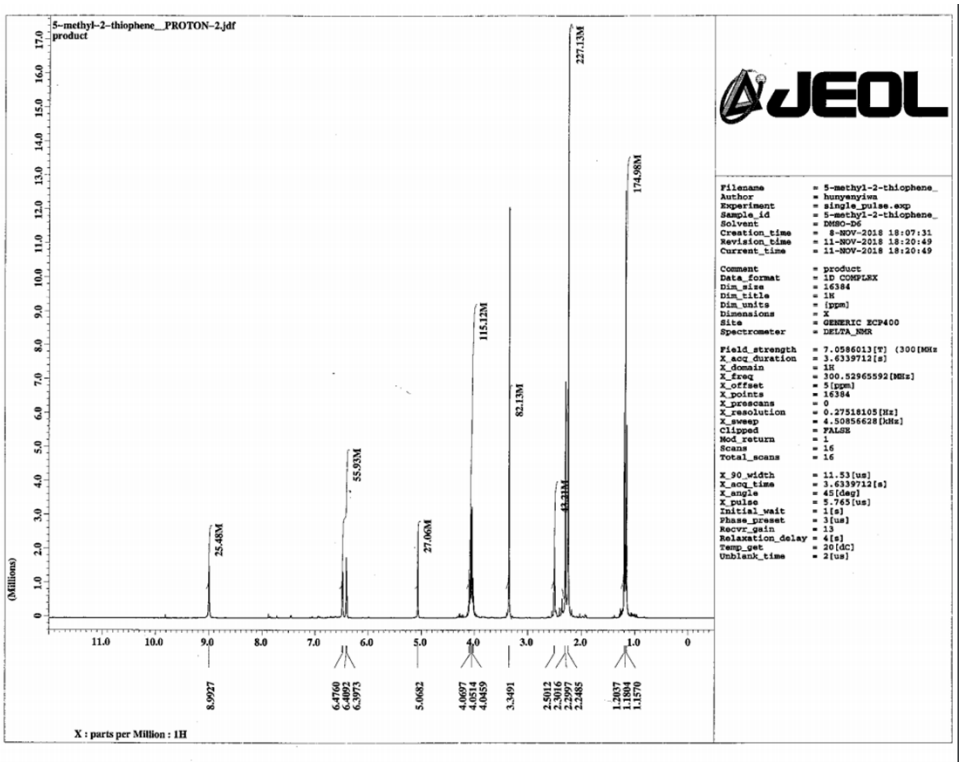
5-methyl-2-thiophene__PROTON-2.jdf
product
(Millions)
X : parts per Million : 1H
25.48M
55.93M
27.06M
115.12M
82.13M
41.31M
227.13M
174.98M
8.9927
6.4760
6.4092
6.3973
5.0682
4.0697
4.0514
4.0459
3.3491
2.5012
2.3016
2.2997
2.2485
1.2037
1.1804
1.1570
JEOL
Filename = 5-methyl-2-thiophene_
Author = hunyamyiwa
Experiment = single_pulse.exp
Sample_id = 5-methyl-2-thiophene_
Solvent = DMSO-D6
Creation_time = 8-NOV-2018 18:07:31
Revision_time = 11-NOV-2018 18:20:49
Current_time = 11-NOV-2018 18:20:49
Comment = product
Data_format = 1D COMPLEX
Dim_size = 16384
Dim_title = 1H
Dim_units = [ppm]
Dimensions = X
Site = GENERIC ECP400
Spectrometer = DELTA_NMR
Field_strength = 7.0586013[T] (300[MHz
X_acq_duration = 3.6339712[s]
X_domain = 1H
X_freq = 300.52965592[MHz]
X_offset = 5[ppm]
X_points = 16384
X_prescans = 0
X_resolution = 0.27518105[Hz]
X_sweep = 4.50856628[kHz]
Clipped = FALSE
Mod_return = 1
Scans = 16
Total_scans = 16
X_90_width = 11.53[us]
X_acq_time = 3.6339712[s]
X_angle = 45[deg]
X_pulse = 5.765[us]
Initial_wait = 1[s]
Phase_preset = 3[us]
Recvr_gain = 13
Relaxation_delay = 4[s]
Temp_get = 20[dC]
Unblank_time = 2[us]

EAA

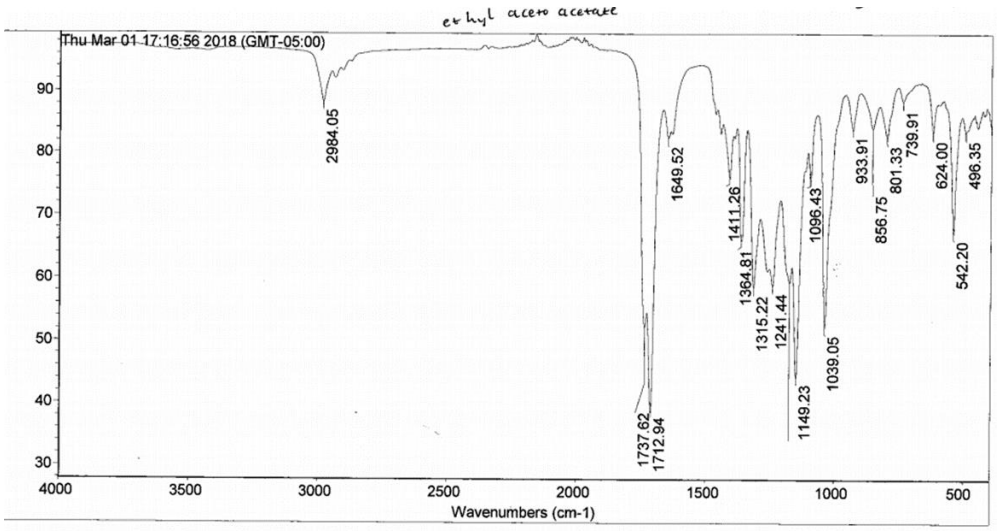

u Mar 01 17:24:42 2018 (GMT-05:00)
ND PEAKS:
Spectrum: Thu Mar 01 17:16:56 2018 (GMT-05:00)
Region: 4000.00 400.00
Absolute threshold: 92.508
Sensitivity: 50
Peak list: